NTNU

Norwegian University of
Science and Technology

Sensitivities in fatigue analysis of offshore wind turbine support structures

Benedicte Hexeberg Hammerstad

Preface

There is an increasing awareness of how finite resources are less than ideal, in the sense of sustainability. Not only because they are finite, but also because they have a negative impact on the environment, and possibly the world's population.

Infinite resources such as water and wind is, if you will excuse me, in the wind. Norway is currently undergoing an oil crisis, and hopefully it will lead to more focus on wind energy. The wind is all around us, without needing to be replenished. What we do need, are structures with special machinery to transform this wind into energy.

A wind turbine is an example of such a structure. There are onshore wind turbines and offshore wind turbines. Onshore wind turbines are cheaper in development, production and installation. [1] Offshore wind turbines give more electricity, because there is less turbulence offshore, and more stable wind conditions leads to more electricity output. Other benefits of offshore wind turbines are the abundant space in which to build wind farms and a smaller visual impact.

Offshore wind turbines, in contrast to onshore wind turbines, needs a support structure. Monopiles are the support structures mostly used; hence, the industry has more experience with it. A jacket structure is an alternative, but it has more unsolved challenges, and is therefore a riskier choice for the time being.

The fact that jacket structures have more unsolved challenges is no surprise, seeing as a lattice structure with several tubular joints is more complex than a single, simple beam with no joints. With more research, these challenges may be resolved.

When designing a jacket structure, the design driving factor is usually the fatigue damage – how well a structure can withstand cyclic loading. [2] Both jacket structures and monopiles are prone to fatigue, but estimating the fatigue damage for a jacket structure is more resource intensive than for a monopile. More joints lead to more calculations.

When it comes to fatigue analysis, there is no exclusively correct way to do it. One of the things affecting which method to choose, is the geometry of the construction components of the structure. On an offshore wind turbine, using the hot spot stress method for fatigue analysis is common for tubular joints in a jacket structure. But even for this method, which is quite specific, there is still no single way to perform the analysis. More on this in chapter 2.

An increased understanding of fatigue damage assessment leads to designs that are more reliable. Among other, maybe safety factors can be reduced. The costs would also be reduced by further optimization of the designs, as the support structure stands for approximately 20 % of the total cost. [3]

Using a program that has been programmed for this purpose, this master thesis will look into the hot spot stress method in detail. The main focus is on selected areas where there are alternatives as to how the analysis should be performed, and a comparison of the results with a sensitivity analysis.

This master thesis shows the theory necessary for understanding this method for fatigue analysis, explains how the sensitivity analysis was performed, and presents and discuss the results. Working with this master thesis has been both demanding and interesting. This study will be continued, using the application that was developed.

The work has been done in co-operation with Fedem Technology AS.

Benedicte Hexeberg Hammerstad

Trondheim, 10.06.2016

Summary

A fatigue analysis gives an answer to the question of whether a structure will resist fatigue throughout its lifetime or not. The hot spot stress method is one of the methods used to find the solution, by looking at points around the circumference of a weld, and finding the stress values at these points. This master thesis investigates fatigue analysis using the hot spot stress method, through a sensitivity analysis. By changing what parameters and approaches the fatigue analysis uses, several fatigue damage values are calculated for each joint.

The design chosen for the study is a single support structure for an offshore wind turbine (OWT) – the UpWind reference jacket from Phase I of the Offshore Code Comparison Collaboration Continuation (OC4) project. [4] The jacket structure supports the NREL 5-MW reference wind turbine. [5] It consist of K-joints, X-joints and Y-joints.

With fatigue damage being the design driving factor, the method for estimating fatigue damage may necessitate different design in the structure. [2] That means that different fatigue damage estimations may result in different costs and a more reliable structure. As anything can be safe and reliable if you just overspend and over-design it, an ideal fatigue analysis can give reliable results, without being too conservative.

During the master work, an application was developed in the .NET framework to work in conjuncture with FEDEM WindPower, a simulation program used for wind turbine systems, that has been verified in the OC4 project. [*4*] The developed application performs all extractions and calculations needed for estimating the fatigue damage using the hot spot stress (HSS) method. The HSSs calculated are linearly extrapolated structural stresses, with the nominal stress in the chord included for the HSSs on the chord side of the weld.

The application performs the fatigue damage estimations using several procedures of the hot spot stress method. This leads to several fatigue damage values for each joint, giving the basis for the sensitivity analysis concerning the hot spot stress method. Common for all variations in these options, are the load simulations and the usage of hot spot stress method, rainflow counting, S-N curve and Palmgren-Miner rule. This is all explained in chapter 2. They also have in common general fixity conditions, chord-end fixity parameter equal to 0.7, and for the joints with two braces – loads occur in both.

The variations consist of the *L* parameter used in the stress concentration factor (SCF) equations, the order in which maximum fatigue damage concerning one hot spot was kept while the others were excluded, the total number of hot spots around the circumference of the weld, and the choice regarding which equations to use for the SCFs at the crown for axial load. For the choice of equations to use for the SCFs, one can choose between solely geometrical SCFs, and SCFs including nominal stress that makes up for local joint flexibility (LJF). Here, all options are evaluated.

Only Y-joints are affected by changes in the *L* parameter after a certain limit, but until this limit is reached it affects all joints. Y-joints are the only ones, regarding the structure analysed and the choices made in this thesis, that have SCFs containing *L* in their equation.

K-joints are those joints that are most affected when all hot spots except the one with the maximum fatigue damage is excluded later in the analysis, compared to excluding them earlier. When they are excluded earlier, the final fatigue damage is built up by only maximum values, while the other alternative estimates all hot spots singularly before keeping the maximum. These procedures are referred to in this thesis as the two estimation approaches.

The fact that K-joints is the joint type showing most differences concerning estimation approach in this thesis, indicates that the spot most prone to fatigue damage varies more within the K-joints than in the other two joint types.

X-joints and K-joints are equally affected by the number of hot spot one uses. Increasing the number of hot spots from 8 to 16 can for several joints give an increase ratio equal to 16 %, the ratio being found by dividing the fatigue damage estimated using 16 hot spots with the fatigue damage estimated using 8 hot spots. Increasing the number of hot spots either gives the same value or a higher value, because increasing the number of hot spots indicates adding hot spots in between the existing ones.

The optional SCFs at the crown for axial load are only evaluated for Y-joints. The equations containing nominal stress shows, for most of the joints, much lower fatigue damage estimations than the solely geometrical ones, for L values at 7.2 m and higher.

The limited selection of parameters, due to limited amount of time, results in a sensitivity analysis that is not sufficient to come up with a final, clear answer regarding the ultimate fatigue analysis. This thesis is therefore intended to be used, with the developed application, as the basis for a larger sensitivity analysis that could provide further knowledge on the preferable procedure concerning fatigue analysis using the hot spot stress method.

Sammendrag

En utmattingsanalyse gir svaret på om hvorvidt en konstruksjon kan motstå utmatting gjennom hele sin livstid eller ikke. Hot spot-metoden er en av metodene som kan brukes til å finne løsningen, ved å se på punkter rundt omkretsen til en sveis i et rørformet ledd, og finne spenningsverdiene i disse punktene. Denne masteroppgaven undersøker utmattingsanalyse utført ved hjelp av hot spot-spenningsmetoden, gjennom en sensitivitetsanalyse. Ved å variere parameterne og fremgangsmåten, har flere utmattingsskadeverdier blitt estimert for hvert ledd.

Konstruksjonen som ble valgt til å utføre analysen på er bærekonstruksjonen til en offshore vindturbin – UpWind referansefagverk fra *Phase I in the Offshore Code Comparison Collaboration Continuation (OC4) project*. [4] Fagverket støtter vindturbinen NREL 5-MW. [5] Denne konstruksjonen består av K-ledd, X-ledd og Y-ledd.

Basert på konstruksjonstypen og forholdene på stedet en offshore støttestruktur skal stå, er utmatting drivende faktor når det gjelder design. Forskjellige fremgangsmåter og diverse valg kan gjøre det nødvendig å endre designet til konstruksjonen. [2] Det indikerer at forskjellige utmattingsanalyser også resulterer i forskjellige kostnader og en mer pålitelig konstruksjon. Siden alt kan bli sikkert og solid så lenge man bruker en betydelig andel penger, og kanskje over-designer, vil en ideell utmattingsanalyse kunne gi pålitelige resultater uten å være for konservativ.

I løpet av master-arbeidet ble det utviklet en applikasjon i rammeverket .NET som samarbeider med FEDEM WindPower, et simuleringsprogram brukt til vindturbinsystemer, som er verifisert av OC4 prosjektet. [*4*] Den utviklede applikasjonen utfører, henter og beregner det som trengs for å finne utmattingen ved å bruke hot spot-metoden. Hot spot-spenningene som blir beregnet er lineært ekstrapolerte strukturelle hot spot-spenninger (HSSer), med nominell spenning i gurtrøret medberegnet i HSSene for gurtsiden av sveisen.

Applikasjonen utfører utmattingsanalysen på flere måter, alle innenfor hot spot-metoden. Dette fører til at hvert ledd får flere utmattingsverdier, noe som gir basisen for en sensitivitetsanalyse av hot spot-metoden. Felles for alle måtene er lastsimuleringene, bruken av hot spot-metoden, rainflow-telling, S-N kurve og Palmgren-Miner-regelen. Dette blir forklart i kapittel 2. De har også til felles generelle festeforhold, festeparameteret for gurtrørene satt til 0.7, og i leddene som har to avstivningsrør er det laster i begge.

Variasjonene består av parameteret *L* som er brukt i stresskonsentrasjonsfaktor-likningene, rekkefølgen på når utmattingen i tilknytning ett hot spot blir beholdt mens resten blir ekskludert, totalt antall hot spots rundt omkretsen av sveisen, og valget angående hvilke likninger man bruker for stresskonsentrasjonsfaktoren i kronen for aksiallast. Dette valget angående stresskonsentrasjonsfaktor og tilhørende likninger står mellom en versjon som er utelukkende geometrisk, og to versjoner som inneholder nominell spenning og gjør opp for lokal leddfleksibilitet. I denne masteroppgaven er alle valgmuligheter evaluert.

Kun Y-ledd er påvirket av variasjonene i *L*-parameteret etter en viss grense, men inntil denne grensen er nådd påvirker det alle leddene. Dette er fordi Y-leddene er de eneste, sett i sammenheng med den analyserte konstruksjonen og valgene tatt, som har stresskonsentrasjonsfaktorer som inneholder *L*.

K-ledd er de som ble mest påvirket av å ekskludere alle hot spotene bortsett fra det med maksimal utmatting senere i analysen, sammenlignet med å ekskludere dem tidligere. Når de blir ekskludert tidligere, er den endelige utmattingsverdien bygget opp kun av maksimale verdier, mens den andre fremgangsmåten estimerer utmatting for alle hot spot hver for seg, før maksimum verdi er den eneste som blir beholdt. Disse er i denne masteroppgaven henvist til som *estimation approach*.

Det at K-leddene viser mest forskjell mellom de to fremgangsmåtene indikerer at hot spotet mest utsatt for utmatting varierer mer blant K-leddene enn i de to andre leddtypene.

X-ledd og K-ledd er begge like påvirket av antallet hot spot man velger å bruke. Når man økte antall hot spot fra 8 til 16, ga dette for flere ledd en økningsratio på 16 %, denne ratioen er da funnet ved å dividere resultatet

fått ved 16 hot spots på utmattingen estimert ved å bruke 8 hot spots. Å øke antall hot spots gir enten samme verdi, eller en høyere verdi, fordi når man øker antall hot spot legger man inn nye verdier mellom de som allerede er der.

De valgfrie stresskonsentrasjonsfaktorene på kronen for aksiallast er kun evaluert for Y-ledd. De likningene som inneholder nominell spenning, viser for de fleste leddene en mye lavering utmattingsestimering enn de som kun baseres på geometri, når *L*-verdien er lik 7.2 m eller høyere.

Det noe begrensede parameter-utvalget, på grunn av begrenset mengde med tid, resulterte i en sensitivitetsanalyse som ikke er dekkende nok til å komme med et klart, endelig svar angående den ultimate utmattingsanalysen. Denne oppgaven er derfor tiltenkt å bli brukt, gjerne med den utviklede applikasjonen, som grunnlag for videre sensitivitetsanalyse som kan gi mer kunnskap om den foretrukne fremgangsmåten for en utmattingsanalyse som bruker hot spot-metoden.

Table of Content

Guide to Reader

Some glossary and theoretical explanations.

Brace: beams connecting the legs together.

Chord: the legs in the structure.

Cumulative damage: the ratio between number of times a certain stress range occurs and how many occurrences a structure can handle, summed up.

HSS: hot spot stress, stresses occurring around the circumference at the weld between to beams. It may elsewhere also be called geometric stress or structural stress. [*6*]

SCF: stress concentration factor, shorter version of structural stress concentration factor. [*7*]

The *L* value is always in the form of *meters*. E.g., L8.4 means *L* = 8.4 m.

DNVGL-RP-0005 is in the text noted as 'the Recommended Practice', or 'the RP'.

List of Figures

List of Tables

List of Symbols

α: alpha, a parameter in the SCF equations.

σ: sigma, nominal stress.

1 Introduction

Renewable energy sources are becoming increasingly important. There is much attention around the world regarding how we affect the environment, and the wind turbine is one of the promising technologies for providing green energy. However, while offshore wind turbines have an increased efficiency due to better wind conditions, they are more expensive than onshore wind turbines. This is partly due to them needing a support structure. [1] While the monopile, with its cheaper design and larger knowledge base is the popular choice for such a support structure, the jacket structure has increased functionality. It can support a wind turbine in deeper waters. [8] To increase the usage of jacket structures there is first a need for increased knowledge about this structure as a construction design.

That is the reason for the choice of case for this master thesis - an offshore wind turbine with a jacket structure as support. Hopefully it can be a step in the right direction when it comes to designing solid jacket structures that are also cost efficient.

Offshore wind turbines (OWTs) are designed for a certain lifetime. The service lifetime for an OWT is typically 20 years or 25 years. [9] [1] A part of this design analysis is the fatigue analysis, giving the fatigue damage. A fatigue analysis is based on S-N curves, giving the number of cycles a material can sustain a certain stress. Fracture mechanics is a possible supplement for fatigue lifetime estimation in the event that a crack is discovered. [7] [2]

The fatigue analysis is performed by using one of three S-N curves. The nominal stress S-N curve, the hot spot stress S-N curve or the notch stress S-N curve. The second handles more complicated structures and site conditions than the first, and the third is only for situations where the other methods are inadequate. [6] [7] [2] In this thesis, only the second alternative is used, the hot spot stress S-N curve.

The hot spot stresses (HSSs) can be calculated using a Finite Element (FE) analysis, but the approach used here is the one that uses equations based on extrapolation of the structural stress. [6] [7] These HSS equations describe how the stress is distributed at the welds in a joint. There are some parts of a joint that have much higher stress than the rest, and it is here the fatigue crack is most likely to initiate. [10]

In the HSS equations, there are stress concentration factors (SCFs) multiplied with nominal stresses. The different SCFs concern certain points around the circumference of a weld between two beams, and for certain load types. They are also divided between the brace side and the chord side of the weld. The SCFs in a joint are themselves found using a set of parametric equations. One SCF can have several possible values in one joint, depending on the conditions. These can be the fixity conditions, whether loads occur in one or two braces, and which value for the parameter L that is used. [7]

The HSSs are further used in rainflow counting, which together with the S-N curves give a cumulative fatigue damage. In the estimation of the final fatigue damage that follows, it is optional when to exclude all hot spots that are not local fatigue damage maximums. The number of hot spot stresses to consider is also optional. While it is common to use eight HSSs per joint weld, it is not a requirement. A closer explanation of the fatigue analysis, specifically using the hot spot stress S-N curve and equations, is found in chapter 2.

This thesis looks into how these points give potentially different fatigue damage, and the purpose of it is to answer these questions:

> *How does the parameter L, the number of hot spots, the approach and choices concerning stress concentration factor equations affect the resulting lifetime fatigue damage? Which factor causes the largest differences?*

The choices concerning stress concentration factor equations is partially whether or not to include local joint flexibility in the fatigue analysis through the SCFs. Notice that this is only partially, because another important

factor is whether or not to let the *L* parameter affect the fatigue analysis. Joint flexibility has been proved to have an effect on an offshore jacket model using finite element models, and is for important cases recommended to include in the fatigue analysis. *[11]*

An application was developed to help answer these questions. The application was made to work together with the simulation program FEDEM WindPower (Version R7.1.4., Fedem Technology AS, Trondheim), to collect information from a wind turbine model, extract results from load simulations and estimate fatigue damages based on the model, the load simulations and selected input values and estimation approaches.

There are some limitations. First, this paper is the master thesis belonging to the marine structural engineering programme, not programming. Lack of programming knowledge have led to things taking more time than necessary; causing limitations to how many variations and calculations there was time for. Second, some factors that would have impacted the fatigue analysis had to be removed from consideration, as they would have made the scope of the task too large. [2] This affects the potential level of detail and accuracy of the sensitivity analysis, but the achieved results still make for a relevant contribution by considering the factors that are most left to individual design choices.

The OWT used is an UpWind design basis used in Phase I of the Offshore Code Comparison Collaboration Continuation (OC4) project. [4] The jacket structure supports the NREL 5-MW reference wind turbine. [5] This is a generic model, and this non-commercial design includes simplifications such as only one element between each joint. This results in fatigue damage estimations that would not occur in an actual design analysis, so the question as to whether the joints can resist fatigue throughout the lifetime or not is therefore not the most interesting one. The part that is interesting is the *differences* caused by different approaches and parameters.

The Recommended Practice published by DNV GL AS, DNVGL-RP-0005 *Fatigue Design of Offshore Steel Structures*, has provided the background used for programming the application and finding parameters and approaches to compare. The next chapter explains the fatigue analysis procedure and all calculations implemented, with this Recommended Practice as the starting point. [7]

The chapter that follows shows how this master thesis' question has been answered, regarding the jacket structure which is analysed, what choices that was made, and the application programmed and used for the calculations. Then follows the results, before a summary and discussion concerning these results, ending with conclusions and recommendations for further work. This is not a simple topic that can be completely answered with one correct answer after 5 months of work, but the work described in the thesis is a beginning.

2 Fatigue Analysis of an Offshore Wind Turbine (OWT) With Tubular Joints

This chapter will summarise and explain the basic elements of a fatigue analysis that uses the hot spot stress method.

2.1 Limit State and Design Load Cases (DLCs)

Offshore structures are designed with respect to ultimate limit state (ULS) and fatigue limit state (FLS). This means that they have to withstand extreme loads and are designed so that fatigue damage will occur only after a certain lifetime.

Offshore wind turbines (OWTs) are highly dynamic, meaning they move around a lot. This is due to the wind and movement of the ocean they are standing in, and to being coupled to a wind turbine which is rotating most of the time. The loads are modelled as (quasi)periodic cycles, and due to this cyclic loading an OWT is prone to fatigue, which is why fatigue damage is the usual design driving factor. [2]

For environmental loads in fatigue analysis, the characteristic load shall be based on the expected load history, for both temporary and operating design conditions. [12] Wind and waves are two of the three environmental loads, the third one is earthquakes. It is the first two loads that causes cyclic loading, which can lead to cumulative damage. Cumulative damage because of cyclic loading is an example of a fatigue limit state, the point before which the structure can be expected not to fail from cyclic loading. [12] [9] [13] [14]

The design load cases (DLCs) DLC 1.2 (operational status) and DLC 6.4 (parked) are the most important ones concerning fatigue damage estimation. They are briefly introduced in Table 1, and more detailed descriptions can be found in Table 4-5 in the offshore standard DNV-OS-J101. [15]

V_{in} is the cut-in wind velocity, which is lowest wind velocity that the turbine is rotating in. V_{out} is the cut-out wind velocity, and this is the upper limit for wind velocities that the turbine is rotating in. They both apply to steady wind without turbulence. [16]

$U_{10,hub}$ is the 10-minute mean wind velocity at the hub height. The hub height is the height above the terrain surface, which for an offshore wind turbine is the mean sea level (MSL). $U_{10,50-yr}$ is the reference wind velocity, which is the 10-minute mean wind velocity at hub-height, with a 50 year return period. The reference wind velocity depends on the site that the structure is to be designed for. [15] [16] [17]

Table 1: Relevant information about two design load cases in fatigue limit state

Load case	Design situation	Wind condition	Wave condition	Limit state
1.2	Power production	Normal Turbulence Model. Wind climate: $V_{in} < U_{10,hub} < V_{out}$	Normal Sea State: H_S according to joint probability distribution of H_S, T_P and $U_{10,hub}$	FLS
6.4	Parked	Normal Turbulence Model. Wind climate: $U_{10,hub} < 0.7U_{10,50-yr}$	Normal Sea State: H_S according to joint probability distribution of H_S, T_P and $U_{10,hub}$	FLS

2.2 Local Joint Flexibility (LJF)

In members of a structure, the brace loading can cause local deformation of the chord wall, and this leads to local joint flexibility (LJF). When a joint shows flexibility, it means that it is not completely rigid. [18] [2] Local joint flexibility may cause braces to rotate, which will get a reaction from the structure, giving additional moments in both chord and brace. [14] In other words, local joint flexibility affects global response. [9]

3

Local joint flexibility can for tubular joints be included in the design analysis by using Buitrago's parametric expressions. These give local joint flexibilities of brace ends for the three actions as mentioned later in sub chapter 2.3 – axial, in-plane and out-of-plane. The LJFs depends on the joint type. [9]

Local joint flexibility can also be included in the SCFs. Since LJF is directly related to loading, these equations use the nominal stress in both the chord and the brace as input, in addition to geometric information. [7] More theory about these SCFs is found in the next sub chapter.

2.3 Stress Concentration Factors (SCFs)

Built structures are not perfectly smooth all over, unlike models used when designing and planning. Irregularities can be due to e.g. welds and notches, and it is at these places that cracks caused by fatigue are most likely to occur. [2] [19] [20] [14] These irregularities are accounted for in calculations using structural stress concentration factors, also more simply called – stress concentration factors. [19] [20] [14]

When exposing a model to load simulations and extracting the load reactions, one good method for finding the nominal stresses is to use classic beam theory. While the nominal stresses take into account the macro-geometric effect, they do not include stress concentration due to irregularities in the structure. [6] [20] Stress concentration is the phenomenon of a structure consisting of tubular beams showing higher stresses in the joints than in other parts of the structure. A stress concentration factor is the dimensionless ratio between the peak stress at the source for irregularity and the nominal stress, and is a crucial part of the hot spot stress equations [19]

By exposing a model to load simulations, extracting the load reactions and calculating SCFs, you get stresses most likely to occur at these irregularities at the welds and notches. [20] For fatigue analysis, the hot spot stress method is the common one. The stresses most likely to occur at the irregularities are called hot spot stresses, and the relation is shown in equation (1). [7] [15] [21] Hot spot stresses are more thoroughly introduced in sub chapter 2.4.

$$\sigma_{hot\ spot} = SCF * \sigma_{nominal} \tag{1}$$

For tubular joints, the SCFs are most commonly derived using parametric equations depending mostly on the geometry of the joint. [21] [7] The Recommended Practice gives the SCFs developed by Efthymiou. [22] [23] [7] These equations differentiate between joint type, which side of the weld one is looking at, and the load type. [7] [24] Three load types are considered, being axial action, in-plane bending and out-of-plane bending. Generally, they all occur in the braces, so usually all relevant nominal stresses in tubular joints originates from the braces. [7] [25]

For joints with long chords, the axial action and in-plane bending in the chord can be included as well. One can look at the brace as being an attachment to the chord, shown in Table A-7, Constructional details 8.-10. in the Recommended Practice. The detail category depends on the thickness of the brace, and this detail category equals the class that this attachment belongs to. The S-N curve corresponding with this class gives the value of the SCF for the attachment, found in Table 2-1 and 2-2 in the Recommended Practice. [7] [19] [21] [26] More about this attachment is in sub chapter 2.4.

As introduced in sub chapter 2.2, LJF can also be included in the SCFs. The SCFs applicable are only those for axial load in the crown, in joints with general fixity conditions and load in one brace only. Figure 1 in the next sub chapter shows the crown positions in a joint. There are two SCF equations regarding this, one SCF for the chord side of the weld, and one SCF for the brace side. These two equations are found in Appendix B in the Recommended Practice as equation (6b) for the chord side, and equation (7b) for the brace side. These equations that account for LJF do not contain the α parameter, nor are they connected to short chord correction factors. [7]

As long as the constraints mentioned in the last paragraph are met, the SCFs in the last paragraph applies to all joint types, and one can choose whether to use these equations, or the equations based solely on geometry.

When these SCFs are referred to as simply equation (6) and equation (7) it means that which equations one is using is not directly relevant for what is being stated.

The α parameter is stated as a function of L, which is a length parameter. It is not specified which L one should use, and while it is possible to use the same L for the whole fatigue analysis, it is related to the chord lengths. The relation between chord and α is that if α is less than 12, the chord is considered a short chord, and the SCF equation shall be multiplied with a short chord correction factor. This only applies to the SCFs at the saddle for axial load, and the SCFs for out-of-plane bending moment. [7] [22] [23]

The optional equations that include LJF do not include the chord-end fixity parameter C either, the parameter which cover the generalised chord-end fixity conditions concerning axial action. This makes these equations a more general option. Hereby, the geometry and load results give these SCFs, not one's choices concerning the fatigue analysis procedure. [7]

These two things, in addition to the joint flexibility, is why these optional equations often are recommended. They are however more demanding to include in the analysis, because, as mentioned in sub chapter 2.2, they rely on the nominal stress in both chord and brace, hence they cannot be calculated until the load simulation is finished. [7]

Table 2 shows which equations from Appendix B in the Recommended Practice that belongs to which SCFs, in relation to joint type, the number of braces that are exposed to loads, the fixity conditions and which side of the weld that is considered. Only the joint types Y, X and K are included in this thesis.

Table 2 also shows which SCFs that contains the α parameter, and if it is included directly into the equation, due to a short chord correction factor (SCCF), or both. The length parameter L only appears in the SCF equations through this α parameter. Since L can be set constant for one structure, and it is somehow optional what it should be equal to, two persons can correctly perform a fatigue analysis using different SCFs. All expressions for the input variables and parameters are found in Appendix B in the Recommended Practice. [7]

The different SCFs are all represented in Table 2 using abbreviations. ASch and ASbr means SCF at the saddle for axial load. ACch and ACbr stands for SCF at the crown for axial load. MIPch and MIPbr concerns SCF for in-plane bending moment, whilst MOPch and MOPbr concerns out-of-plane bending moment. All loads are in the brace, and 'ch' and 'br' stands for which side the reaction relates to, 'ch' meaning chord, 'br' meaning brace. [7]

A gap joint is a K-joint that has some space between the two braces where they both meet the chord. For an overlapping K-joint the braces are connected to each other as well, not only to the chord. [7]

Table 2: Overview of the different SCFs in Y-, X- and K-joints

Joint type	Number of braces with loads	Fixity conditions, chord ends	SCF	Equation number in the RP	α in the equation	α in the SCCF
Y						
	1 brace	Fixed	ASch	(1)		|
			ACch	(2)	|	
			ASbr	(3)	|	|
			ACbr	(4)	|	
		General	ASch	(5)	|	|
			ACch	*(6a)*	|	

5

					(6b)		
			ASbr		(3)	|	|
			ACbr		*(7a)*	|	
					(7b)		
			MIPch		(8)		
			MIPbr		(9)		
			MOPch		(10)		|
			MOPbr		(11)		|
X							
	2 braces	Fixed	ASch		(12)		|
			ACch		(13)		
			ASbr		(14)		|
			ACbr		(15)		
		Pinned	ASch		(12)		|
			ACch		(13)		
			ASbr		(14)		|
			ACbr		(15)		
			MIPch		(8)		
			MIPbr		(9)		
			MOPch		(16)		|
			MOPbr		(17)		|
	1 brace	Fixed	ASch		(18)	|	|
			ACch		*(6a)*	|	
					(6b)		
			ASbr		(19)	|	|
			ACbr		*(7a)*	|	
					(7b)		
		Pinned	ASch		(18)	|	|
			ACch		*(6a)*	|	
					(6b)		
			ASbr		(19)	|	|
			ACbr		*(7a)*	|	
					(7b)		
			MIPch		(8)		
			MIPbr		(9)		
			MOPch		(10)		|
			MOPbr		(11)		|
K							
	2 braces		Asch ACch		(20)		
			ASbr ACbr		(21)		
			MIPch		(8)		
			MIPbr	Gap joint	(9)		
				Overlap	(22)		
			MOPch		(23)		|
			MOPbr		(24)		|

6

		ASch	(5)	|	|
		ACch	(6a)	|	
			(6b)		
		ASbr	(3)	|	|
1 brace		ACbr	(7a)	|	
			(7b)		
		MIPch	(8)		
		MIPbr	(9)		
		MOPch	(25)		|
		MOPbr	(26)		|

2.4 Hot Spot Stresses (HSSs)

The hot spot stress method is a common approach for a fatigue analysis. As explained in sub chapter 2.3, a SCF gives the relation between the nominal stress occurring in an ideal model, and the hot spot stress. The SCF takes into account how the geometry affects the stress distribution, and by using an S-N curve later in the fatigue analysis, also the stress concentration due to the weld is implemented in the fatigue analysis. [7] [14]

One way to estimate hot spot stresses (HSSs) is to use influence functions. The method used in this thesis is superposition of stresses, and it is this method that will be explained further. [22] [7]

In a joint one looks at hot spots around the intersection, on both the chord and the brace side. [26] Figure 1 shows the crown and saddle points. [23] By extrapolating the nominal stresses occurring right outside the area not affected by the geometry of the weld, and sum up the single stress components after multiplying them with corresponding SCF, one finds the hot spot stress. The single stress components consists of axial action at the crown and saddle, and bending in-plane and out-of-plane, as mentioned in sub chapter 2.3. In points between these four, the axial action is linearly interpolated, and the bending is variated sinusoidal. [7]
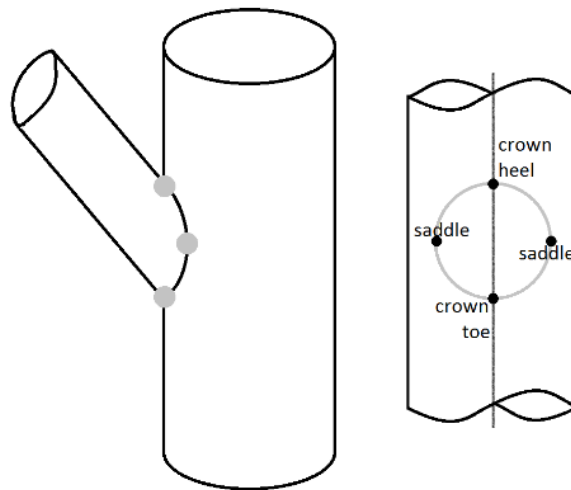
Figure 1: Hot spots in a tubular joint, crown and saddle positions

The Recommended Practice gives equations corresponding to eight hot spots, and it explains how to derive equations for intermediate points. The equations consist of SCFs, nominal stresses and variables. [7] Equation (3) shows a skeleton of these equations, which are to be used together with the variable skeleton shown in equation set (2). They are written here in a programming way, but can also be used without programming.

The equations are most compatible when the total number of hot spots that can be divided by eight, apart from that the number of hot spots is arbitrary. If one were to use 12 hot spots together with this equation set one

7

would not get the saddle points, because the hot spots are divided with equal distance around the whole circumference, starting at the crown heel.

The equations differ whether it is being calculated on the chord side or the brace side of the weld. All equations include nominal stresses in the brace, multiplied with corresponding SCF – chord SCF on the chord side, brace SCF on the brace side. [7] In addition, when looking at the joint as the brace being an attachment to the chord, the HSS equations on the chord side also contains nominal stress on the chord side, multiplied with the attachment SCF that is described in the previous sub chapter. [7] [19] [21] [26]

The variables shown in equation (2) all have a length equal half the number of hot spots, the latter noted as *nHS*. Equations (2) and (3) uses zero-based index. [27] If e.g. one is using MATLAB, the start and end indexes should be one integer higher to make them fit a one-based index. [28]

$$
\begin{aligned}
varAtt &= \left[0:1:\frac{nHS}{4}:1:\left(\frac{nHS}{2}-1\right)\right] \\
varAS &= \left[0:1:\frac{nHS}{4}:-1:1\right] \\
varAC &= \left[\frac{nHS}{4}:-1:0:1:\left(\frac{nHS}{4}-1\right)\right] \\
varMIP &= \left[\frac{nHS}{2}:-2:0:2:\left(\frac{nHS}{2}-2\right)\right] \\
varMOP &= \left[0:2:\frac{nHS}{2}:-2:2\right]
\end{aligned}
\tag{2}
$$

By putting the equation skeleton into a loop with laps equal one fourth of the total number of hot spots, one can easily calculate HSSs with varying amount of hot spots without a lot of changes for each possibility. In equation (3), *iHS* indicates which hot spot one is looking at, and the different σ variables, are the nominal stress time series.

By setting *nHS* equal to 8, one would for the brace side get the same equations as those given in the Recommended Practice.

$$
\begin{aligned}
HSSbrace_{iHS} &= \frac{4.0}{nHS}(varAS_{iHS} * SCF_{AS\,brace} + varAC_{iHS} * SCF_{AC\,brace})\sigma_{X\,brace} + \sin\left(\frac{varMIP_{iHS} * \pi}{nHS}\right)SCF_{MIP\,brace} \\
&\quad * \sigma_{MY\,brace} - \sin\left(\frac{varMOP_{iHS} * \pi}{nHS}\right)SCF_{MOP\,brace} * \sigma_{MZ\,brace}
\end{aligned}
$$

$$
\begin{aligned}
HSSbrace_{iHS+\frac{nHS}{4}} &= \frac{4.0}{nHS}\left(varAS_{iHS+\frac{nHS}{4}} * SCF_{AS\,brace} + varAC_{iHS+\frac{nHS}{4}} * SCF_{AC\,brace}\right)\sigma_{X\,brace} \\
&\quad - \sin\left(\frac{varMIP_{iHS+\frac{nHS}{4}} * \pi}{nHS}\right)SCF_{MIP\,brace} * \sigma_{MY\,brace} - \sin\left(\frac{varMOP_{iHS+\frac{nHS}{4}} * \pi}{nHS}\right)SCF_{MOP\,brace} \\
&\quad * \sigma_{MZ\,brace}
\end{aligned}
\tag{3}
$$

$$
\begin{aligned}
HSSbrace_{iHS+\frac{nHS}{2}} &= \frac{4.0}{nHS}(varAS_{iHS} * SCF_{AS\,brace} + varAC_{iHS} * SCF_{AC\,brace})\sigma_{X\,brace} \\
&\quad - \sin\left(\frac{varMIP_{iHS} * \pi}{nHS}\right)SCF_{MIP\,brace} * \sigma_{MY\,brace} + \sin\left(\frac{varMOP_{iHS} * \pi}{nHS}\right)SCF_{MOP\,brace} * \sigma_{MZ\,brace}
\end{aligned}
$$

$$HSSbrace_{iHS+\frac{3*nHS}{4}}$$
$$= \frac{4.0}{nHS}\left(varAS_{iHS+\frac{nHS}{4}} * SCF_{AS\ brace} + varAC_{iHS+\frac{nHS}{4}} * SCF_{AC\ brace}\right)\sigma_{X\ brace}$$
$$+ \sin\left(\frac{varMIP_{iHS+\frac{nHS}{4}} * \pi}{nHS}\right)SCF_{MIP\ brace} * \sigma_{MY\ brace} + \sin\left(\frac{varMOP_{iHS+\frac{nHS}{4}} * \pi}{nHS}\right)SCF_{MOP\ brace}$$
$$* \sigma_{MZ\ brace}$$

$$HSSchord_{iHS} = \cos\left(\frac{varAtt_{iHS} * 2.0 * \pi}{nHS}\right)SCF_{Att} * (\sigma_{X\ chord} + \sigma_{MY\ chord})$$
$$+ \frac{4.0}{nHS}(varAS_{iHS} * SCF_{AS\ chord} + varAC_{iHS} * SCF_{AC\ chord})\sigma_{X\ brace}$$
$$+ \sin\left(\frac{varMIP_{iHS} * \pi}{nHS}\right)SCF_{MIP\ chord} * \sigma_{MY\ brace} - \sin\left(\frac{varMOP_{iHS} * \pi}{nHS}\right)SCF_{MOP\ chord} * \sigma_{MZ\ brace}$$

$$HSSchord_{iHS+\frac{nHS}{4}} = \cos\left(\frac{varAtt_{iHS+\frac{nHS}{4}} * 2.0 * \pi}{nHS}\right)SCF_{Att} * (\sigma_{X\ chord} + \sigma_{MY\ chord})$$
$$+ \frac{4.0}{nHS}\left(varAS_{iHS+\frac{nHS}{4}} * SCF_{AS\ chord} + varAC_{iHS+\frac{nHS}{4}} * SCF_{AC\ chord}\right)\sigma_{X\ brace}$$
$$- \sin\left(\frac{varMIP_{iHS+\frac{nHS}{4}} * \pi}{nHS}\right)SCF_{MIP\ chord} * \sigma_{MY\ brace} - \sin\left(\frac{varMOP_{iHS+\frac{nHS}{4}} * \pi}{nHS}\right)SCF_{MOP\ chord}$$
$$* \sigma_{MZ\ brace}$$

$$HSSchord_{iHS+\frac{nHS}{2}} = -\cos\left(\frac{varAtt_{iHS} * 2.0 * \pi}{nHS}\right)SCF_{Att} * (\sigma_{X\ chord} + \sigma_{MY\ chord})$$
$$+ \frac{4.0}{nHS}(varAS_{iHS} * SCF_{AS\ chord} + varAC_{iHS} * SCF_{AC\ chord})\sigma_{X\ brace}$$
$$- \sin\left(\frac{varMIP_{iHS} * \pi}{nHS}\right)SCF_{MIP\ chord} * \sigma_{MY\ brace} + \sin\left(\frac{varMOP_{iHS} * \pi}{nHS}\right)SCF_{MOP\ chord} * \sigma_{MZ\ brace}$$

$$HSSchord_{iHS+\frac{3*nHS}{4}}$$
$$= -\cos\left(\frac{varAtt_{iHS+\frac{nHS}{4}} * 2.0 * \pi}{nHS}\right)SCF_{Att} * (\sigma_{X\ chord} + \sigma_{MY\ chord})$$
$$+ \frac{4.0}{nHS}\left(varAS_{iHS+\frac{nHS}{4}} * SCF_{AS\ chord} + varAC_{iHS+\frac{nHS}{4}} * SCF_{AC\ chord}\right)\sigma_{X\ brace}$$
$$+ \sin\left(\frac{varMIP_{iHS+\frac{nHS}{4}} * \pi}{nHS}\right)SCF_{MIP\ chord} * \sigma_{MY\ brace} + \sin\left(\frac{varMOP_{iHS+\frac{nHS}{4}} * \pi}{nHS}\right)SCF_{MOP\ chord}$$
$$* \sigma_{MZ\ brace}$$

When increasing the number of hot spots, the resulting fatigue damage estimate will either stay the same, or increase. It will not decrease, because the final fatigue damage estimate uses the maximum value, and when increasing the number of hot spots, one does not replace the already existing hot spots, but one *adds* hot spots. This means that if the value stays the same after one has performed a new analysis where the only difference is more hot spots, the governing hot spot was already a part of the hot spots evaluated. Equally, if the value increases, the new governing hot spot is amongst the new, intermediate hot spots.

2.5 Rainflow Counting and S-N curve

One of the common design approaches for performing fatigue analysis, is to use S-N curves, as mentioned in sub chapter 2.4. These curves come from fatigue tests, and they give a structure's resistance against fatigue, shown by the number of cycles it can handle for a certain stress range. Fatigue initiation comes from a crack starting to grow, and when the crack is through the thickness of the structural element, fatigue failure occurs. [12] [14] [7]

Cycle counting shall be performed on the stress time history, and one of the two methods that are the most accepted ones, is the rainflow counting method. [2] This gives a stress range history and the number of cycles per stress range. [10] It is this stress range history that is used for the S-N curve, and also for the cumulative damage estimation, see sub chapter 2.6. [9]

For constant amplitude loading, the stress ranges are consistent, and for design analysis one can simply consider the endurance limit stress. This approach is inadequate when it comes to environmental loads, as introduced in sub chapter 2.1. These loads cause large variation amongst the stress ranges, it is therefore recommended to look at the required fatigue life – perform a fatigue analysis. [14] The fatigue lifetime for an OWT is typically 20 years or 25 years. [15] [29] [12] [1]

For S-N classes in air, this endurance limit stress for cut-off stress occurs after 10^7 cycles. [10] In relation to variable amplitude, this limit decreases as the fatigue crack grows. For environmental loads, the slope changes after 10^7 cycles. No fatigue occurs below the cut-off stress, and the stress ranges relevant for fatigue analysis are those who contribute to fatigue damage in the structure. [12] [14]

For welded joints, the S-N curve takes into account the thickness effect, depending on whether the thickness is larger than a given reference thickness or not. For attachment joints, the thickness can be replaced by an effective thickness, also this depending on its ratio to the reference thickness. [7]

2.6 Cumulative Damage

The *characteristic cumulative damage* multiplied by the load factor equals the *design cumulative damage*. In this case, as the load factor concerning fatigue limit state is equal to one, there is no difference between characteristic cumulative damage and design cumulative damage. [12]

To use the S-N curve to find the cumulative damage, the varying amplitude stress cycles calls for a supplementary rule. The Palmgren-Miner rule, assuming linear relationship between the load and the load effect, can be used for this. [14] [7] [2] For each stress range in one specific load case, the fatigue damage is the number of cycles that occurs in that stress range, divided by the number of cycles the joint can handle.

The value belonging to each stress range can be summed up, [14] giving a fatigue damage value for one load case. The Palmgren-Miner rule is shown in equation (4), exemplified as being the accumulated fatigue damage for one load case, where i indicates the stress range index.

$$D = \sum_i \frac{n_i}{N_i}$$

(4)

Further summation is accepted when several load cases are involved, but for fatigue analysis each load case fatigue damage must also be multiplied with factors concerning site conditions, length of the load case time series and fatigue lifetime. Cumulative damage should be found separately for each connection exposed to fatigue loading in a structure. [9]

For the hot spot method, cumulative damage is found using hot spots. The common approach is to sum up all maximums from each load case. An alternative approach is proposed and explained in chapter 3.3.

3 Fatigue Analysis Application

This master thesis is answering questions regarding fatigue analysis, not programming, but a lot of the work has been to make an application. The application is made with the purpose of being used for fatigue analysis later, not only for this master thesis. It is made to perform fatigue analysis on other constructions as well, but the main focus has been to perform an analysis, with several options, with the UpWind reference jacket introduced in sub chapter 3.1. [4] [5]

3.1 Offshore Wind Turbine Model

The OWT model consists of the UpWind reference jacket used within Phase I of the Offshore Code Comparison Collaboration Continuation (OC4) project, supporting the NREL 5-MW reference wind turbine. [4] [5] This model was already implemented in FEDEM WindPower (Version R7.1.4., Fedem Technology AS, Trondheim). The length of the jacket is 70.15 m, and it is located at clamped rigid mudline 50 m below the mean seal level (MSL). [30]

This jacket is four-legged and is built up by 24 K-joints, 16 X-joints and 16 Y-joints. [30] These are all tubular joints, hence hot spot stress S-N curve class T is used. [7] They have been evaluated as the brace being an attachment to the chord, causing the nominal stresses in the chord to be included in the HSS equations for the chord side. [26] More about this is found in sub chapter 2.3 and sub chapter 2.4.
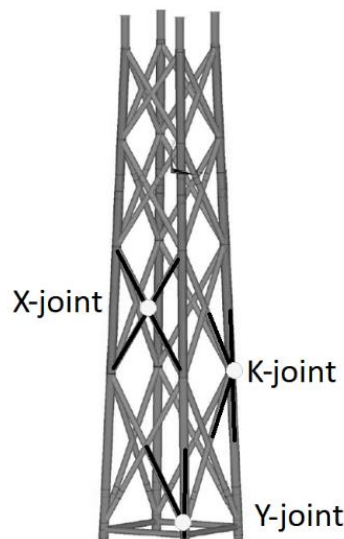
Figure 2: Jacket structure model [30]

K-joints connects two X-joints to the legs, each K-brace belonging to a separate X-joint. [30] All K-joints in this jacket structure are gap joints. This affects the SCFs due to ξ and α, which are explained in Appendix B in the Recommended Practice, and the latter is explained in sub chapter 2.3 as well. In two of the SCF formulas for K-joints used in this thesis, some of the variables are connected to a certain brace. [7]

These SCFs were interpreted as being equal for both braces, except for those parameters that does not show a specific affiliation, regardless of which of the two braces one is finding the belonging SCFs to. At the end of the fatigue damage estimation period, when it was too late to perform all the fatigue analyses again, another interpretation, the correct one, occurred. In Appendix B in the Recommended Practice, it is stated that the equations are for the chord adjacent to brace A, and for brace A. This means that one should swap which brace that belongs to which part of the equation when calculating for brace B. [7]

In this thesis however, the lower brace is used as 'brace A' in Appendix B in the Recommended Practice, and this was the case for both braces in all K-joints. [7]

The X-joints all consists of beams with thickness smaller than the reference thickness. Even though the S-N curve used is the one that takes the thickness effect into account, this has because of the small thickness, given the same values as the basic design S-N curve would give. [7]

In addition, all beams building the X-joints had the same diameter and thickness. There was therefore no obvious telling of which beam that was chord, and which one that was brace. Hence all possibilities were calculated, and the maximum was kept. Meaning that for one X-joint there were four estimated fatigue damage values, contrary to K-joints that only had two values, and Y-joints that only had one value.

Each Y-joint connects only one X-joint to the leg, as opposed to the K-joints. Y-joints are positioned at the top and the bottom of the jacket structure, equally divided. [30] In this thesis the Y-joints are the only ones with load only in one brace, hence the LJF included by the optional equations, see sub chapters 2.2 and 2.3, only affects these joints.

3.2 Load simulation

The DLCs used are DLC 1.2 and DLC 6.4 because, as explained in sub chapter 2.1, they both apply to FLS. [15] [16] In total 15 load cases were simulated, and they covered every other wind velocity between 2 m/s and 30 m/s. The simulation inputs were found in the UpWind Design Basis, and for the UpWind reference jacket model, the cut-in wind velocity is 3 m/s, and the cut-out wind velocity is 25 m/s. [17]

The site condition looked at is the generic deep water site, described in the UpWind Design Basis. From there, the reference wind velocity is found to equal 42.73 m/s. The upper limit for DLC 6.4 is 0.7 times the reference wind velocity, as shown in Table 1, and this was rounded off to 30 m/s. [17]

Therefore, the simulation contained four load cases in DLC 6.4 (2 m/s, 26 m/s, 28 m/s and 30 m/s), and eleven load cases in DLC 1.2.

The load simulation was conducted in FEDEM WindPower (Version R7.1.4, Fedem Technology AS, Trondheim), with analysis time and usable time set to 4 000 seconds. The first 400 were removed in order to remove transients, giving 3 600 seconds, which is the recommended minimum for fatigue analysis. [14] [13] With the time step set to 0.025, this gave time series containing 144 000 points.

3.3 Fatigue Damage Estimation

The flowchart in Figure 3 shows the procedures used for these fatigue analyses. It includes both the common approach, and the alternative approach. These are two approaches that are both within the hot spot stress method.

Common for both approaches is that one first estimates cumulative damage for each weld, each hot spot and each event. Each value is multiplied with the corresponding factor that takes into account the site conditions, length of the load case time series and fatigue lifetime, as explained in sub chapter 2.6. The lifetime chosen is 20 years. One then looks at one weld at a time.

For the common approach, one only keeps the maximum value for each event, cuts thus down the number of hot spots to one, giving for one weld only one value per event. These values are then summed up. This is done for each weld in one joint, and on each side of the weld. E.g. for a K-joint, this would give four potential fatigue damage values. The maximum of these is the final fatigue damage estimation for this joint.

The alternative approach continues with all hot spots. Each hot spot has one value per event, and these values are summed up, giving one value for each hot spot. And it is the maximum of these values that is kept. Also here it is done for each weld, and each side of the weld, giving several potential fatigue damage values for each joint. As in the common method, the maximum is kept as the final fatigue damage estimation for this joint.

When using the alternative approach, it requires more values to be kept. How much more effort this demands depends on how one performs the fatigue analysis. Both approaches have been performed in this thesis, and when building the application, they both required the same amount of coding. It probably did affect the memory usage on the computer while the analysis was running, but how much was never measured.
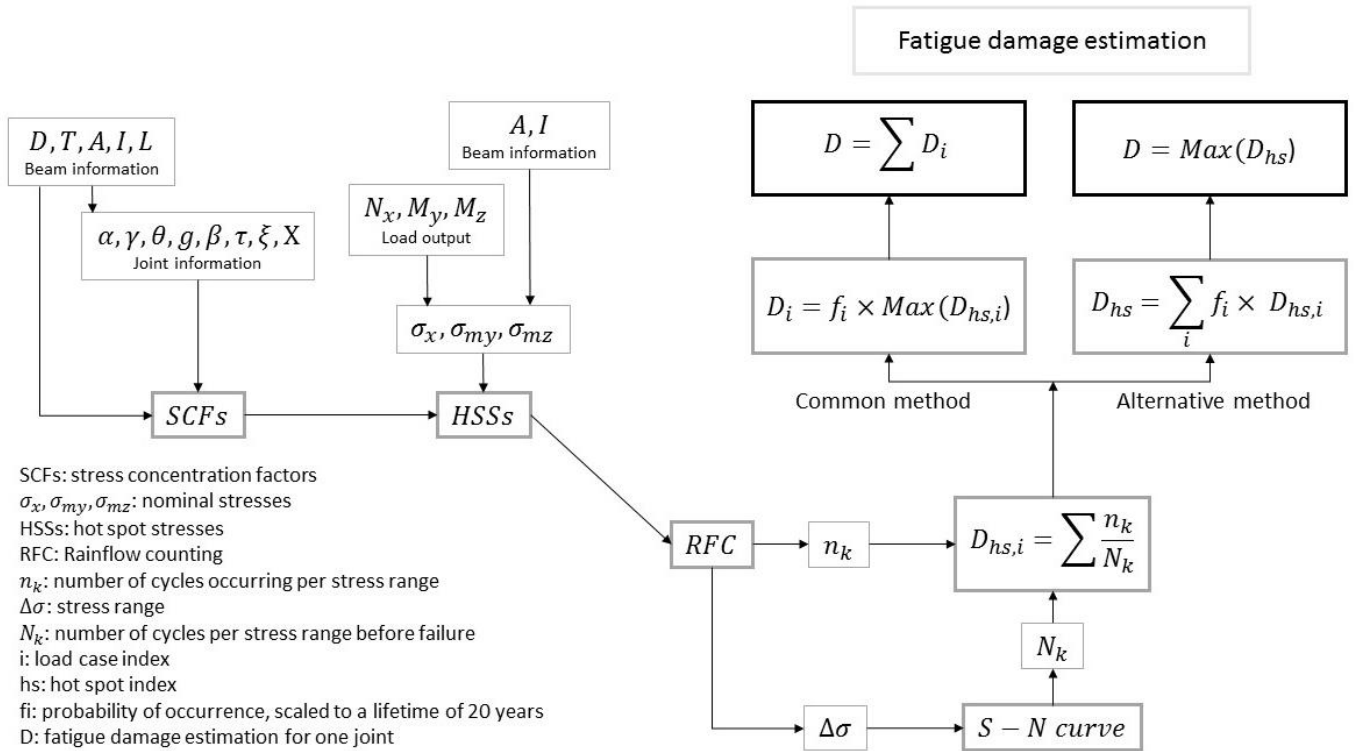
Figure 3: Flowchart showing the procedure used for fatigue damage estimation

It was chosen to set a cut-off value at 1 MPa for the rainflow counting, to reduce the stress range series. This was assumed as okay for a construction of this size, exposed to these load cases. Since these joints have been considered as attachment joints, the thickness effect is included when calculating the S-N curve. [7]

The hot spot stress equations used are those that for the chord side of the weld includes nominal stress in the chord, as explained in sub chapter 2.4 and shown in equation (3). They were implemented in the application using a loop, with the number of laps set to one fourth of the number of hot spots. The nominal stress time series, σ, all covered 3600 seconds, and made HSS time series with equivalent length. This whole loop was run for all load cases for each weld, in each joint. Since all braces in the structure evaluated has a thickness smaller than 25 mm, the attachment SCF equals 1.13 for all joints. [7]

It is stated in sub chapter 2.3 that the brace can only be considered as an attachment for long chords. Whether a SCF is to be multiplied with the short chord correction factor or not, depends on whether α is above the limit at 12 or not, and α is dependent of the L parameter. [7] This thesis perform calculations using L values both small and large, but in all cases the chords are considered long with regards to the brace being an attachment. In this thesis, there is difference between the parameter L used in the SCF equations, which varies, and the geometric length of the chords in the jacket structure, which stay constant through across the fatigue analyses.

This thesis has expanded the equations given in the Recommended Practice, going from 8 hot spots to 256 hot spots. To get an indication whether it is actually beneficial to add hot spots, results have been made corresponding to 8, 16, 32, 64, 128 and 256 hot spots. Previous study shows that increasing the number of hot spots from 8 to 32 for some joints give noticeable differences. [31]

13

The equations including LJF only applies to joints with load action in one brace only. For this thesis, this only occurs in the Y-joints. Fatigue damage for Y-joints have therefore been calculated three times:

> i) equations (6a) and (7a) from Appendix B in the Recommended Practice,
>
> ii) equations (6b) and (7b) based on σ_{my}, nominal bending stress in the chord around local y-axis, and
>
> iii) equations (6b) and (7b) based on σ_{mz}, nominal bending stress in the chord around local z-axis.

Both options concerning equations (6b) and (7b) also includes the nominal axial stress in the brace.

In addition to the LJF addition, also the parameter L varies between different fatigue analyses. The calculations in this thesis are based on 5 different L values concerning K-joints and X-joints, and 8 different L values concerning Y-joints. The SCFs have all been calculated using 59 different L values.

3.4 The Application

A lot of effort was spent on making an application that could easily perform a fatigue analysis in several ways. It is also meant to be used on other structures, but to not spend too much time on programming, and too little time on the fatigue analyses in question, it is somewhat fitted for this jacket structure, because it only includes K-joints, X-joints and Y-joints. It also calculates for all the different number of hot spots, instead of making this an option for the user.

This application works together with FEDEM WindPower (Version R7.1.4, Fedem Technology AS, Trondheim), and it is programmed in the .NET framework using C# programming language.

Figure 4 shows how this application looked. The user must first select the coordinate system that corresponds with the one in the model opened in FEDEM WindPower, the model one wants to perform the analysis on. Choosing the correct coordinate system is necessary for calculating angles in the joints, and when deciding the joint type.

One can then, if one wants to, decide to use another L than the default one, which is 8.4 m. The same is possible with the chord-end fixity parameter C, where the default is set to 0.7. The fixity conditions must be selected, as do the number of braces where loads occur.

The application was also made so that the fatigue analysis could be performed without looking at the brace as an attachment to the chord, and the nominal stress in the chord would then be excluded in the HSS equations.

The part about first and last BaseID is included to make it easier to find the joints that are to be included in the analysis. The BaseID is a parameter found in FEDEM WindPower. When pressing either 'User defined' or 'Default values', the application calculates the SCFs. Concerning equation (6) and equation (7), it is (6a) and (7a) that is calculated here. Of all calculations from this part, six matrices are kept to be used later. Three SCF matrices, one for each joint type, and three matrices with joint information, also these for each joint type.

When the SCFs are calculated, one can go to the next step. iJoint-start and iRow-start makes it possible to choose which joint type and which weld to start with. This was preferable when using equations (6b) and (7b), to be able to start directly at the Y-joints. The HSS equations and fatigue damage estimations are performed inside a large loop. The first step in the loop is the joint type, and this is what iJoint-start is related to. iJoint 0 means K-joint, iJoint 1 means X-joint and iJoint 2 means Y-joint.

The second step in the loop is the weld, which is what iRow-start relates to. K-joints have two welds, due to two braces, and likewise Y-joints only have one weld. Even though also X-joints only have two welds, X-joints had four possibilities. iRow corresponds with the row number in the matrices made in the first part of the application. Fatigue damage on the chord side and on the brace side are both calculated in the same step.

After specifying where to start, one selects which SCF at the crown for axial load that the fatigue estimation should include. By clicking on 'Results', the analysis starts, and the application extracts the results from load simulations conducted in FEDEM WindPower. Due to long time series, the analysis took quite some time. For the jacket structure looked at in this thesis, the total number of rows were 128, and for each of these it

went through 15 load cases and found six time series for each load case. The time series each had 144 000 values, due 3 600 seconds with a time step equal to 0.025 seconds.

When the analysis was finished, the result was an Excel document showing a matrix containing estimated fatigue damage for each joint, for each number of hot spots, for each estimation approach. For K-joints this was a 24×12 matrix, for X-joints and Y-joints the matrix size was 16×12.

These results were afterwards plotted using MATLAB (Version R2016a).
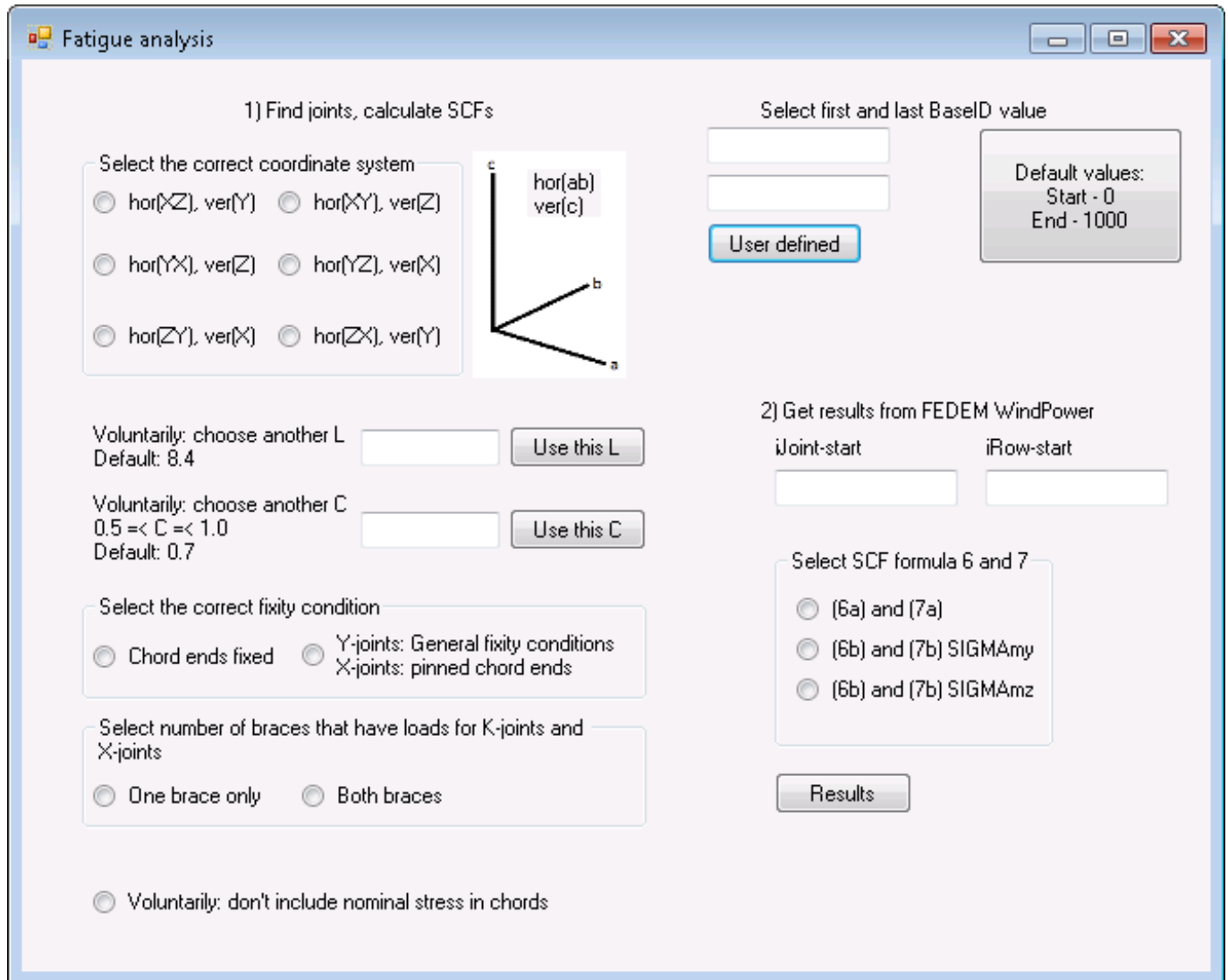
Figure 4: The application used to perform all fatigue analyses

4 Results

This chapter describes the results of the calculations done in the application, what the different fatigue analyses shows. It is allocated by each variation in the fatigue analysis.

The damage values vary between the joints. Figure 5 shows where the different joints are in the jacket model, and this is useful to take a look at for all results shown in this chapter.
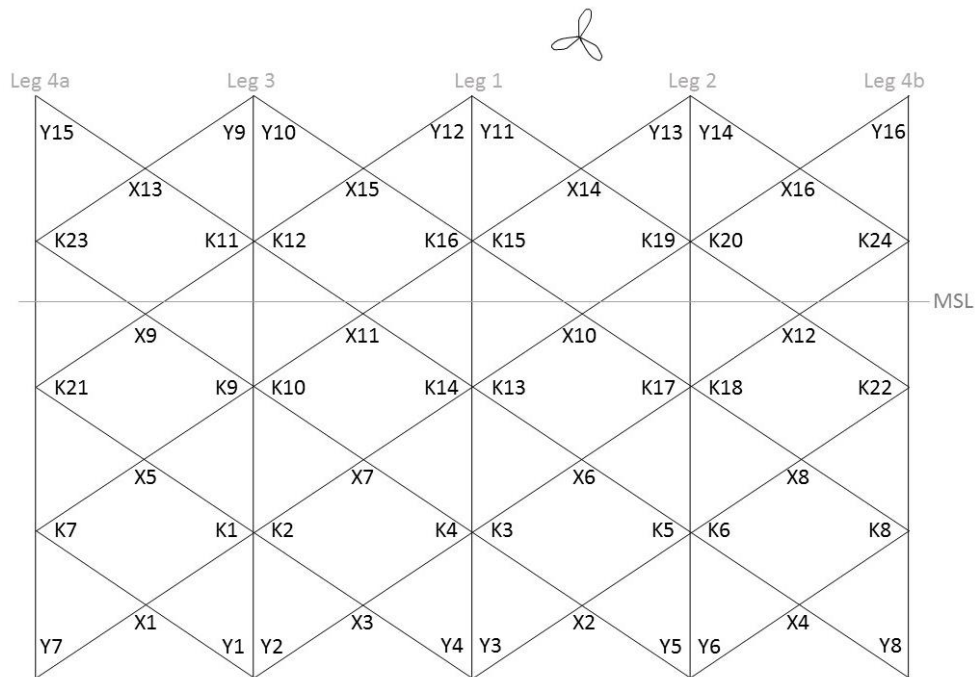
Figure 5: Simplified sketch of the model showing the placement of the different joints

4.1 SCFs

This sub chapter is about how the L value affects the SCFs. In this thesis, all SCFs concern general fixity conditions, and load in both braces in joints that have more than one brace. The SCFs at the crown for axial load are in this chapter found using equation (6a) and equation (7a) from Appendix B in the Recommended Practice. [7]

The SCFs shown in this sub chapter are only those SCFs affected by α. All other SCFs, apart from the optional equations (6b) and (7b) that contains nominal stresses, were constant. The SCFs that were constant are shown in Appendix B.

For the beams in the UpWind reference jacket, the largest chord diameter was 1.2 m, and the corresponding L causing α to meet its limit at 12 is 7.2 m. This was the situation for all K-joint and Y-joints. All the X-joints had a chord diameter equal to 0.8 m, so for these joints α meet its limit when L is equal to 4.8 m. [17] The figures in this sub chapter shows where in the plot that α goes from being below the limit, to being above.

When α is above the limit, the SCF only varies if α is in the equation itself. This is shown in Figure 7, Figure 8, Figure 9, Figure 10, Figure 11, Figure 12 and Figure 13 in sub chapters 4.1.1, 4.1.2 and 4.1.3, along with more description. All SCFs were calculated with L going from 0.8 m to 24 m with a step set to 0.4 m, but because of this linearity, only the SCFs that are affected by the short chord correction factor and keeps varying after the α limit is reached, is shown with all 59 L values, in Figure 11. The rest is only showing L values up to 16.4 m.

All figures mentioned in the previous paragraph have the same limit for the y-axis, to in addition show how the size of the different SCFs is compared to each other.

The short chord correction factors are non-linear, and goes toward 1, exemplified using short chord correction factor F3 in Y-joints, in Figure 6. This explains the shape of the SCF plots.
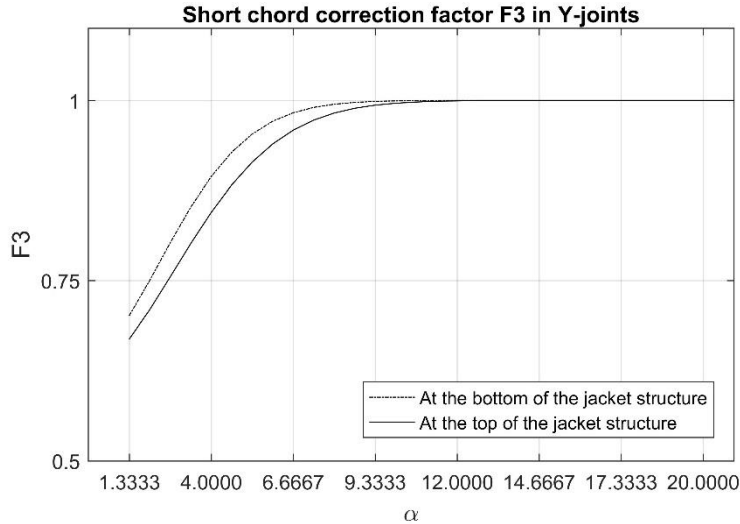
Figure 6: Short chord correction factor F3 for the Y-joints

4.1.1 K-joints

For K-joints, only the SCFs for out-of-plane bending moment is affected by *L*. All joints show the same shape, but values increase, as do the difference between brace side and chord side, when the location height increases. These SCFs are affected by short chord correction factor F4. [*7*]

Figure 7 shows two plots for one joint, because K-joints at the lower part of the structure has different SCFs inside one joint. The difference between the lower weld and the upper weld is because the upper chord and the lower chord does not have the same thickness, and this variable affects several of the expressions in both the chord and the brace equation. The diameter also affects several of the expressions, but for this structure, even though they are different, the difference equals to 1.4×10^{-7}, and is therefore too small to make an impact. Concerning the chord thickness however, the lower chord thickness is 1.4 times the upper chord thickness.

For the lower part of the joint, the SCF for out-of-plane bending moment is higher on the brace side than on the chord side, but for the upper part and both parts in all joints on the other levels, this SCF is lower on the brace side.
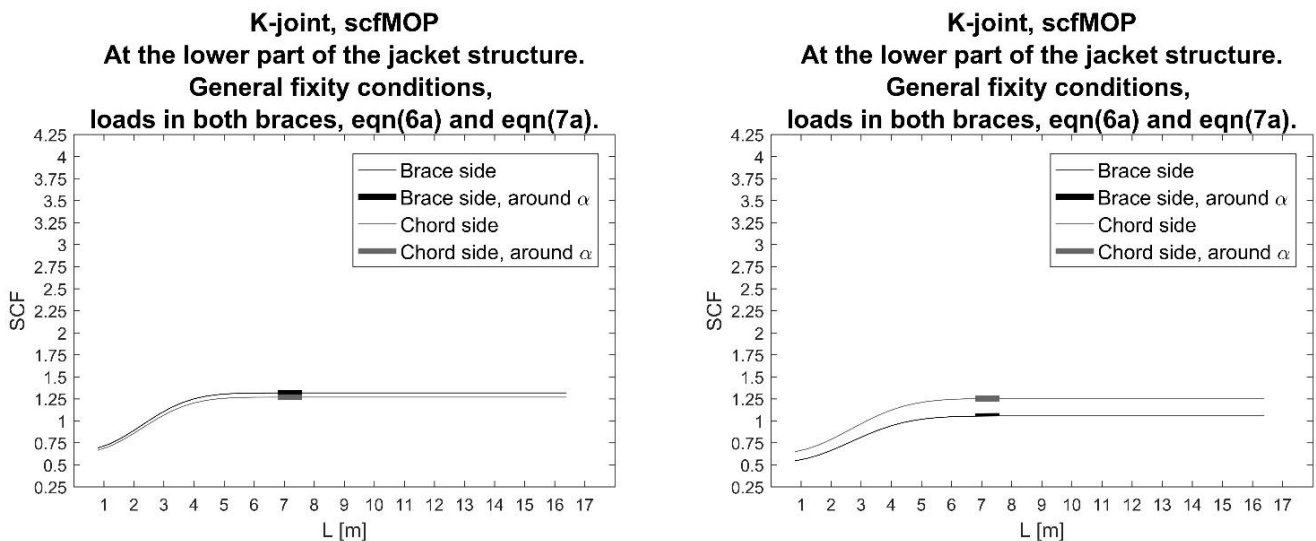
Figure 7: SCFs for out-of-plane bending moment in K-joints. Lower part of the weld to the left, upper part to the right

17

Figure 8 shows the SCFs for out-of-plane bending moment for the two next levels, and for these joints the SCFs did not differ between the upper part and the lower part.
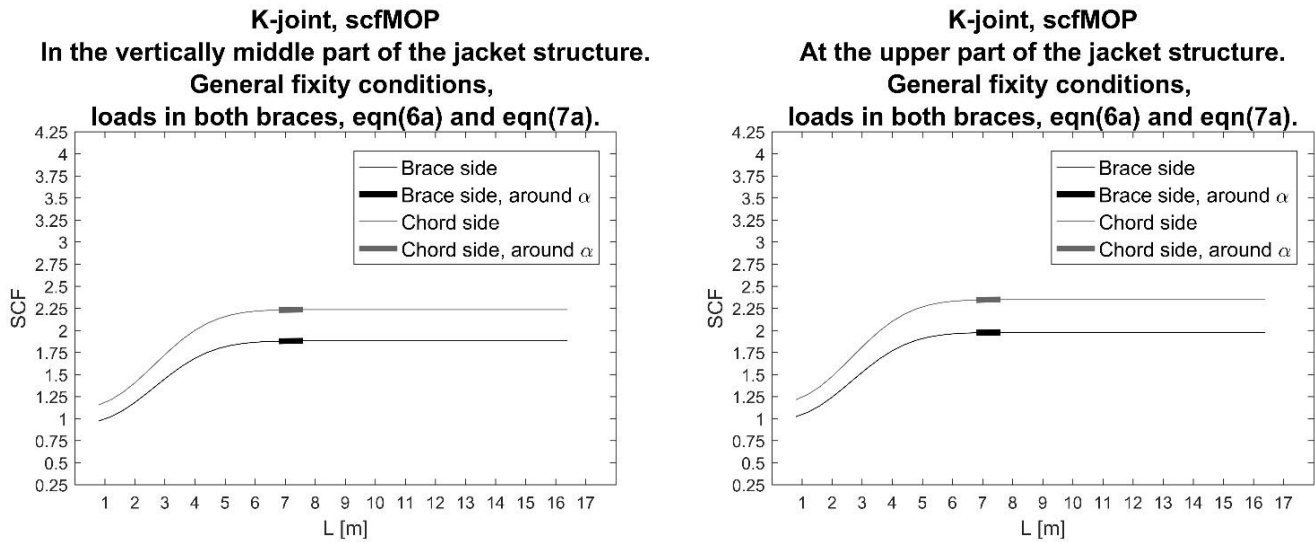
Figure 8: SCFs for out-of-plane bending moment in K-joints

4.1.2 X-joints

The SCFs at the saddle increases together with the location height for all X-joints, as shown in Figure 9 below. This applies to both the chord side and the brace side of the weld. The difference between the joints on different location heights is the angle between chord and brace.

There is also here difference between the angle on the upper side of the joint, and the angle on the lower side, but this difference is too small to be seen in a figure, the largest difference being equal to 0.0003. Figure 9 therefore only uses one plot to represent a whole joint.
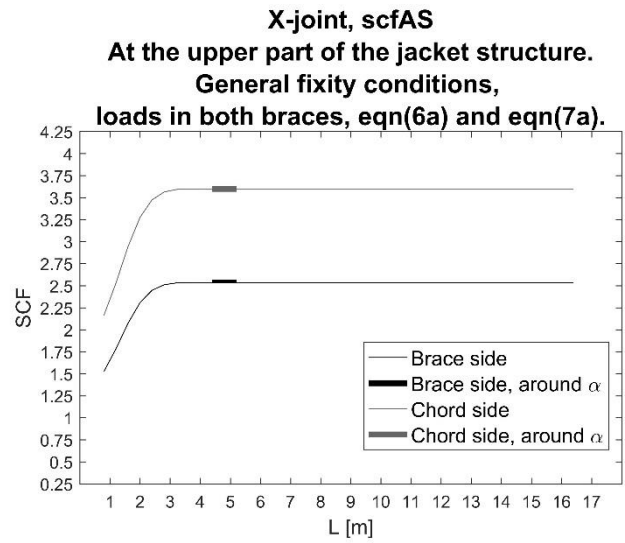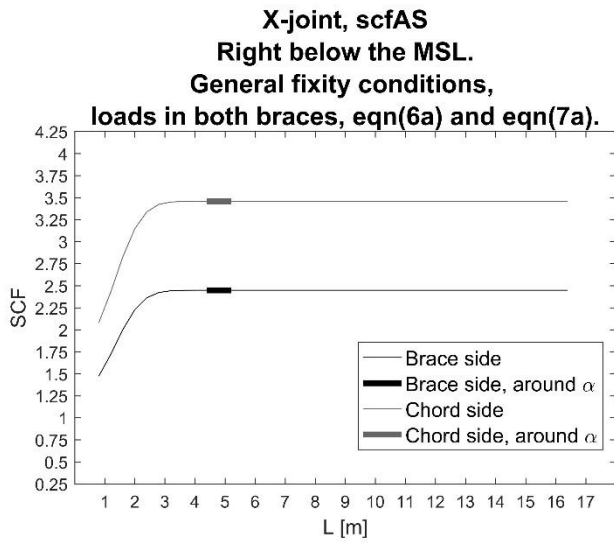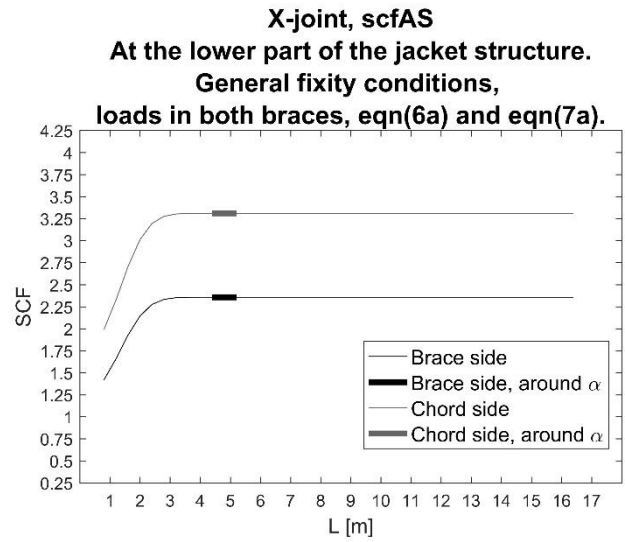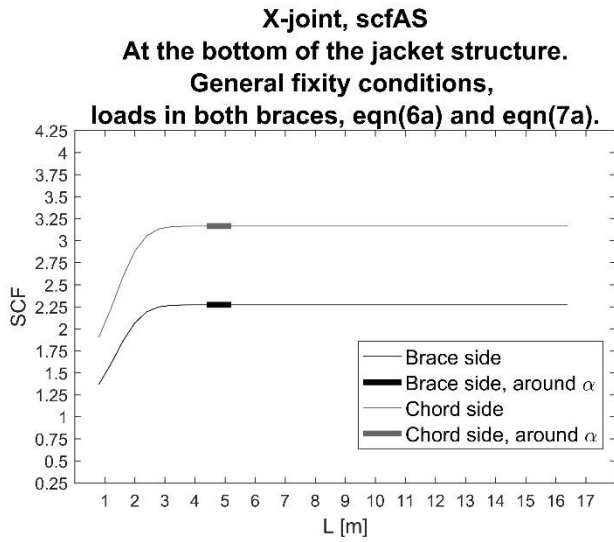
Figure 9: SCFs at the saddle for axial load in X-joints

Concerning the SCFs for out-of-plane bending in the X-joints we see the same trend as for axial loading at the saddle, except that these values are approximately 0.9 lower. The value increases together with the location due to different angle between chord and brace. The differences within one joint are at the maximum 0.0002, so Figure 10 also represents a whole joint with one plot.

It is for these SCFs, for this joint type, that one clearly sees the variation around the α limit, the part that is bold is visibly not linear.
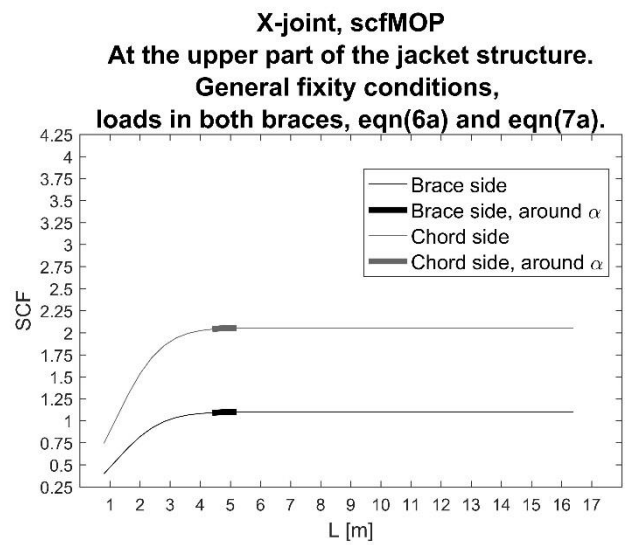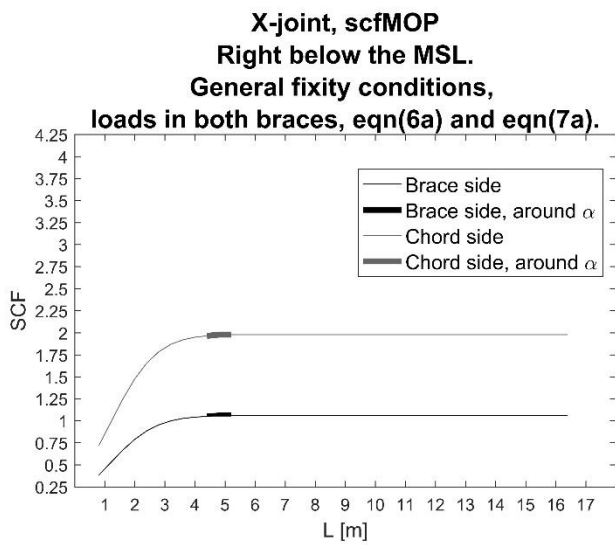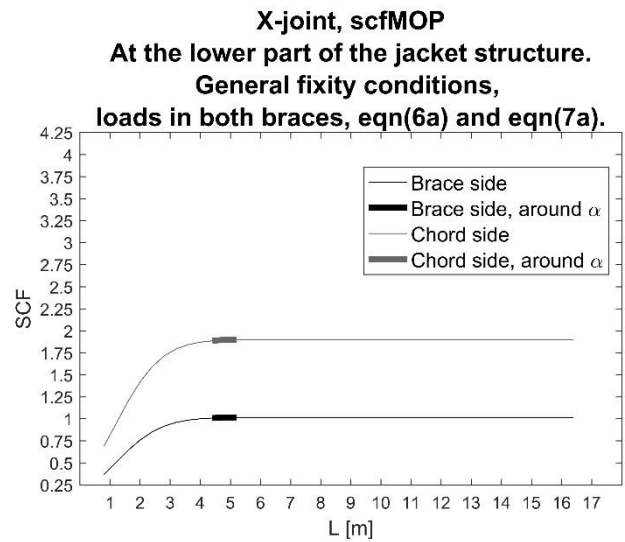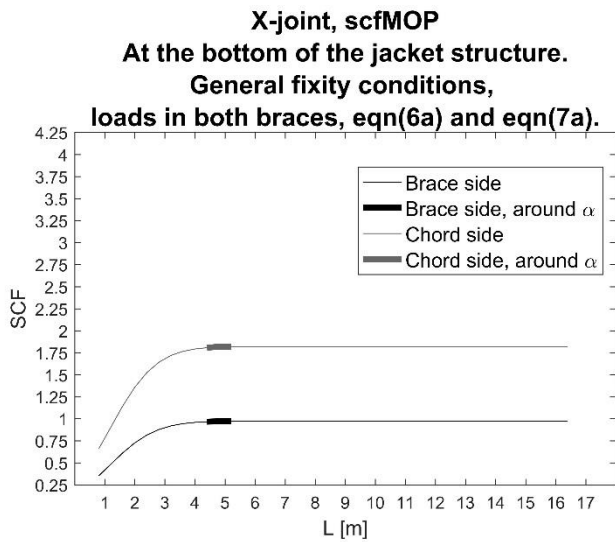
Figure 10: SCFs for out-of-plane bending moment in X-joints

4.1.3 Y-joints

The SCFs related to the Y-joints mainly varies between those belonging to the joints on top of the structure, and those on the bottom. Internally, the variations depend on which load the SCF applies to.

Figure 11 shows how the SCFs for axial load at the saddle point varies due to increasing *L*. The SCF on the chord side increases faster than the SCF on the brace side. For low *L*, they start very close to each other on top of the structure, and the SCF on the chord side quickly gets much larger than the one on the brace side. It is not so clearly shown, but also the SCF on the brace side at the bottom of the jacket structures keeps increasing.

At the bottom of the structure, the SCF on the chord side does not catch up with the SCF on the brace side until *L* is very close to 24 m. This is also difficult to see in the figure, but at the end of the plot belonging to the bottom of the structure in Figure 11, the chord value is slightly higher than the brace value.

20
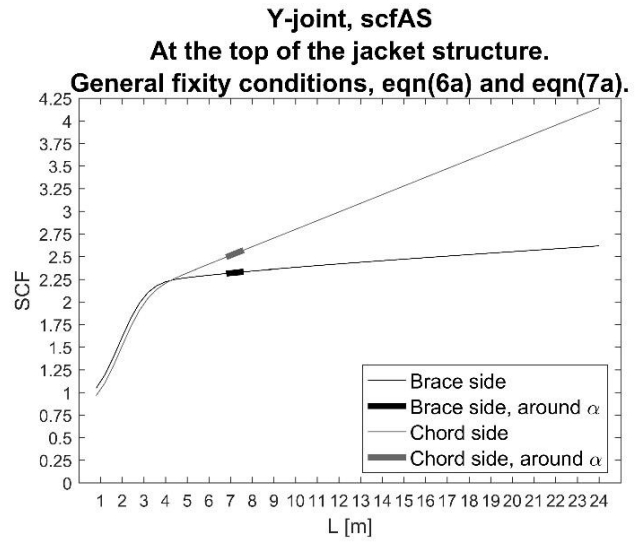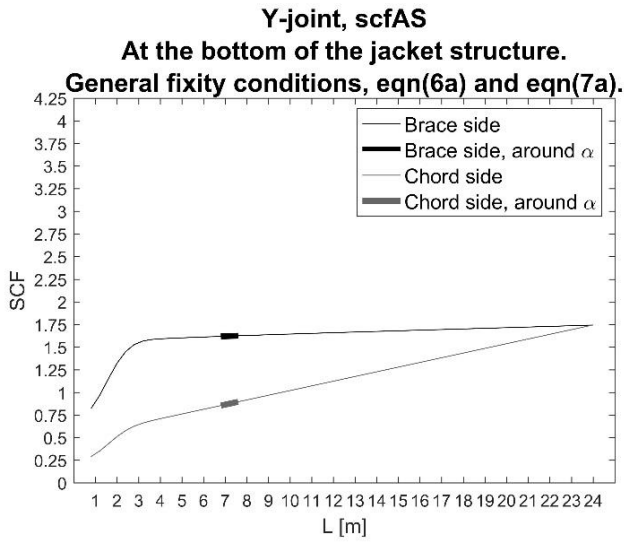
Figure 11: SCFs at the saddle for axial load in Y-joints

The SCFs for out-of-plane bending moment in Y-joints is shown in Figure 12. These SCFs do not contain α in itself, the SCFs are therefore constant after α has reached the limit. The two SCFs, respectively on the brace side and on the chord side, are very close at the bottom of the structure, a difference equal to 0.027, but a bit more apart at the top of the structure, where the difference is 0.338. Both differences are for the L values larger than 7.2 m.
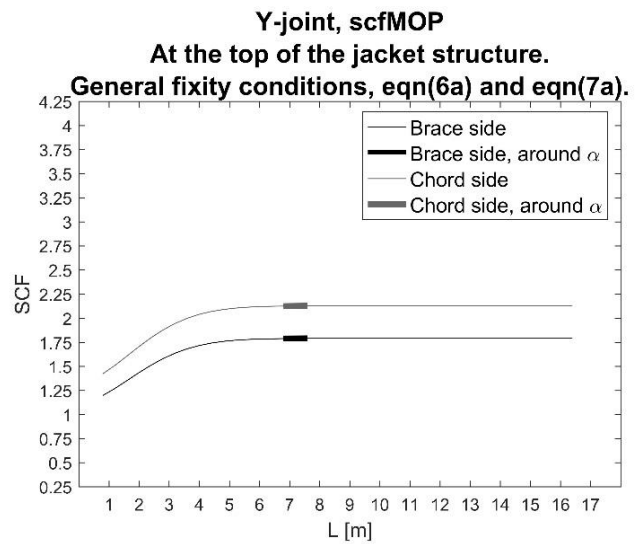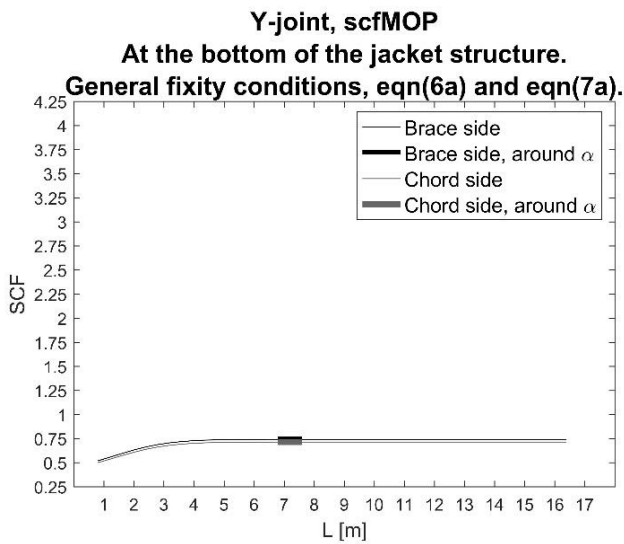
Figure 12: SCFs for out-of-plane bending moment in Y-joints

The SCFs without short chord correction factor, even though they include α and therefore vary along with L, vary linearly. This is shown in Figure 13, for the SCFs at the crown for axial load. It also shows that the increase is steeper for the SCF on the chord side than for the SCF on the brace, the same as for the saddle.
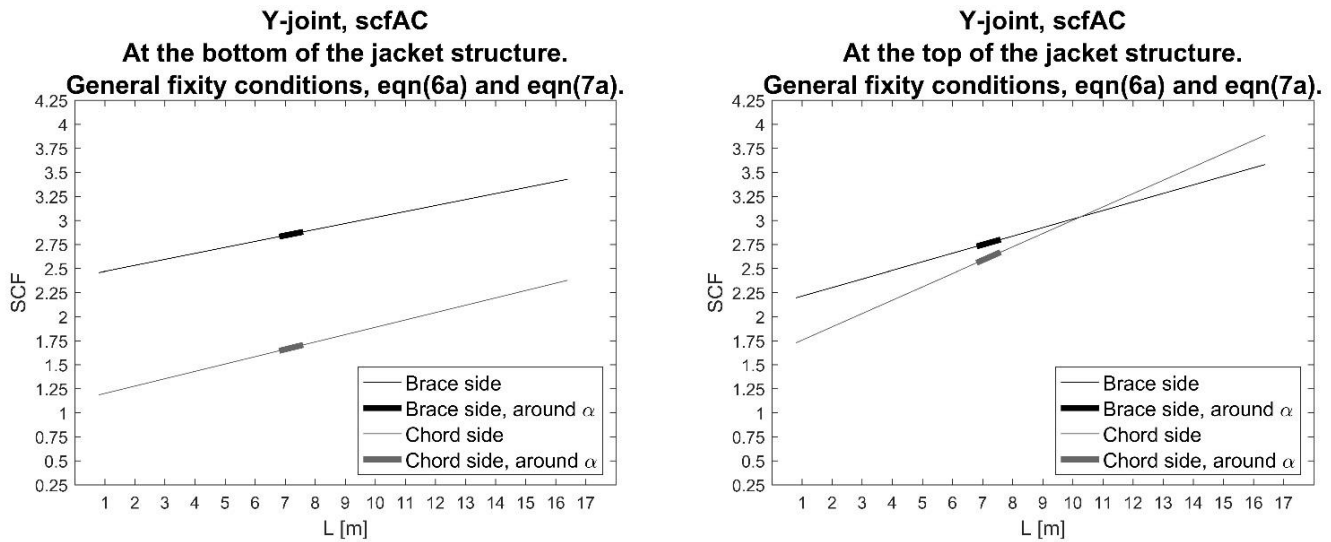
Figure 13: SCFs at the crown for axial load in Y-joints

4.2 Normalised Fatigue Damage in Relation to Estimation Approach and *L* value

All results, regardless of both *L* value and approach, are normalised with what is interpreted as the common procedure, which is *L* equal to 8.4 m and common approach. Equation (6a) and equation (7a) from Appendix B in the Recommended Practice has also been used in all cases in this sub chapter. [7]

There are two figures showing normalisation for each joint – one where all fatigue damages are estimated with results gotten with 256 hot spots, and one where they are estimated using 8 hot spots. The purpose of this was to look at the difference between the two methods and different *L* values, and also to see how these differences depended on the number of hot spots.

Before comparing results across joint types, remember that the y-axes limits are not the same for all joints. This is due to much larger normalised differences for Y-joints than for K- and X-joints. It is also important to remember that all figures in this chapter shows the relation between the fatigue damage estimation two different approaches give, not the estimated fatigue damage. All fatigue damage estimations for X-joints are shown in tables in Appendix C: Estimated Fatigue Damage for Different *L* Values and Different Number of Hot Spots.

The chord stress subsection in the HSS equations for the chord side is independent of the *L* value. Differences caused by different *L* values are therefore not related to this, because this part of the equations only vary due to nominal stress in the chord, which is the same regardless of the input parameters.

Variation between the methods is caused by which hot spot that gives largest fatigue damage estimation. When both methods give the same value, it means that the hot spot giving the largest value, is the same for all load cases. When both methods give values that are very similar to each other, this can mean that the hot spots giving largest fatigue damage estimate is the same for most of the load cases, or it can mean that several hot spots give similar fatigue damage estimates. The common method is noted as 'Approach Com', and the alternative method is called 'Approach Alt'.

4.2.1 K-joints

Figure 14 shows the estimated fatigue damage for all K-joints using 256 hot spots, normalised to the fatigue damage estimated using *L* equal to 8.4 m and Approach Com. Figure 15 shows almost the same thing, but all fatigue damages are estimated using only 8 hot spots. Notice that the y-axis doesn't start before 0.85, so the differences are not as extreme as they appear to be.

When using 8 hot spots, 13 out of 24 joints gets the same fatigue damage estimation for all Ls and both methods. This is the case only for 2 out of 24 joints when using 256 hot spots. Several of the differences are however minor. K-joints showing small variation due to L are barely affected by out-of-plane moment.

20 out of 24 K-joints shows difference between the two approaches when using 256 hot spots. The same is 11 out of 24 K-joins for 8 hot spots.

The first 9 K-joints gives quite similar results when comparing results using 256 hot spots with results using 8 hot spots. Out of these, K-joint 5, 7 and 9 shows variation mainly due to the approach. These are all joints at the lower part of the structure.

The K-joints in the vertically middle part of the structure are also quite similar to each other, when comparing 8 joints and two different amount of hot spots. K-joint 9 and K-joint 17 are those K-joints at this level that shows largest variation between approach, meaning that which hot spots with maximum fatigue damage varies for several load cases. K-joint 9 is at the front of the jacket structure, according to the wind turbine, and K-joint 17 is at the back. They are both at the same side of the structure, to the right when looking at it from the front. K-joint 13 is equally independent of method, L and number of hot spots, and this joint is also at the front, but on the left side.

The trend amongst K-joints at the upper part of the jacket structure is also similar between using 256 hot spots and using 8 hot spots. Except for K-joint 20 and K-joint 24, they are those with least equal differences across the number of hot spots. The difference between the two approaches is quite large when using 8 hot spots, but much smaller when using 256 hot spots. Also, for K-joint 20 there is no difference between different L values when using 8 hot spots and the alternative approach.

K-joint 15 is the joint that captures one's attention quickest, because this joint has the largest variation between methods, with a decrease ratio equal to 7 %. This joint is above the mean sea level (MSL), at the front of the jacket structure, to the left. It is an interesting observation that for the two lower levels the most difference at the front occurs in joints to the right. This large difference between the methods means that the hot spots with maximum fatigue damage keeps on varying. Another interesting observation is that the joint on the same level, and at the front of the jacket structure – but on the other side, is K-joint 19, which shows very little variation.

For all joints there is no difference between L16, Approach Com and L8.4, Approach Com. This corresponds with what was seen in sub chapter 4.1.1, that the SCFs for K-joints stops varying after L7.2. When L equals 7.2 m, one of the welds in eight of the K-joints have α slightly less than 12, while the rest are above 12. This is due to different chord diameters, as included in sub chapter 4.1.1, but unlike that case, the diameter difference causes difference in the fatigue damage estimation.

This explains why L7.2, Approach Com normalised to L8.4, Approach Com does not equal 1 for all joints. This difference is however very small, and increase ratio at only 0.03 % at the largest.
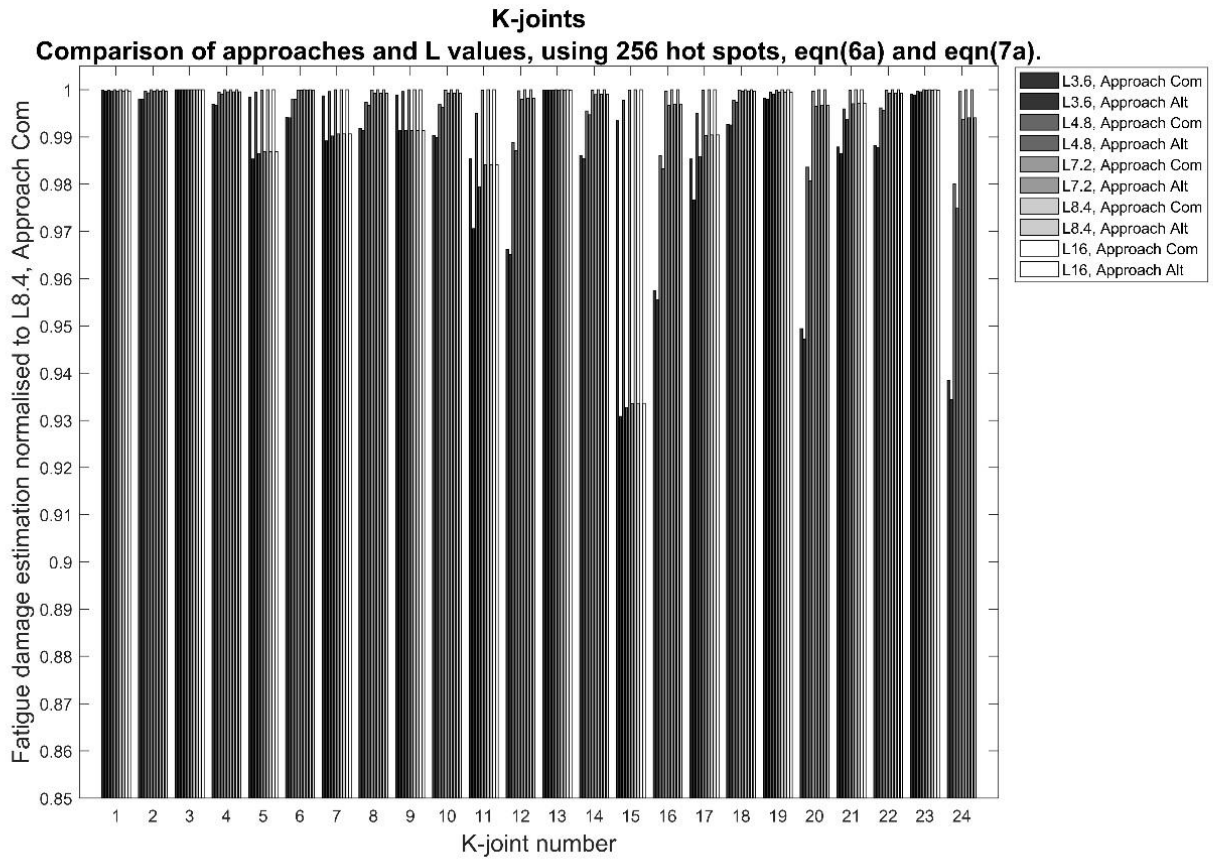
Figure 14: Fatigue damage for the different K-joints using 256 hot spots, normalised to L8.4, Approach Com
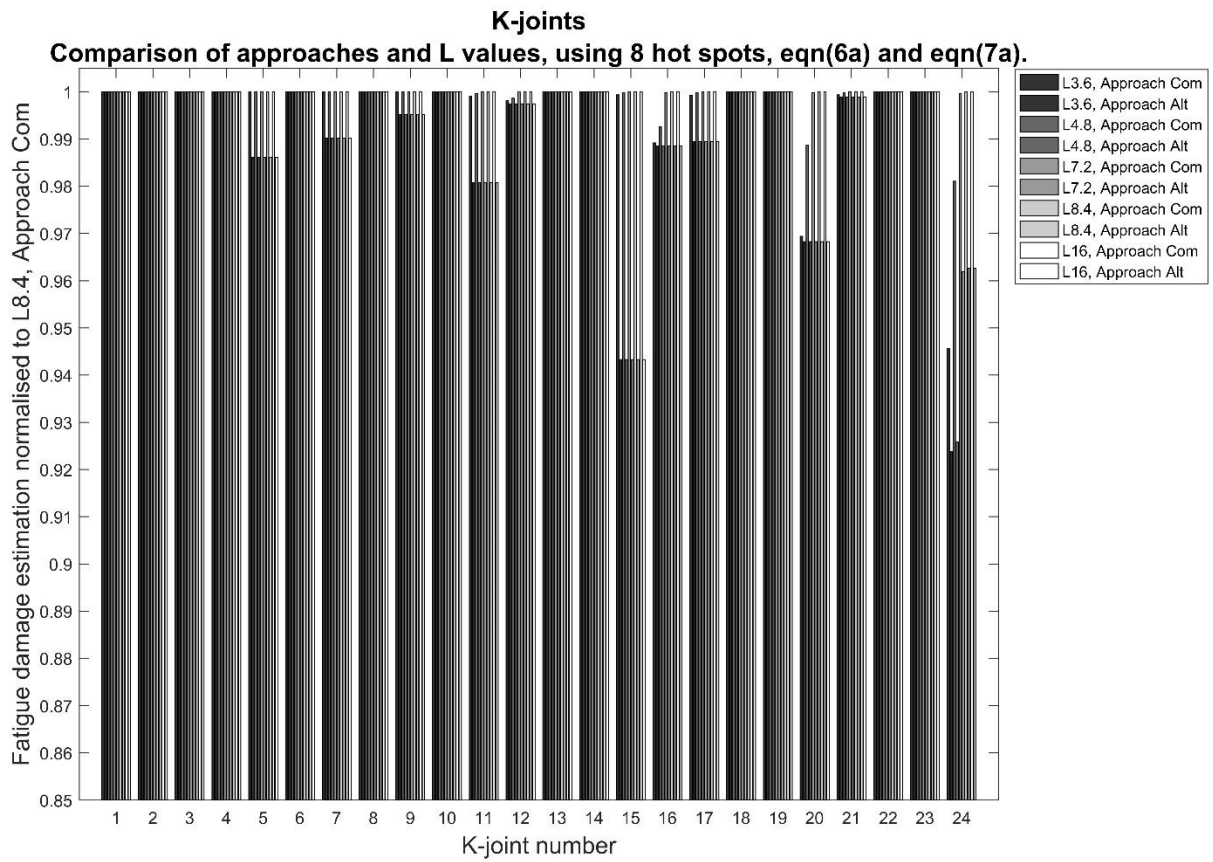
Figure 15: Fatigue damage for the different K-joints using 8 hot spots, normalised to L8.4, Approach Com

4.2.2 X-joints

Figure 16 shows the estimated fatigue damage for the different X-joints using 256 hot spots, normalised to the fatigue damage estimated using L equal to 8.4 m and Approach Com. Figure 17 shows the same, except for the number of hot spots, which is 8. It is important to note that the y-axis doesn't start before 0.85, so the differences are smaller than they appear to be.

By only looking at the common method, it is seen that only one L gives different results than the other Ls. Seeing as L3.6 is the only L below the limit, which for X-joints is reached when L equals 4.8 m, this is no surprise.

The alternative approach gives other results, compared to common approach using L8.4, for all joints when 256 hot spots are used, the same for when 8 hot spots is used. Although this depends on how many decimals one considers. If excluding L3.6, four of the X-joints gets the same value when using the alternative approach, as when using common approach and L8.4, when using 8 hot spots.

The X-joint with most difference between methods is X-joint 10 when using 256 hot spots, and X-joint 5 and 6 when using 8 hot spots. In addition, X-joint 6 is the only joint in addition to X-joint 1 that gives the same values for all Ls when using the alternative approach and 8 hot spots. When only using 8 hot spots the hot spot with maximum fatigue damage is the same for almost all load cases in X-joint 10, but there is more variation when using 256 hot spots.

From the tables in Appendix C: Estimated Fatigue Damage for Different L Values and Different Number of Hot Spots one sees that for all Ls included in this thesis, the fatigue damage estimated using 8 hot spots gives a value that is 0.02 smaller than when using 256 hot spots, for X-joint 5 and 6. Hence, the hot spots giving maximum fatigue damage estimations lies within these "new" hot spots. The same difference, but between 256 hot spots and 16 hot spots, is 0.0002.

X-joint 15 and 16 are those joints that gives largest difference between L3.6 and the other Ls, and this is the same independent of the number of hot spots. These joints are at the top of the jacket structure, on each side. The SCFs at the saddle for axial load, and the SCFs for out-of-plane bending moment are all affected by L. Of these four, those at the saddle for axial load have a larger increase before the α limit is reached, and they have larger value than the two others for all Ls.
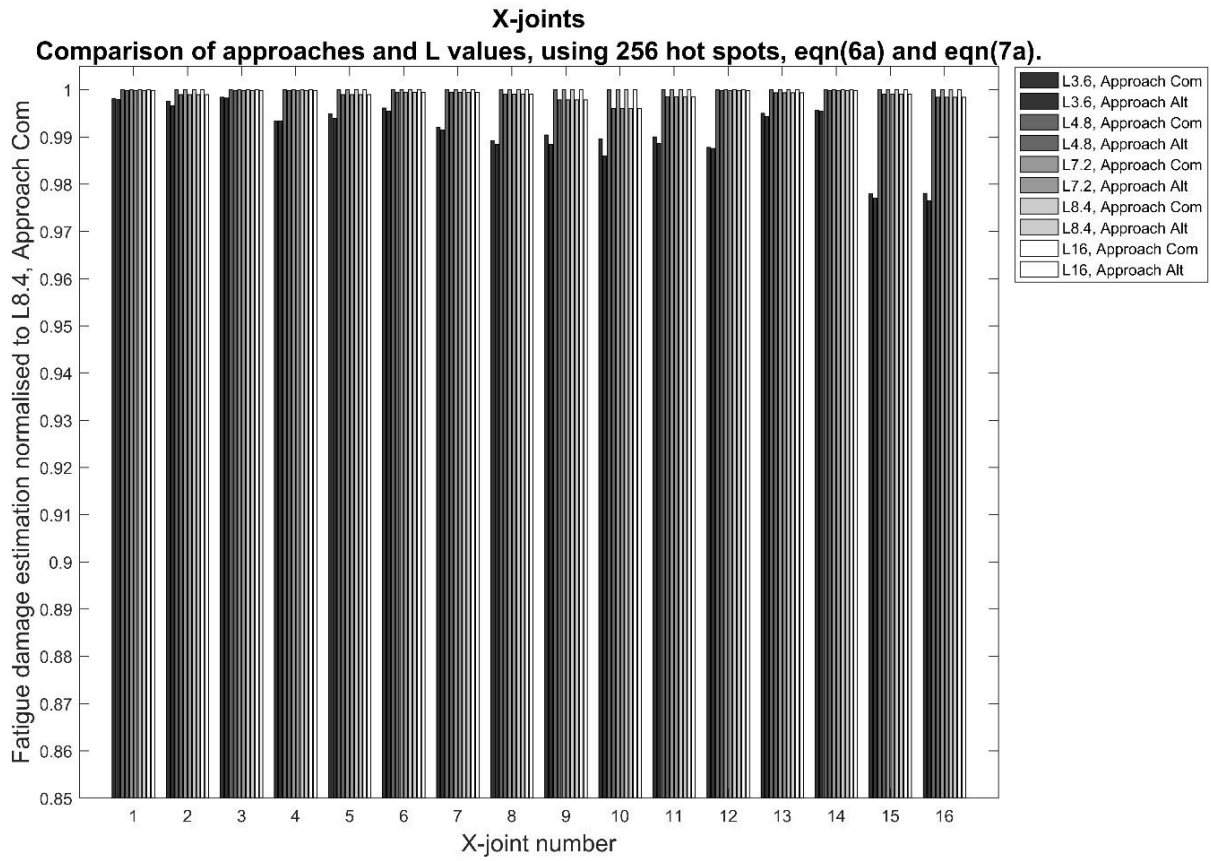
Figure 16: Fatigue damage for the different X-joints using 256 hot spots, normalised to L8.4, Approach Com
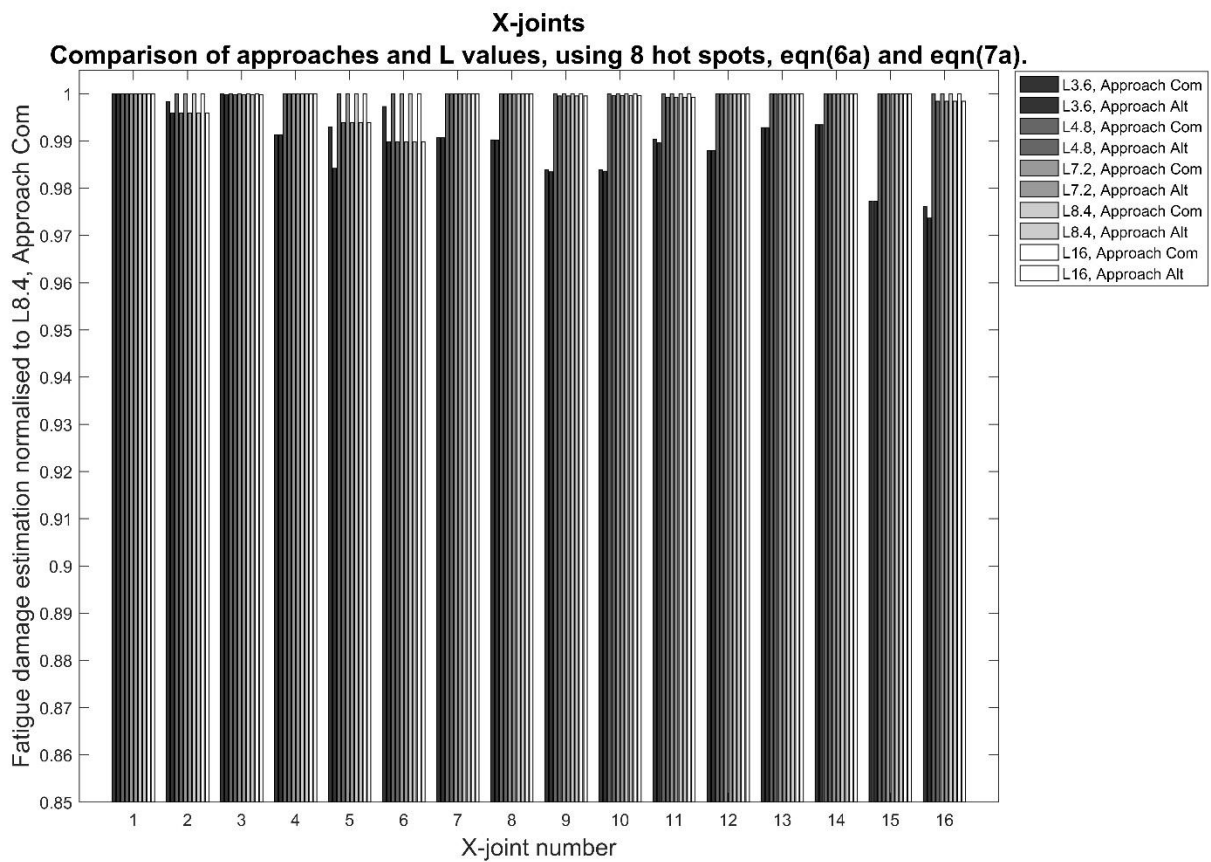
Figure 17: Fatigue damage for the different X-joints using 8 hot spots, normalised to L8.4, Approach Com

26

4.2.3 Y-joints

Figure 18 and Figure 19 shows the estimated fatigue damage for all Y-joints, normalised to the fatigue damage estimated using L equal to 8.4 m, Approach Com and equations (6a) and (7a) from Appendix B in the Recommended Practice. [7] The first one is for fatigue damages estimated using 256 hot spots, whilst the fatigue damages in the second are estimated using 8 hot spots. For this joint type, the y-axis starts at 0, so the difference due to L actually is quite large. Another thing to keep in mind is that the first four L values are quite close.

As already stated, the differences concerning the Y-joint are large. The largest differences are due to L equal 16 m, therefore Figure 18 and Figure 19 also shows a close-up that shows the differences between the lower L values more clearly. For L16, the alternative approach shows 20 % lesser increase than the common approach does, when normalised to L8.4, common approach. Amongst the two L16 approached, the decrease is 6 %.

As shown in sub chapter 4.1.3, Y-joints have six SCFs that vary due to L, three on each side of the weld, and four of them continues to vary after the limit of α is reached. It is therefore no surprise that there is difference between all Ls.

None of the joints at the bottom of the structure, Y-joint 1 to Y-joint 8, shows difference between fatigue damage estimated using different approach. Not for 256 hot spots, nor for 8 hot spots.

Y-joint 13, 14, 15 and 16 shows little to no difference between the approaches as well. These joints are all at the top of the jacket structure. To the left at the front and at the back, and on the left part. The other four joints at the top of the jacket structure, all shows difference between the two approaches. Except for joint 10 which does not show difference for all L values when using 8 hot spots.
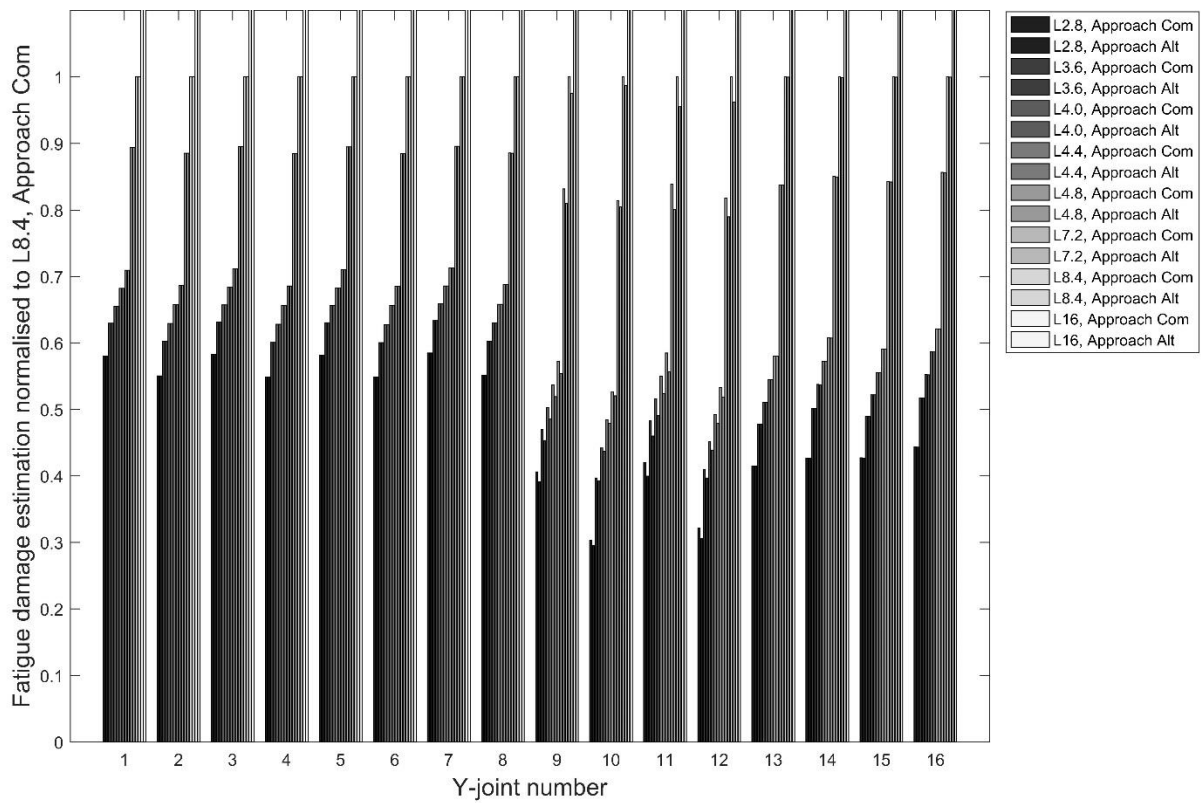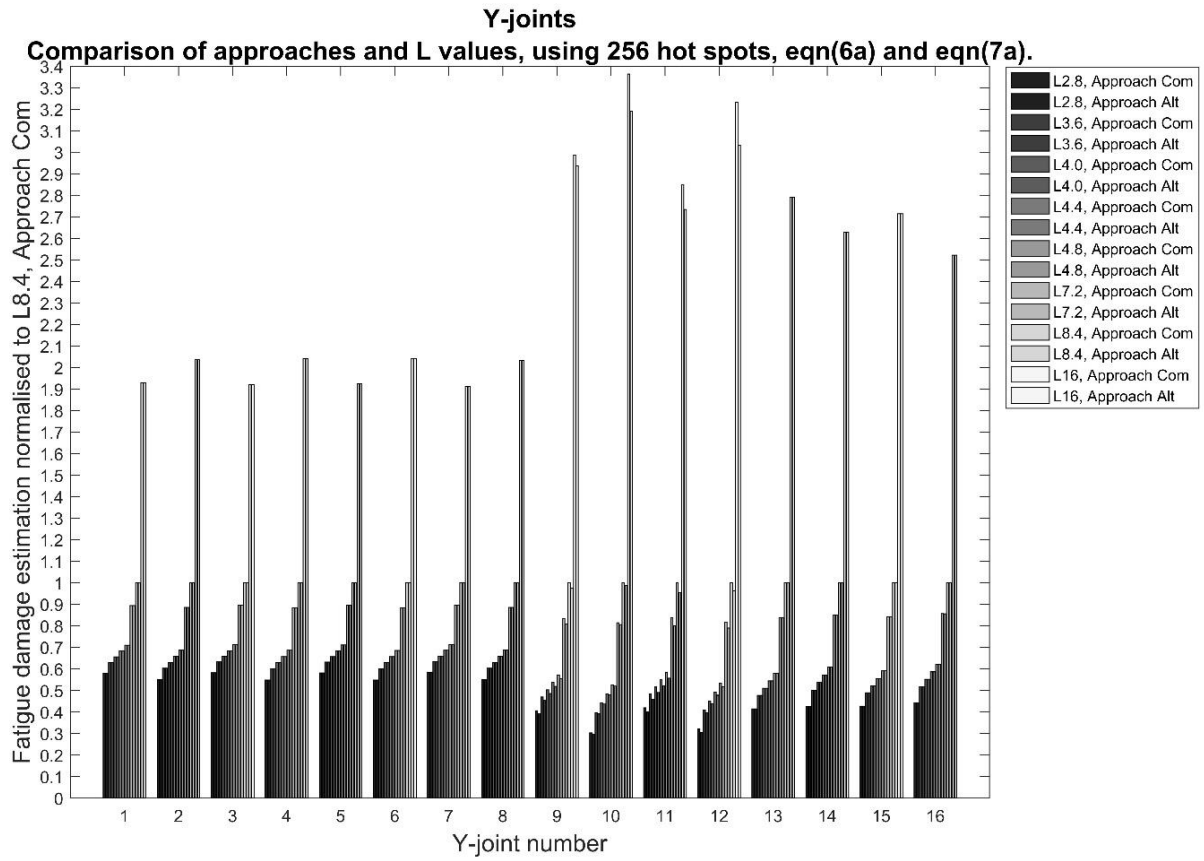
Figure 18: Fatigue damage for the different Y-joints using 256 hot spots, normalised to L8.4, Approach Com
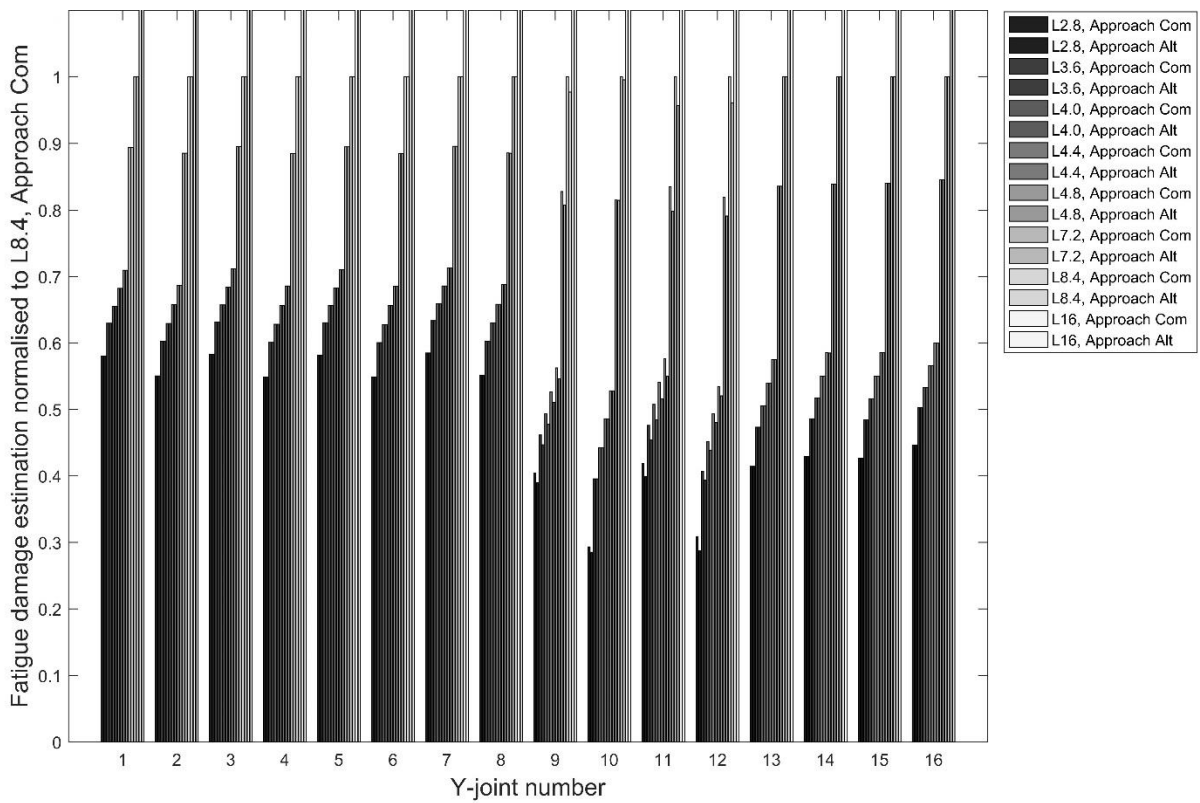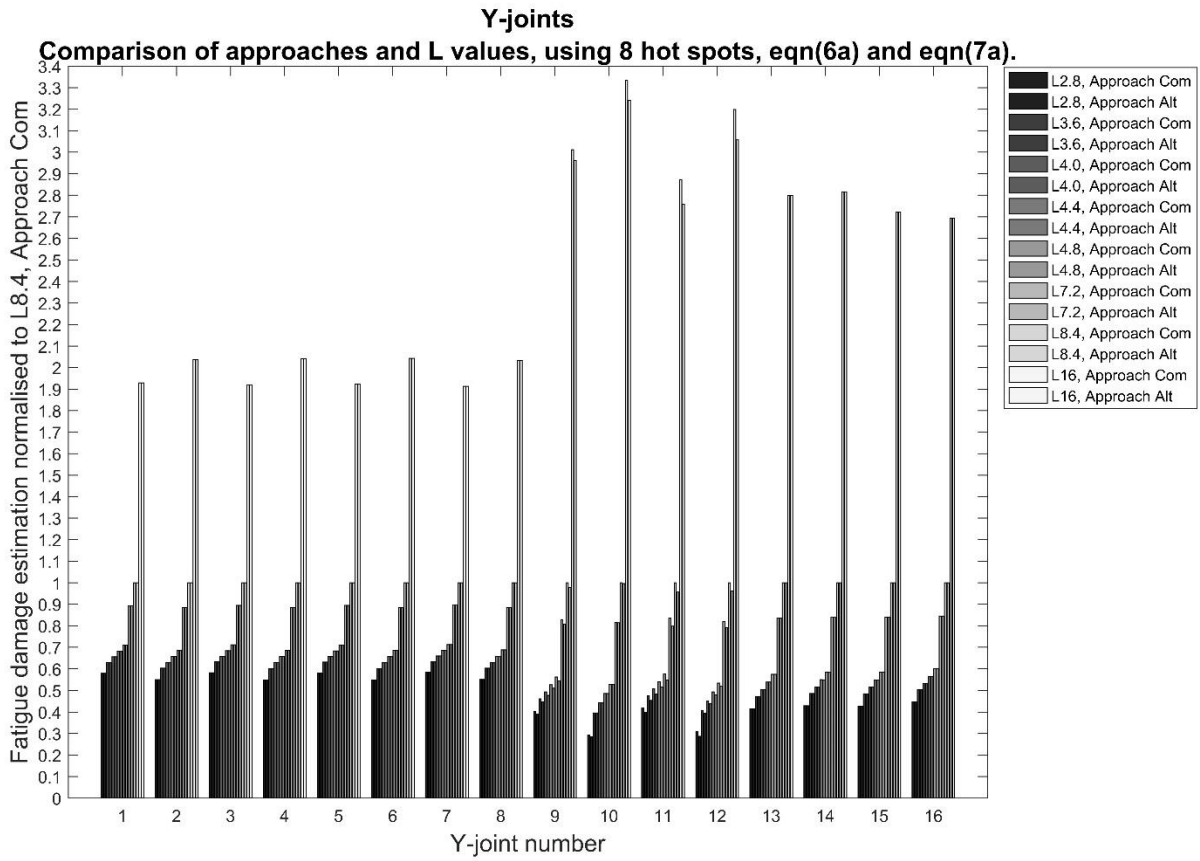
Figure 19: Fatigue damage for the different Y-joints using 8 hot spots, normalised to L8.4, Approach Com

4.3 Fatigue Damage in Relation to Number of Hot Spots

For the comparison of what different number of hot spots estimates the fatigue damage to be, it was for all joints used L equal to 8.4 m, the common approach and equations (6a) and (7a) from Appendix B in the Recommended Practice. [7] The fatigue damages has been normalised to the results gotten when using 8 hot

spots, to show how the results differ when increasing the number of hot spots. More specifically, the results have been divided by the estimations based on 8 hot spots.

4.3.1 K-joints

Most of the K-joints show difference due to the number of hot spots. As expected, the value either stays the same or it increases, because the hot spot with maximum value when using few hot spots still has the same value when using more hot spots.

As is seen in Figure 20, the largest differences lie between results from 8 hot spots and results from 16 hot spots. For the four joints that shows this the most, the increase ratio ranges between 10 % and 16 %. The increase ratio when going from 8 hot spots to 32 hot spots lies within the same range.

Those four K-joints that shows largest difference in Figure 20 are for this jacket structure joints with fatigue damage estimation equal to 0.43 or lower, these are all above the mean sea level, on the two sides of the jacket structure. K-joint 1 and 3 are both close to the bottom of the structure, and K-joint 13 is at the next level up, at the front of the structure.
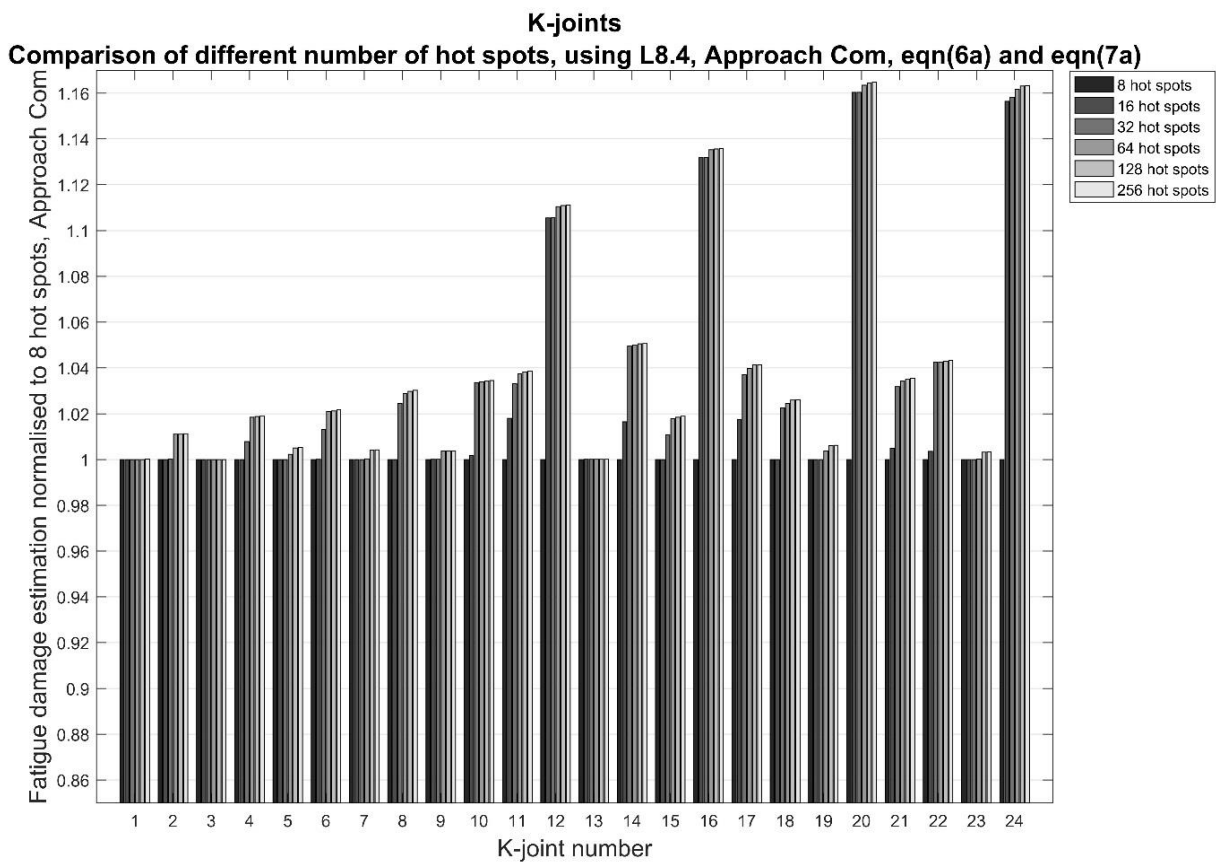
Figure 20: Fatigue damage estimations with different number of hot spots for all K-joints, normalised to 8 hot spots

4.3.2 X-joints

As seen in Figure 21, increasing the number of hot spots either give the same fatigue damage estimation, or it gives a higher one. This is especially interesting in X-joint 3, where fatigue damage estimated using 8 hot spots says the joint will resist fatigue throughout its entire lifetime, whilst fatigue damage estimated using 16 hot spots and more says that it will not. In addition, this difference is quite large. The fatigue damage estimates are shown in Appendix C: Estimated Fatigue Damage for Different *L* Values and Different Number of Hot Spots.

Those five X-joints that shows largest difference has an increase ratio between 8 hot spots and 16 hot spots in the area between 10 % and 16 %, the same as for K-joints. But unlike the K-joints, these are all at the two

lowest levels of the structure. X-joint 11 and 12, those with increase ratio close to zero, are on either side of the jacket structure.

The largest difference is shown to lie between 8 and 16 hot spots, but for joints at the two highest levels regarding the distribution of X-joints in the structure, 32 hot spots gives an additional 2 % increase.
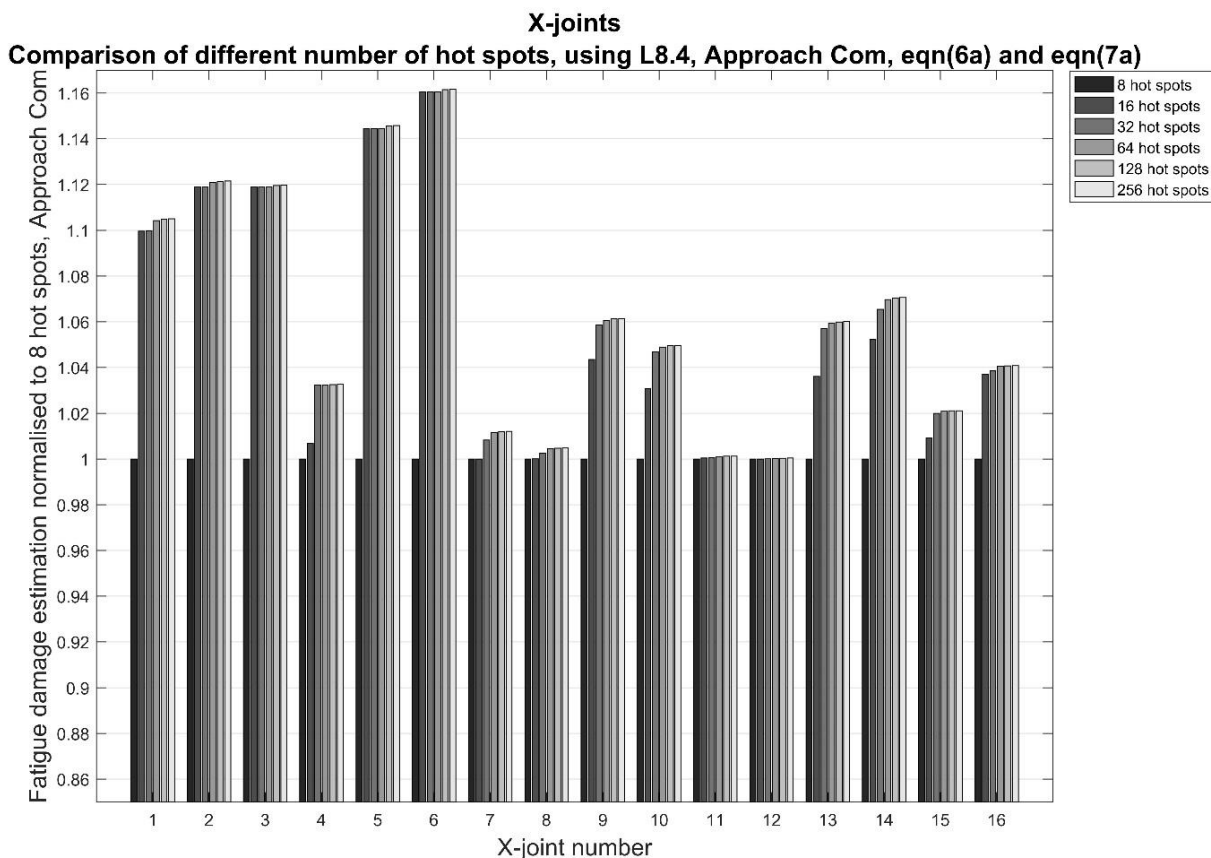
Figure 21: Fatigue damage estimations with different number of hot spots for all X-joints, normalised to 8 hot spots

4.3.3 Y-joints

The results are constant for all 8 Y-joints at the bottom of the structure – increasing the number of hot spots did not make any difference. For all Y-joints on top of the structure, however, increasing the number of hot spots also increases the estimated fatigue damage. These joints are also the joints with an overall smaller fatigue damage, compared to the joints on the bottom.

Y-joint 14 and 16 shows an increase ratio at 10 % when using 16 and 32 hot spots, and 11 % when using more. Increase ratios for all other joints are 2 % or less. These two joints with highest difference, meaning the hot spot giving maximum fatigue damage estimation lies somewhere in between the original 8 hot spots, are both on the right side of the jacket structure.

This is the results when using equation (6a) and equation (7a) from Appendix B in the Recommended Practice. [7] The same plot, but with fatigue damages estimates using equations (6b) and (7b) is shown in sub chapter 4.4.
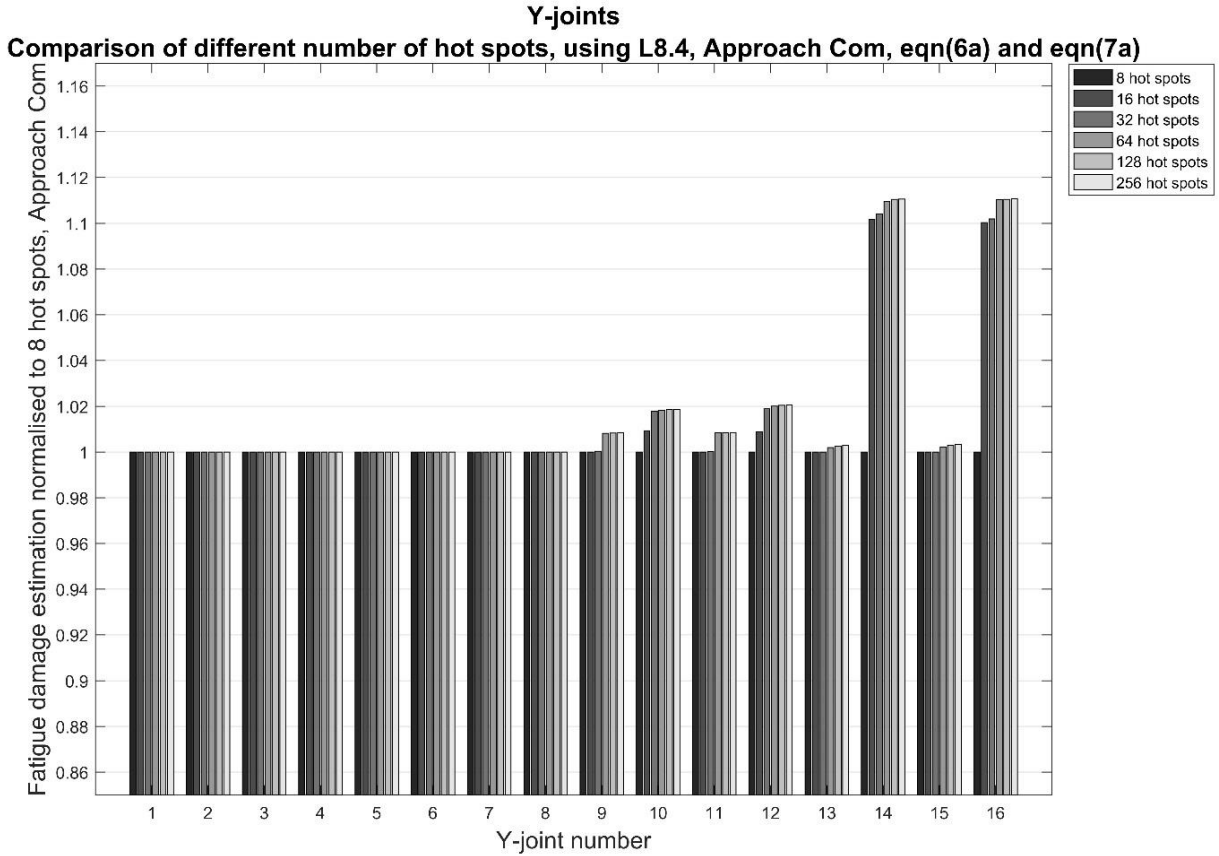
Figure 22: Fatigue damage estimations with different number of hot spots for all Y-joints, normalised to 8 hot spots

4.4 Fatigue Damage in Relation to Local Joint Flexibility

As mentioned previously, since only the Y-joints have loads in only one brace, they are the only ones affected by the SCFs that account for joint flexibility. This sub chapter shows the results of fatigue damage estimations based on different *L* values and different equations for the SCFs at the crown for axial load.

The SCFs at the saddle for axial load is still the same, and this one is affected the *L* parameter. Therefore the fatigue damage continues to be affected by the *L* parameter.

First, fatigue damage estimates using L8.4 and varying number of hot spots, normalised to results gotten when using 8 hot spots, as shown in Figure 23 and Figure 24. Results in Figure 23 have been found using the nominal stress in the chord due to in-plane bending moment, whilst for the results in Figure 24 the nominal stress in the chord used is due to out-of-plane bending moment.

The biggest difference between these two results lies in Y-joint 16. When using nominal stress due to in-plane bending moment, the increase ratio between 8 hot spots and 16 hot spots is almost 0 %, and the same between 8 hot spots and 32 hot spots and above, is 1 %. When using nominal stress due to out-of-plane bending moment, this increase ratio is up to 12 % when going from 8 hot spots to 16 hot spots, and 13 % when going from 8 to 32.

Apart from this exception, the increase ratio is quite similar for all joints when comparing the chord stress alternatives, lying between 8 % and 11 % for three of the Y-joints on top of the structure. Y-joint 11 and 13 are at the front of the jacket structure, Y-joint 15 is at the back.

Only four Y-joints shows no difference regarding choice of nominal bending stress – Y-joint 7, 10, 12 and 14. For these joints the nominal bending stress in the chord is either equal in both planes, or the axial load in the brace is zero.

32

When comparing the option using nominal stress due to in-plane bending, with the alternative that uses equation (6a) and equation (7a), the results are completely different, apart from the 8 first joints that shows no difference. When comparing the nominal stress due to out-of-plane bending option with the option using equations (6a) and (7a), it is not quite the same, because these two have in common the increase ratio for Y-joint 16. While the out-of-plane option shows increase ratio of 1 % between 16 hot spots and 32 hot spots, this is almost zero for the equations (6a) and (7a) option.
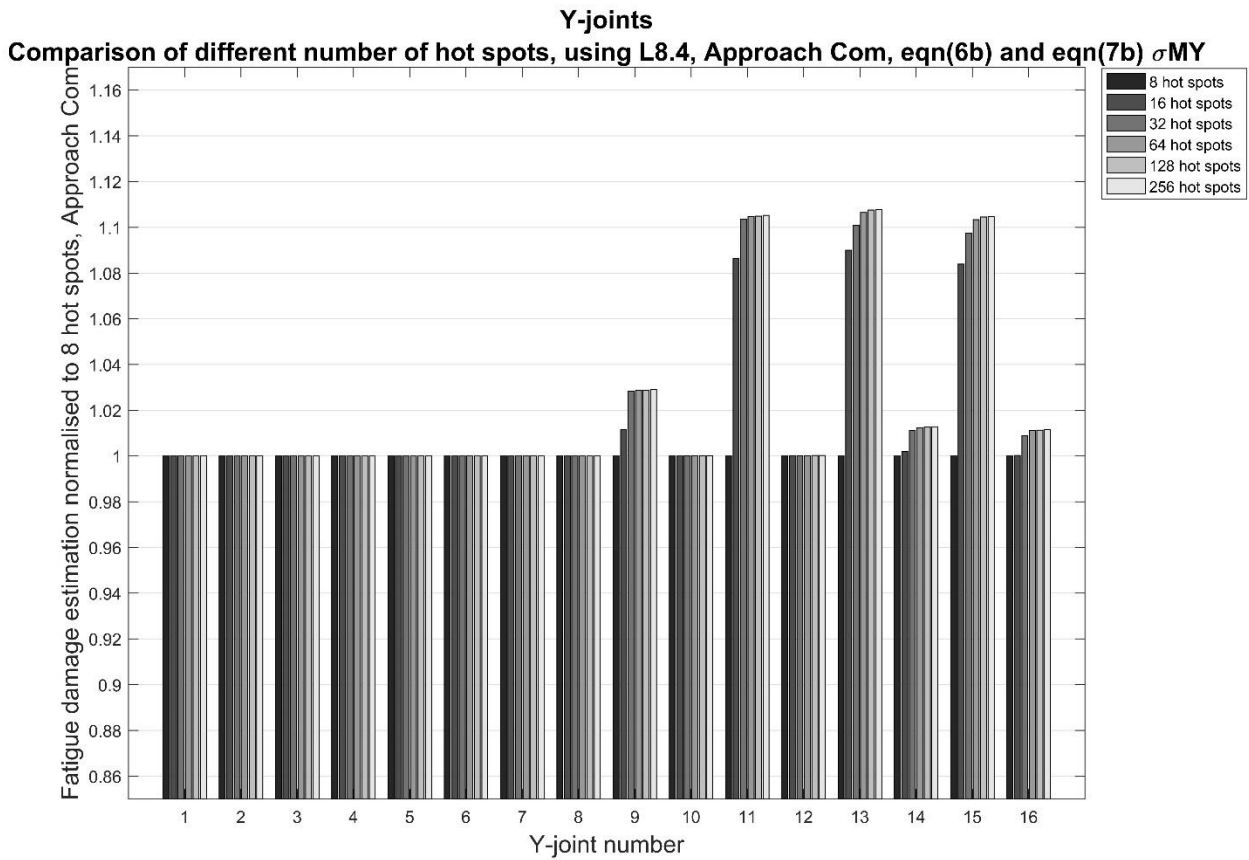
*Figure 23: Fatigue damage estimations with different number of hot spots for all Y-joints, normalised to 8 hot spots*
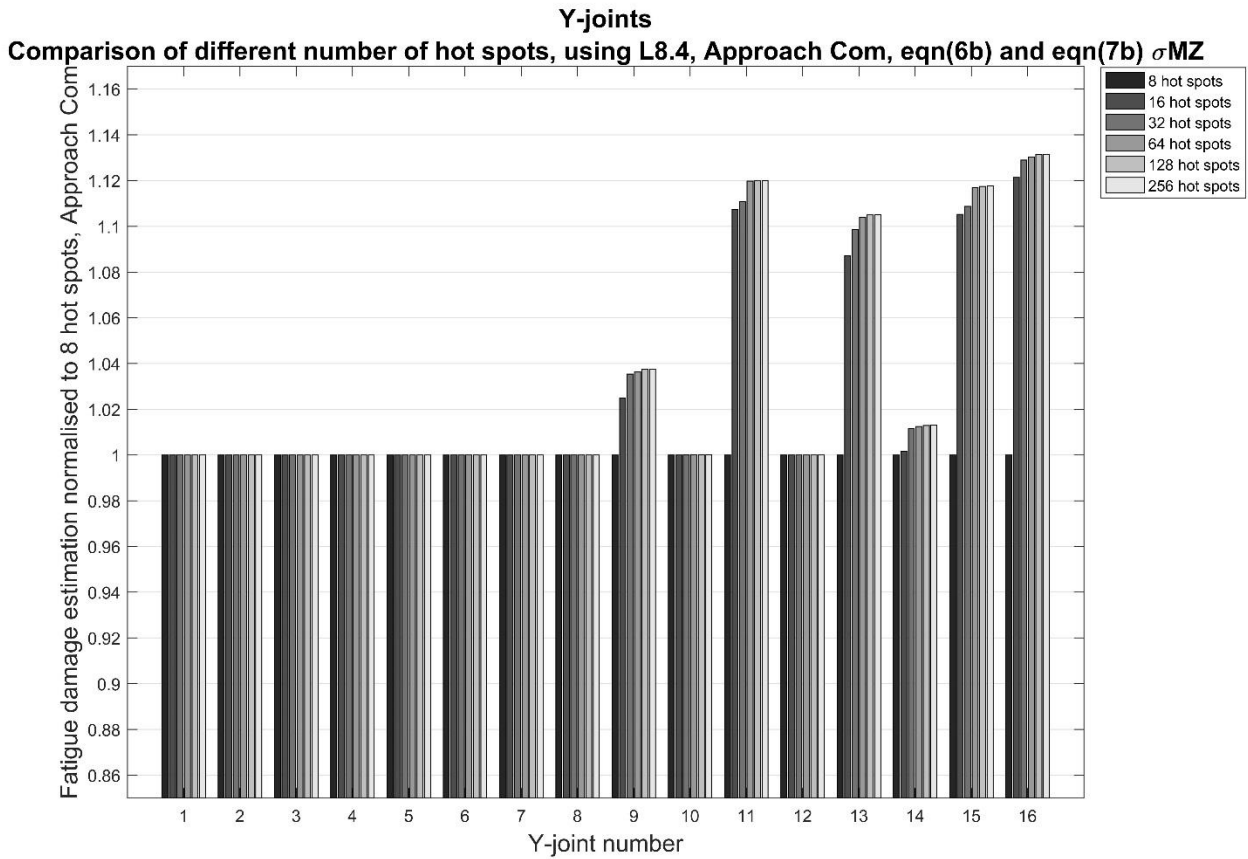
Figure 24: Fatigue damage estimations with different number of hot spots for all Y-joints, normalised to 8 hot spots

The next figures, Figure 25, Figure 26, Figure 27, Figure 28 and Figure 29, will show more directly the comparison between the different versions of equation (6) and equation (7) from Appendix B in the Recommended Practice. [7] Each figure shows plots relating to several joints, and all three equation possibilities. The different joints have been sorted based on the plot shapes and fatigue damage estimates.

The figures show that whether one uses nominal stress in the chord due to in-plane bending moment or out-of-plane bending moment does not make a big difference, but whether one uses equations (6a) and (7a) or equations (6b) and (7b) from the Recommended Practice [7] do makes a clear difference already at an *L* value equal to 3.6 m.

For the *L* values included in this thesis, it is not before L8.4 that the difference affects the answer to whether the structure is sturdy enough or not. Results gotten using equations (6a) and (7a) has steeper increase than the two other options for all joints.

For all Y-joints at the bottom of the structure, the results based on equations (6b) and (7b), both nominal bending stress options, are almost constant, the largest difference occurring here is 0.0004, which occurs when using nominal stress due to out-of-plane bending moment, in Y-joint 3, between the value regarding L16 and the value regarding L8.4. This difference almost close to zero is due to the axial stress in the brace being close to zero, because this is the nominal stress in the HSS equations that is multiplied with the SCFs at the saddle for axial load.

Y-joint 10 and 12 are those that shows the most similar results across all three alternatives.
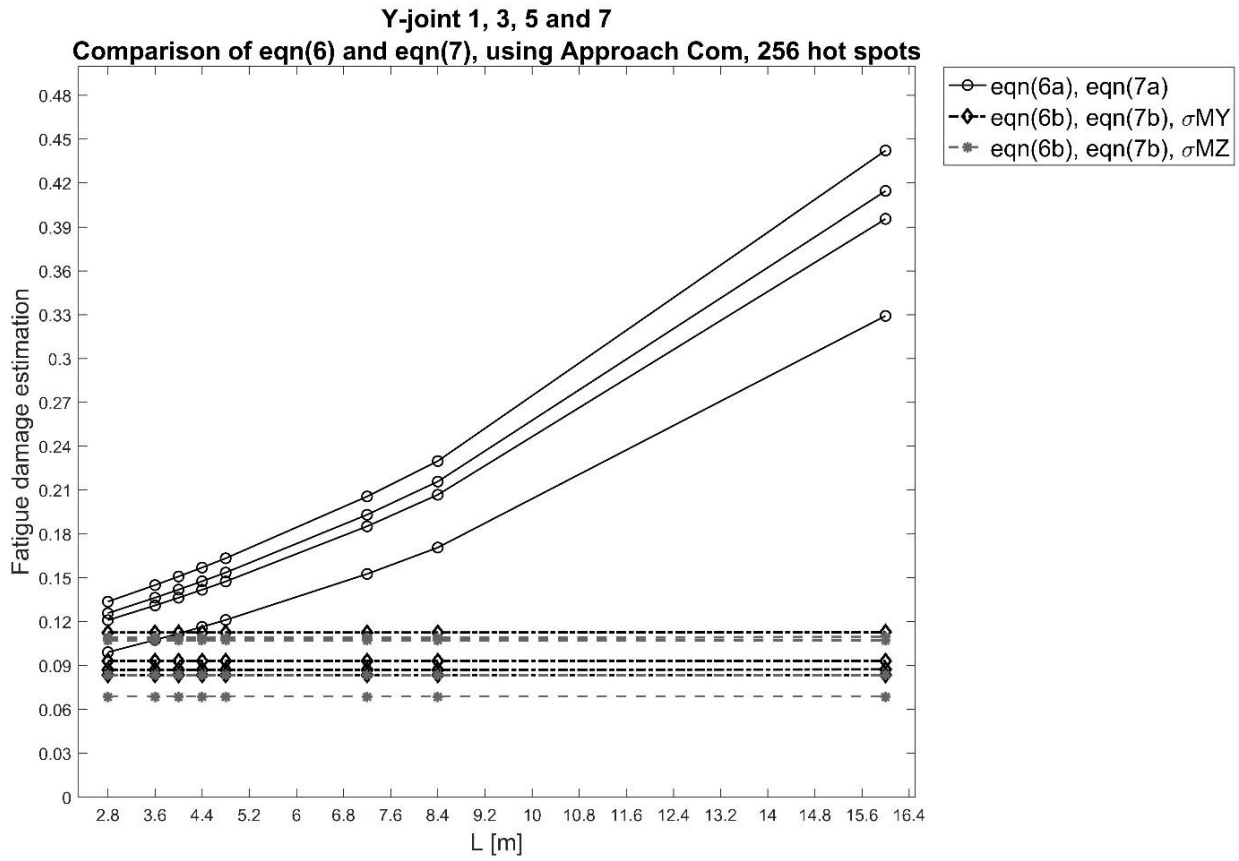
Figure 25: Fatigue damage estimations for Y-joint 1, 3, 5 and 7, with varying eqn(6), eqn(7) and L
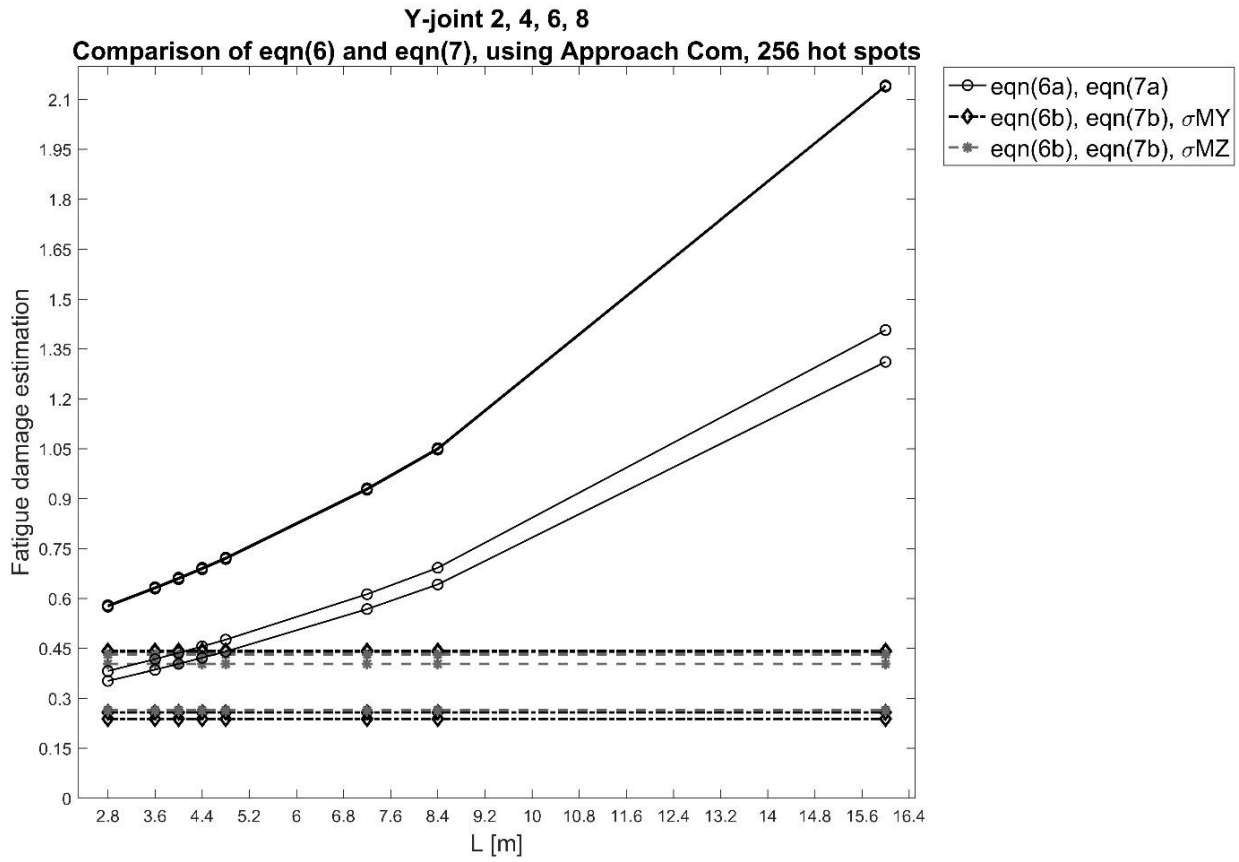
Figure 26: Fatigue damage estimations for Y-joint 2, 4, 6 and 8, with varying eqn(6), eqn(7) and L
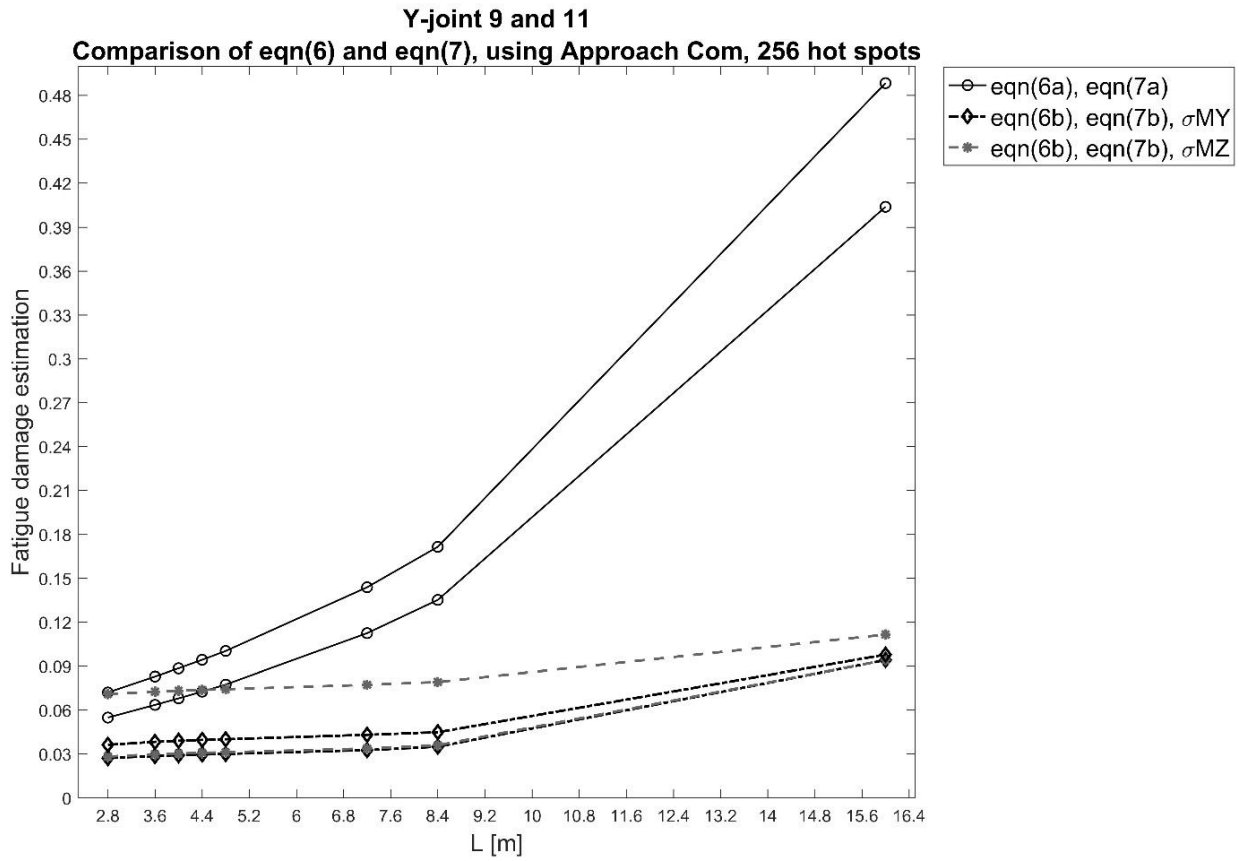
Figure 27: Fatigue damage estimations for Y-joint 9 and 11, with varying eqn(6), eqn(7) and L
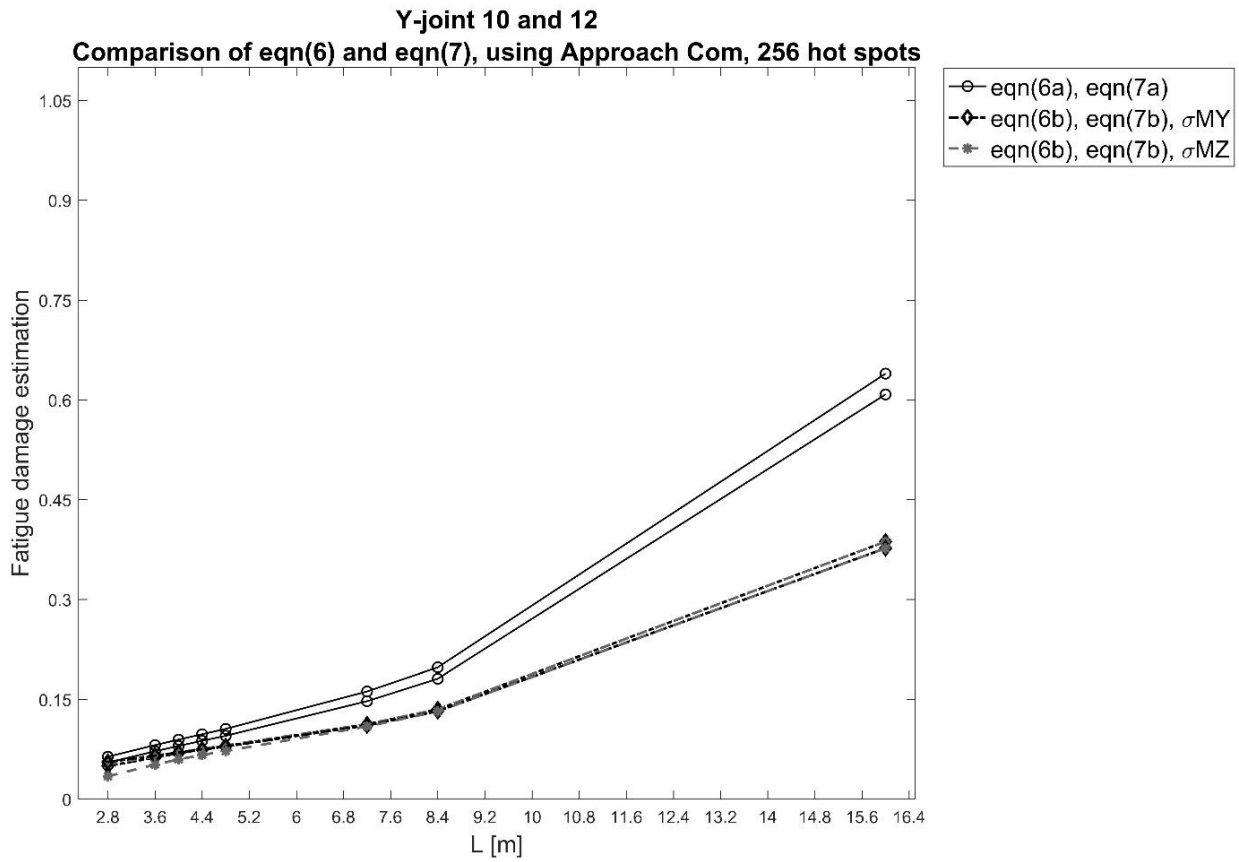
Figure 28: Fatigue damage estimations for Y-joint 10 and 12, with varying eqn(6), eqn(7) and L
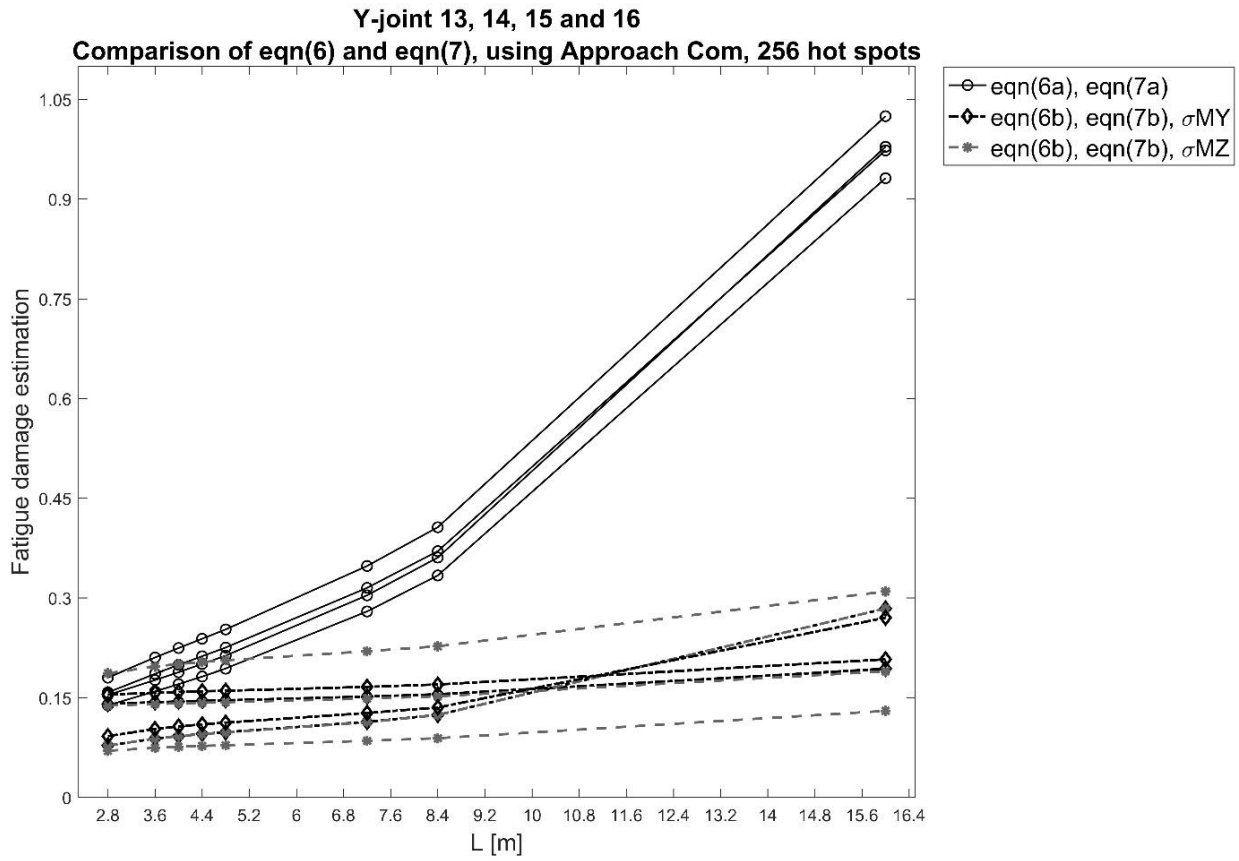
Figure 29: Fatigue damage estimations for Y-joint 13, 14, 15 and 16, with varying eqn(6), eqn(7) and L

5   Result Summary and Discussion

This chapter contains the evaluation of the results, starting with a summary of the results regarded as most interesting and relevant, and then discussing the potential sources and whether these results seem important or not.

Regarding L, K-joints and X-joints are only affected by the L value until it causes α to exceed the limit that decides whether the SCF should be multiplied with the short chord correction factor or not. This connection is also seen in the final fatigue damage estimates for these joint types. The choice of this L value is therefore only relevant until this limit is reached, but before this, it is an important parameter concerning the final fatigue damage estimations.

The question is – does one really use an L lower than this limit value? If using the expression for α as basis, this limit is crossed when L equals 7.2 m for K-joints, and L equal 4.8 m for X-joints. For this UpWind reference jacket, none of the K-joints have chord lengths lower than this, neither does the X-joints.

In Y-joints, the SCFs at both the saddle and crown in Y-joints continues to increase together with increasing L value, when using equation (6a) and equation (7a) from Appendix B in the Recommended Practice. [7] This shows up in the final fatigue damage estimates as well, and they quickly get very large. The SCFs for out-of-plane bending moment is constant after α has exceeded the limit.

Also Y-joints have been considered as if the brace is an attachment to the chord. Even though the upper Y-joints may be interpreted as having a short chord, this attachment is equal for all three alternatives concerning equations (6) and (7), and cannot be the reason for large gaps between the results.

The size on the nominal axial stress in the brace is important. If this is large, it causes the part of the HSS equation that contains the SCF at the crown for axial load to have a bigger impact on the resulting HSS. It also makes the SCFs found using equations (6b) and (7b) smaller, because the nominal axial stress in the brace is included in these equations as a denominator.

The fatigue damage estimated using equations (6b) and (7b) does not increase as steeply as those resulting from equations (6a) and (7a), since only the SCFs at the saddle for axial load is affected by the L value. The results across the three possibilities are closest for the two Y-joints at the top of the structure, to the left of the wind turbine. This relates to the nominal axial stress in the brace. It is small enough to give some size to the SCFs at the crown for axial load, and large enough to make the SCFs at the saddle for axial load to make an impact on the result.

The two approaches considered give different results in some joints, where the hot spots with maximum value are not equal for each load case. For Y-joints, only one fourth showed difference between the two approaches, and the largest decrease ratio when going from the common approach to the alternative approach was 6 %.

None of the Y-joints at the bottom of the structure showed a difference between the estimation approaches, so for these joints the hot spot giving maximum fatigue damage seems to be constant, indicating that the loads are also seemingly constant at the bottom. X-joints does not show a considerable amount of difference between the two approaches, neither when using 256 hot spots nor when using 8 hot spots.

The two K-joints showing largest difference between the two approaches are close to the top of the structure, above the MSL, with a decrease ratio equal to 7 %. This is the largest decrease ratio between the two approaches for the whole jacket structure, and in total the K-joints had most variation concerning which hot spots that gave largest fatigue damage estimation. If the decrease ratio plays a significant role in a fatigue analysis or not, depends on how exposed the joint is to fatigue damage. If the fatigue damage estimation is high enough, one method can approve the joint, while the other method can find the joint as insufficient.

There are differences concerning number of hot spots, and these differences could play a bigger role for other structures.

The largest differences in K-joints and X-joints were found when comparing results found using 16 hot spots with results from using 8 hot spots, where the increase ratio ranged between 10 % and 16 % for several joints. Simply doubling the number of hot spots give large differences, showing that the location most exposed to loads often lies in-between the most common 8 hot spots. In some joints the increase ratio was larger between 32 and 8 hot spots, than between 16 and 8 hot spots, respectively 4 % and 0.5 %. These joints have the most exposed points in-between the 16 hot spots, not in them.

For Y-joints the number of hot spots makes no difference at the bottom of the structure, and little to no difference at the top, except for two joints. The largest increase ratio between fatigue damage estimations based 8 hot spots and 16 hot spots was 10 %.

As mentioned in the introduction, some choices have been made that may affect the results. The chord-end fixity parameter equals the typical value, 0.7, throughout this whole thesis. [7] In this thesis, due to the fixity conditions and the number of braces with loads, this parameter only affects the SCFs in Y-joints at the saddle on the chord side for axial load, and at the crown on both the brace and the chord side for axial load. It has only affected the crowns when equation (6a) and equation (7a) from Appendix B in the Recommended Practice was used. [7]

This difference in when the crowns were affected can be some of the reason as to why the fatigue damages estimated using equations (6a) and (7a) are much higher than the two other alternatives. But since they in some cases start very close to each other, and the big differences comes with bigger Ls, this does not seem like a probable reason.

Another choice that was made concerns the K-joints. As stated in sub chapter 3.1, the lower weld in all K-joints were selected as 'brace A'. [7] In all joints, brace A and brace B had different angle between itself and the chord, and for the K-joints at the lowest K-joint level, the upper and lower chord had different thickness and diameter, which affected the SCFs. In this thesis, this only affects the SCFs for out-of-plane bending moment in the K-joints, where both braces are represented, but with some difference concerning the parameters.

As mentioned in sub chapter 3.1, the SCFs for out-of-plane moment in K-joints was misinterpreted, causing on weld in each K-joint to have wrong SCFs value. This has caused the SCFs for out-of-plane bending moment in K-joints to be approximately 4 % different than it should be. As shown, the L value does not affect the fatigue damage estimation a great deal, and these SCFs are not the ones with highest value in K-joints. This mistake should not be repeated, but it has not affected the results of this thesis a lot.

The Recommended Practice used for the calculations is DNVGL-RP-0005, not the edition that came out in April 2016 – DNVGL-RP-C203, after the thesis work had begun. There are differences concerning the S-N curves, hence the results here are not the ones recommended for further use in design analysis. However, seeing as this master thesis is about comparison, it has not directly affected the credibility of the results.

6 Conclusion and Recommendations

6.1 Conclusion

L is an important parameter, because it visibly affects the fatigue damage estimations. For K-joints and X-joints there is however no need to consider L values that causes alpha to exceed its limit, which is 12, as this does not affect the results any further. This applies to fatigue analysis using general fixity conditions and a structure where loads occur in both braces.

For Y-joints, when using general fixity conditions, the L value affects the results much less when using equation (6b) and equation (7b) from Appendix B in the Recommended Practice. [7] This difference between fatigue damages estimated with equations (6a) and (7a), and fatigue damages estimated with equations (6b) and (7b) can, in addition to be related to the L value, also be affected by the nominal axial stress in the brace.

The two approaches, when using L8.4, shows largest difference in K-joints and Y-joints at the top of the structure.

Different number of hot spots give different results in most cases. Increasing the number of hot spots either increases the fatigue damage estimation or does not make a difference. This is because increased number of hot spots indicates that hot spots are added, and the old ones are still kept. For some of the K-joints and X-joints, increasing the number of hot spots from 8 to 16 gave an increase in fatigue damage up to 16 %.

Using too few hot spots may cause one to miss a joint that cannot resist fatigue throughout the lifetime, so it is recommended to use at least 16 hot spots for joints that are notably exposed to cyclic loading.

The largest difference is related to the choice regarding the SCFs at the crown for axial load. Here the fatigue damage estimations found using the SCF equations based on nominal stress, those that accounts for LJF, were for some joints down to only 20 % of the value found using the solely geometric equations.

6.2 Recommendations for Further Research

One of the parameters that have stayed constant throughout this whole thesis is the chord-end fixity parameter C. A sensitivity analysis with a variation regarding this is recommended. [7] [22]

This thesis has looked at varying numbers of hot spots, but which hot spots that gave the largest fatigue damage was not observed. Observing the hot spots with the largest fatigue damage, while comparing the two approaches, could give more information regarding about these hot spots. This could e.g. tell if it is enough to add a few hot spots at specific places, instead of using many enough to cover the whole circumference. Previous study shows that K-joins in several cases had the hot spot with maximum value close to, but not directly at, the crown toe. [31]

The attachment SCF has been used for all calculations in this thesis. Another recommendation is to perform the exact same study, but without this attachment, and see what difference it makes, and where in the structure it differs the most. This is especially relevant for the Y-joints and X-joints at the top of the structure, because these have the shortest chords.

The SCFs including LJF has been used, but the new SCF values have not been noted. Only the resulting fatigue damage has been compared, not the SCFs themselves. Nor have the nominal axial stress been noted. By looking at both of these – the SCFs that includes LJF and the size of the nominal axial stress compared with the other stresses, it can give a better answer regarding what causes these large differences, and when to use which equations.

Comparisons of L values in Y-joints for Ls between 4.8 m and 7.2 m could be advantageous, to see if there is an exact point at which the difference between the different equations for the SCF at the crown for axial load starts to increase. To find an exact point, the Ls should be close to each other. A delta equal to 0.1 would be a good beginning, and the results gotten from this could indicate if a smaller delta is necessary.

A third thing regarding LJF – a structure with more joints that only has loads in one brace could give more information regarding the difference that this choice for SCF equations causes.

As mentioned in sub chapter 3.2, the time series for each load response for each beam, consisted of values representing 3600 seconds. This caused the analysis to take larger amount of time than predicted, hence processes compared were not many enough to give concrete results. It is therefore recommended to extend this parameter study, e.g. by using an application like the one developed for this thesis.

References

[1]   The European Wind Energy Association. The Economics of Wind Energy. 2009 Mar.

[2]   Karadeniz H. Stochastic Analysis of Offshore Steel Structures: An Analytical Appraisal. London: Springer; 2013.

[3]   International Renewable Energy Agency. Wind Power. IRENA Working Paper: Renewable Energy Technologies: Cost Analysis Series. 2012 Jun: 1(5).

[4]   Popko W, Vorpahl F, Zuga A, Kohlmeier M, Jonkman J, Robertson A, Larsen TJ, Yde A, Sætertrø K, Okstad KM. Offshore Code Comparison Collaboration Continuation (OC4), Phase 1-Results of Coupled Simulations of an Offshore Wind Turbine With Jacket Support Structure. 22nd International Offshore and Polar Engineering Conference. International Society of Offshore and Polar Engineers; 2012.

[5]   Jonkman J, Butterfield S, Musial W, Scott G. Definition of a 5-MW Reference Wind Turbine for Offshore System Development. Technical Report NREL/TP-500-38060. National Renewable Energy Laboratory, Golden, Colorado; 2009.

[6]   China Classification Society. GD 09-2013: Guidelines for Fatigue Strength Assessment of Offshore Engineering Structures. 2013 Oct.

[7]   DNV GL AS. DNVGL-RP-0005: Fatigue Design of Offshore Steel Structures. 2014 Jun.

[8]   The European Wind Energy Association. Deep Water: The Next Step for Offshore Wind Energy. 2013 Jul.

[9]   DNV GL AS. DNVGL-ST-0126: Support Structures for Wind Turbines. 2016 Apr.

[10]   Maddox SJ. Fatigue Strength of Welded Structures, 2nd ed. Abington Publishing; 1991.

[11]   Mirtaheri M, Zakeri HA, Alanjari P, Assareh MA. Effect of Joint Flexibility on Overall Behavior of Jacket Type Offshore Platforms. American J. of Engineering and Applied Sciences. 2009: 2(1): 25-30.

[12]   DNV GL AS. DNVGL-OS-C101: Design of Offshore Steel Structures, general - LRFD method. 2015 Jul.

[13]   The International Electrotechnical Commission. International standard IEC 61400-3: Wind turbines – Part 3: Design Requirements for Offshore Wind Turbines. 2009 Feb.

[14]   Barltrop NDP, Adams AJ. Dynamics of Fixed Marine Structures, 3rd ed. Butterworth Heinemann; 1991 Jun.

[15]   DNV GL AS. DNV-OS-J101: Design of Offshore Wind Turbine Structures. 2014 May.

[16]   The International Electrotechnical Commission. International standard IEC 61400-1: Wind turbines – Part 1: Design Requirements. 2005.

[17]   Fischer T, de Vries W, Schmidt B. UpWind Design Basis. WP4: Offshore Foundations and Support Structures. 2010 Oct.

[18]   Chen B, Hu Y, Tan M. Local Joint Flexibility of Tubular Joints of Offshore Structures. Marine Structures. 1990: 3(3):177-197.

[19]   Karamanos S A, Romeijn A, Wardenier J. Stress Concentrations in Tubular Gap K-joints: Mechanics and Fatigue Design. Engineering Structures. 2000 Jan: 22(1):4-14.

[20]   Schijve J. Fatigue of Structures and Materials. 2nd ed. Delft: Springer; 2009.

[21]   Lotsberg I. On Stress Concentration Factors for Tubular Y- and T-Joints in Frame Structures. Marine Structures. 2011 Jan: 24(1):60-69.

[22]   Efthymiou M. Development of SCF Formulae and Generalised Influence Functions for Use in Fatigue Analysis. Recent development in tubular joint technology, OTJ'88. London: 1988 Oct.

[23]   Efthymiou M, Durkin S. Stress Concentrations in T/Y and Gap/Overlap K-joints. Behaviour of Offshore Structures, BOSS'85. The Netherlands: Elsevier Science Publishers B.V.; 1985.

[24]   Pilkey WD, Pilkey DF. Peterson's Stress Concentration Factors. 3rd ed. New Jersey: John Wiley & Sons, Inc.; 2008.

[25]   Wægter, John. Stress Concentrations in Simple Tubular Joints [Internet]. [Place unknown]: 2009 Apr. Available from:
http://homes.civil.aau.dk/lda/Advanced%20Structural%20Engineering/Stress%20concentrations%20in%20simple%20tubularjoints.pdf

[26]   Lotsberg, Inge. [E-mail]. Message to: Benedicte Hexeberg Hammerstad. 2015 Dec.

[27]   The International Organization for Standardization, the International Electrotechnical Commission. International standard ISO/IEC 23270: Information technology – Programming languages – C#. 2006 Sep.

[28]   MathWorks. MATLAB Mathematics, R2016a. 2016.

[29]   DNV GL AS. DNVGL-ST-0262: Lifetime Extension of Wind Turbines. 2016 Mar.

[30]   Vorpahl F, Popko W, Kaufer D. Description of a basic model of the 'UpWind reference jacket' for code comparison in the OC4 project under IEA Wind Annex 30. Germany: Fraunhofer Institute for Wind Energy and Energy System Technology IWES; 2013.

[31]   Hammerstad BH, Schafhirt S, Muskulus M. On Fatigue Damage Assessment for Offshore Support Structures with Tubular Joints. Deep Sea Offshore Wind R&D Conference, EERA DeepWind'2016. Norway: ScienceDirect; 2016 Jan.

Appendix 1: Master thesis (TBA4920 Marine Civil Engineering)

MASTER THESIS
(TBA4920 Marine Civil Engineering, master thesis)

Spring 2016
for
Benedicte Hexeberg Hammerstad

Sensitivities in fatigue analysis of offshore wind turbine support structures

Sensitiviteter i pålitelighetsanalyser av understell for offshore vind turbiner

BACKGROUND

In offshore steel structures such as jackets for offshore wind turbines, tubular joint connections are driving fatigue design of the structures. Fatigue calculations of tubular joints require compliance with the relevant standards such as DNV-RP-C203. The calculations are based on stress combinations described by the use of hot spot stresses (HSS) and stress concentration factors (SCF). Uncertainties regarding the fatigue damage estimates lead to conservative designs (using large fatigue safety factors) and increase costs.

TASK DESCRIPTION (Tentative work for the thesis)

Description of task
The main scientific task is to **investigate the sensitivity of fatigue damage estimates in the hot spot stress (HSS) approach** to the parameters and details of the calculation method, such as stress concentration factors (SCF) or the number/position of hot spots.

Aims and purpose
The aim with this task is to quantify (parts of) the uncertainty regarding fatigue damage estimates for offshore wind turbine support structures. As these estimates depend a lot on the details of the loading, it is planned to implement and verify code checks for joint fatigue as a post-processing tool in the FEDEM simulation software, using the application programming interface. The implemented post-processing tool shall then be used to identify the sensitivities of the HSS-approach both in terms of number/position of hot spots, as well as their dependency on changes of the SCFs. It is also relevant to identify influences of joint flexibility to the fatigue calculations. If time allows, further work can be done on the investigation of uncertainties in the fatigue calculations of tubular joints, such as the joint type classification in dynamic analyses, tolerances of S-N-curves, or geometrical parameter used in the SCF-calculation.

Subtasks and research questions

As an introduction, the candidate must write an outline of the thesis work (**research plan**) within the first two weeks that will be reviewed and commented on by the supervisors. This outline should show that the candidate understands the aims of the thesis, has the knowledge necessary to perform the tasks, that his approach is suitable for approaching the problem(s), and that the timing is adequate.

1. Writing of research plan [2 weeks]
2. Getting familiar with the FEDEM simulation software and the .NET framework. [2 weeks]
3. Specification of the post-processing tool [1 week].
4. Development and implementation of the tool [4 weeks]
5. Sensitivity analysis. [4 weeks]
6. Consideration of local joint flexibilities or additional factors [4 weeks]
7. Writing of thesis [3 weeks]

General about content, work and presentation
The text for the master thesis is meant as a framework for the work of the candidate. Adjustments might be done as the work progresses. Tentative changes must be done in cooperation and agreement with the professor in charge at the Department.

In the evaluation thoroughness in the work will be emphasized, as will be documentation of independence in assessments and conclusions. Furthermore the presentation (report) should be well organized and edited; providing clear, precise and orderly descriptions without being unnecessary voluminous.

The report shall include:

- Standard report front page (from DAIM, http://daim.idi.ntnu.no/)
- Title page with abstract and keywords.(template on: http://www.ntnu.no/bat/skjemabank)
- Preface
- Summary and acknowledgement. The summary shall include the objectives of the work, explain how the work has been conducted, present the main results achieved and give the main conclusions of the work.
- Table of content including list of figures, tables, enclosures and appendices.
- A list explaining important terms and abbreviations should be included.
- List of symbols should be included
- The main text.
- Clear and complete references to material used, both in text and figures/tables. This also applies for personal and/or oral communication and information.
- Text of the Thesis (these pages) signed by professor in charge as Attachment 1.
- The report musts have a complete page numbering.

The thesis can as an alternative be made as a scientific article for international publication, when this is agreed upon by the Professor in charge. Such a report will include the main points as given above, but where the main text includes both the scientific article and a process report.

Advice and guidelines for writing of the report is given in: "Writing Reports" by Øivind Arntsen. Additional information on report writing is found in "Råd og retningslinjer for rapportskriving ved prosjekt og masteroppgave ved Institutt for bygg, anlegg og transport" (In Norwegian). Both are posted on It's-learning.

Submission procedure
Procedures relating to the submission of the thesis are described in DAIM (http://daim.idi.ntnu.no/). Printing of the thesis is ordered through DAIM.

On submission of the thesis the candidate shall submit also to the professor in charge a CD/DVD with the paper in digital form in pdf and Word (editable) version, the underlying material (such as data collection, time series etc., if possible) in digital form.

Documentation collected during the work, with support from the Department, shall be handed in to the Department together with the report.

According to the current laws and regulations at NTNU, the report is the property of NTNU. The report and associated results can only be used following approval from NTNU (and external cooperation partner if applicable). The Department has the right to make use of the results from the work as if conducted by a Department employee, as long as other arrangements are not agreed upon beforehand.

Tentative agreement on external supervision, work outside NTNU, economic support etc.
Separate description is to be developed, if and when applicable.

Health, environment and safety (HSE) https://innsida.ntnu.no/hms-for-studenter
NTNU emphasizes the safety for the individual employee and student. The individual safety shall be
in the forefront and no one shall take unnecessary chances in carrying out the work. In particular, if
the student is to participate in field work, visits, field courses, excursions etc. during the Master
Thesis work, he/she shall make himself/herself familiar with "Fieldwork HSE Guidelines". The
document is found on the NTNU HMS-pages at
https://innsida.ntnu.no/wiki/-/wiki/English/Fieldwork+-+for+participants

The students do not have a full insurance coverage as a student at NTNU. If you as a student want
the same insurance coverage as the employees at the university, you must take out individual travel
and personal injury insurance.

Start and submission deadlines
The work on the Master Thesis starts on (date) _15.01.2016_

The thesis report as described above shall be submitted digitally in DAIM at the latest
(date:) _10.06.2016_ at 3pm.

Professor in charge: _Dr. Michael Muskulus_

Other supervisors: _Dr. Daniel Zwick (Fedem Technology)_
Mr. Sebastian Schafhirt

Trondheim, 15.01.2016 (initial version)

Michael Muskulus
Professor in charge (sign)

Appendix B: Stress Concentration Factors Unaffected by Short Chord Correction Factor

K-joints

The SCFs in K-joints differ between the upper and lower part of the joint throughout the whole jacket structure for in-plane bending moment and at the chord and saddle for axial load. Figure 30, Figure 31 and Figure 32 shows SCFs at the saddle and chord for axial load in K-joints. Figure 33, Figure 34 and Figure 35 shows SCFs for in-plane bending moment in K-joints.
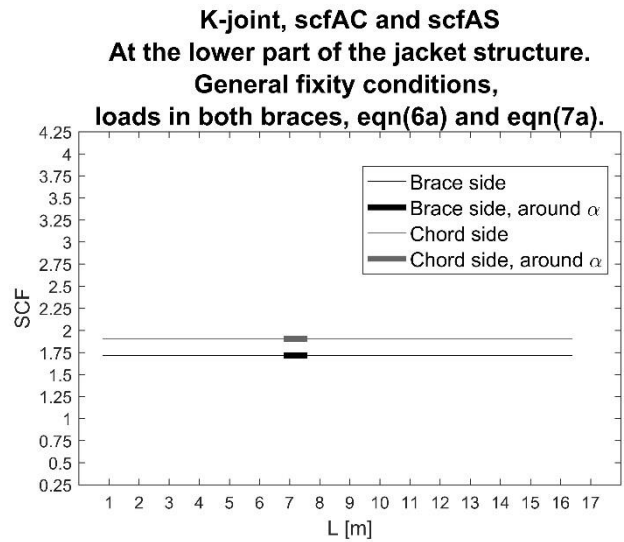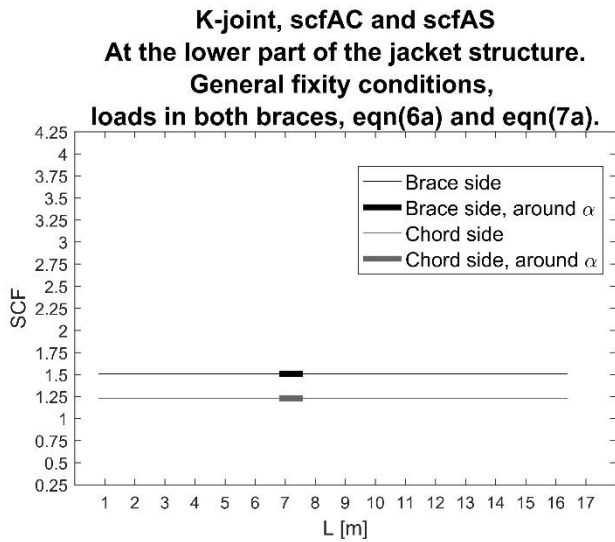
Figure 30: SCFs at the saddle and chord for axial load in K-joints. Lower part of the weld to the left, upper part to the right
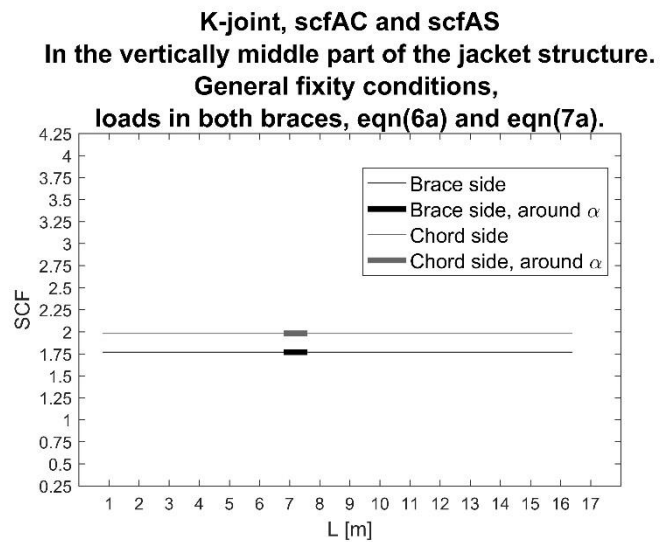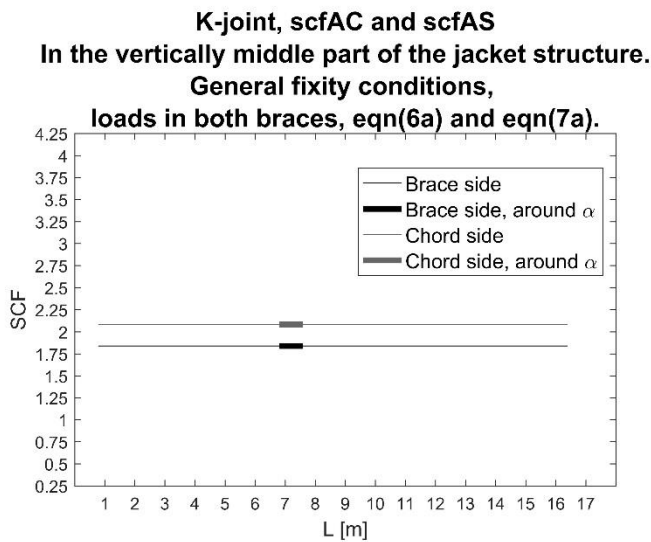
Figure 31: SCFs at the saddle and chord for axial load in K-joints. Lower part of the weld to the left, upper part to the right
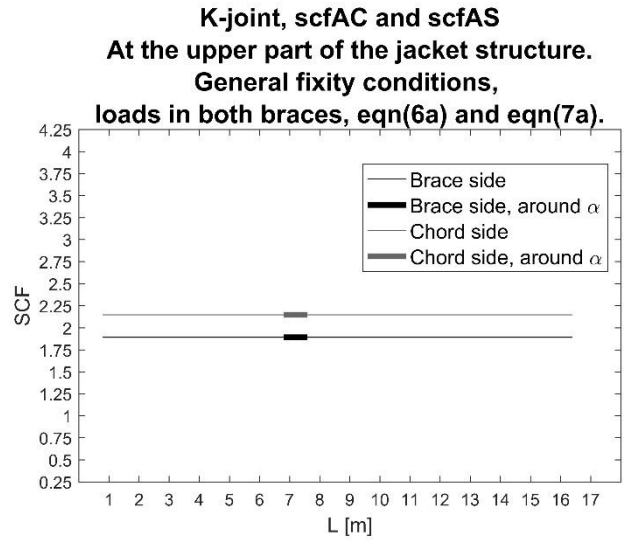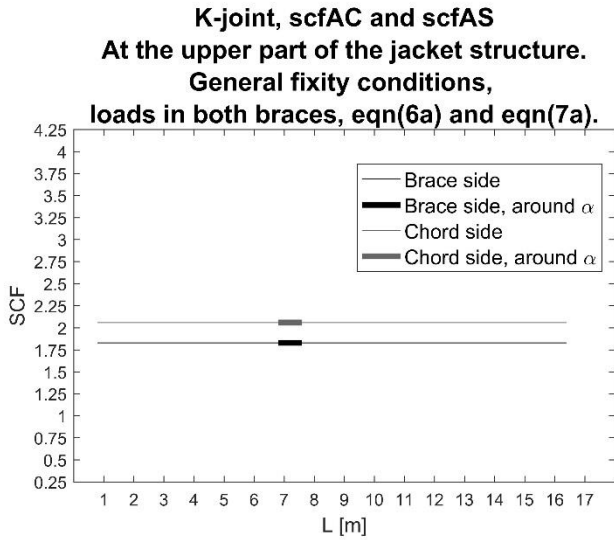
Figure 32: SCFs at the saddle and chord for axial load in K-joints. Lower part of the weld to the left, upper part to the right
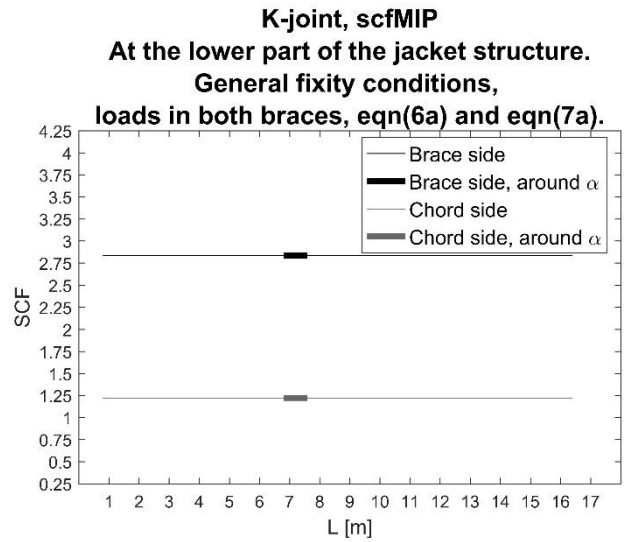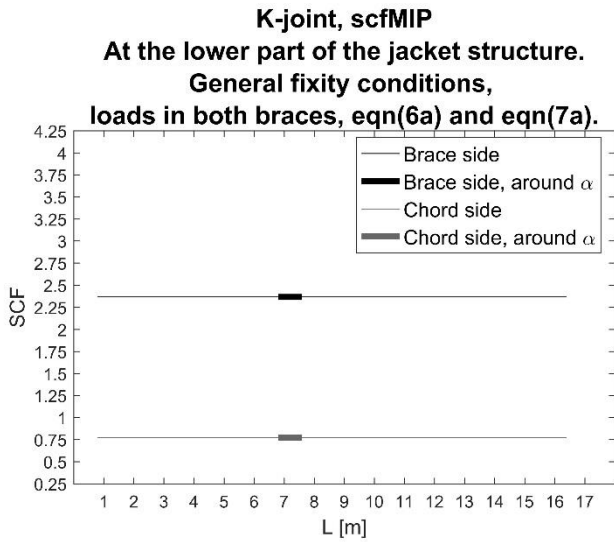
Figure 33: SCFs for in-plane bending moment in K-joints. Lower part of the weld to the left, upper part to the right
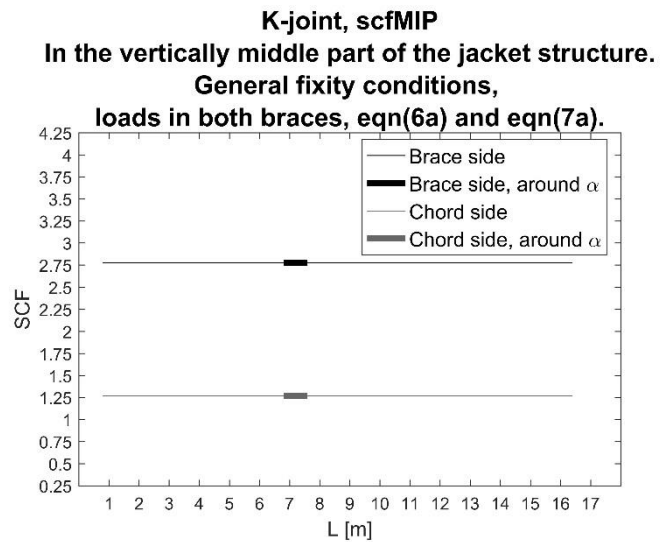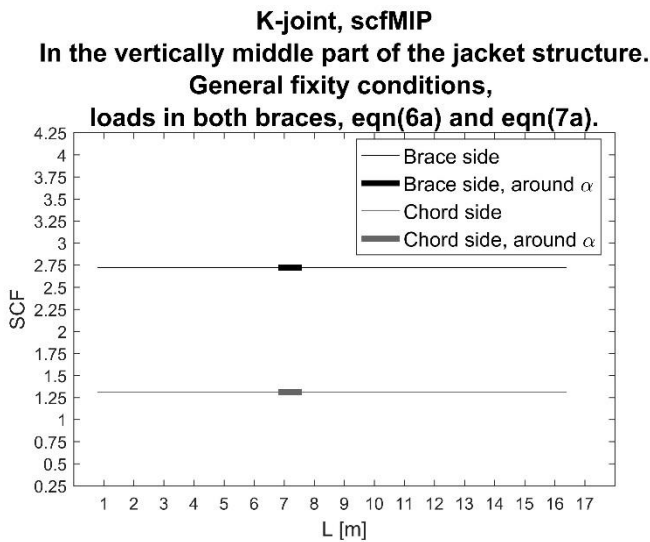
Figure 34: SCFs for in-plane bending moment in K-joints. Lower part of the weld to the left, upper part to the right
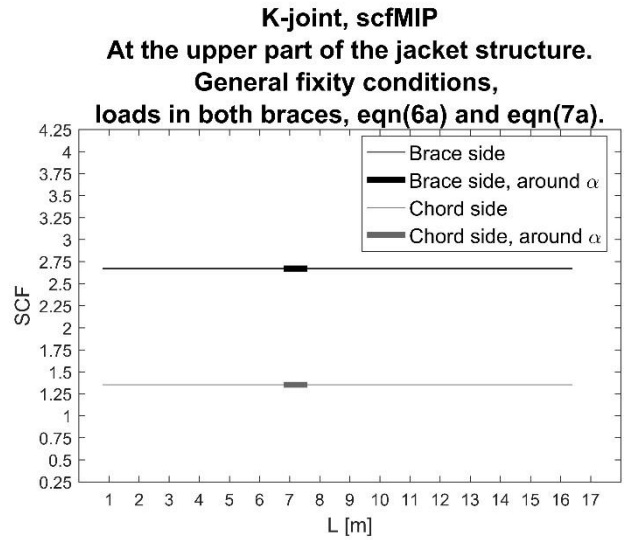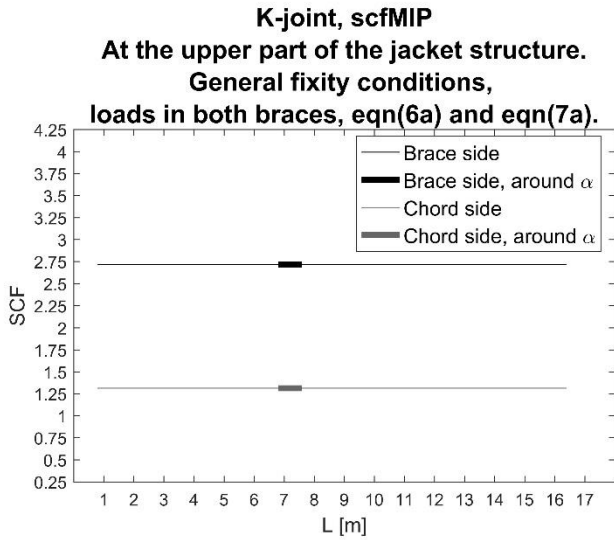
Figure 35: SCFs for in-plane bending moment in K-joints. Lower part of the weld to the left, upper part to the right

X-joints
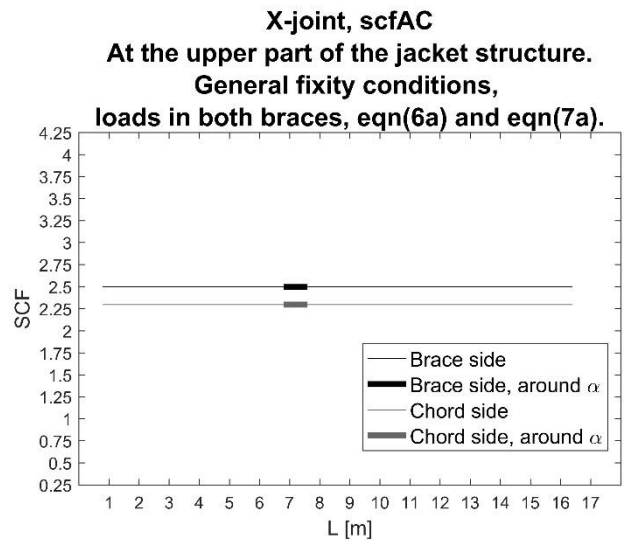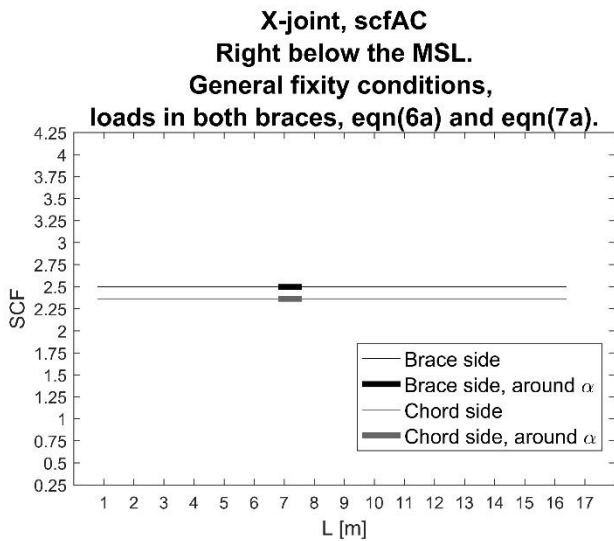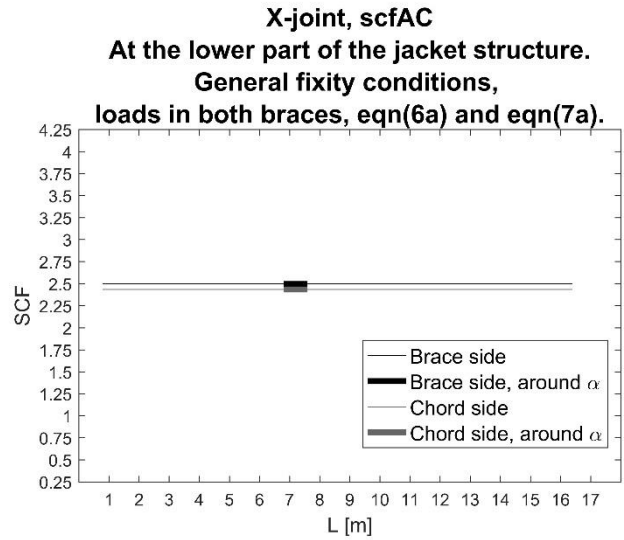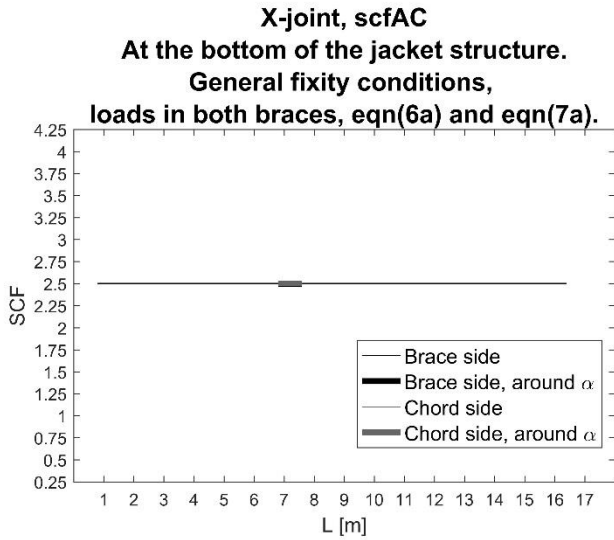
Figure 36: SCFs at the crown for axial load in X-joints

X-joint, scfMIP
At the bottom of the jacket structure.
General fixity conditions,
loads in both braces, eqn(6a) and eqn(7a).

X-joint, scfMIP
At the lower part of the jacket structure.
General fixity conditions,
loads in both braces, eqn(6a) and eqn(7a).

X-joint, scfMIP
Right below the MSL.
General fixity conditions,
loads in both braces, eqn(6a) and eqn(7a).

X-joint, scfMIP
At the upper part of the jacket structure.
General fixity conditions,
loads in both braces, eqn(6a) and eqn(7a).

Figure 37: SCFs for in-plane bending moment in X-joints

Y-joints

Y-joint, scfMIP
At the bottom of the jacket structure.
General fixity conditions, eqn(6a) and eqn(7a).

Y-joint, scfMIP
At the top of the jacket structure.
General fixity conditions, eqn(6a) and eqn(7a).
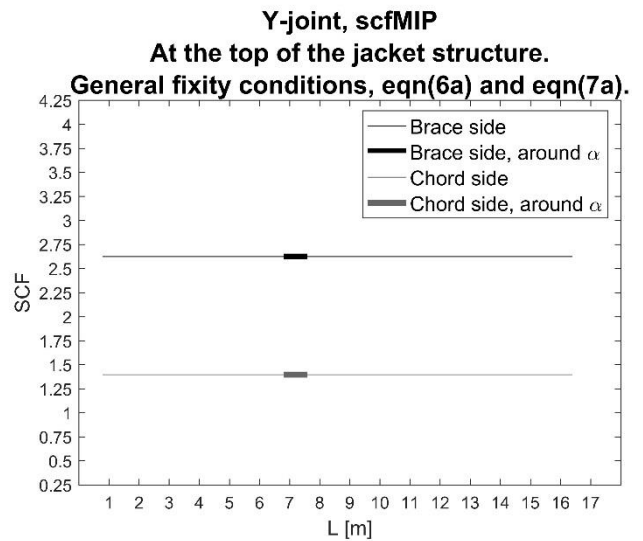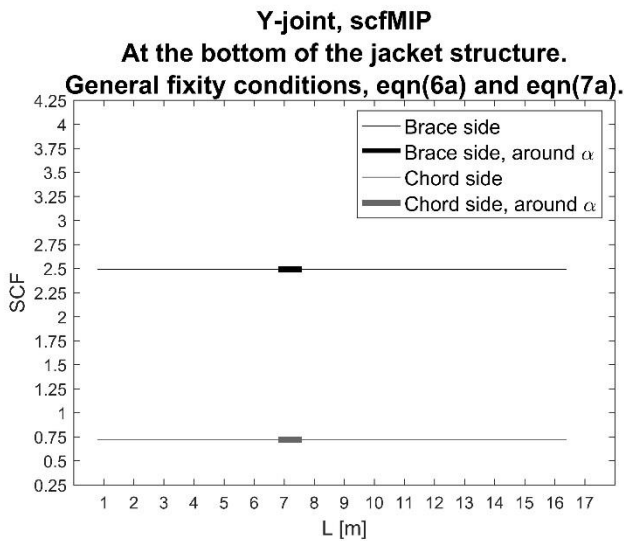
Figure 38: SCFs for in-plane bending moment in Y-joint

B4

Appendix C: Estimated Fatigue Damage for Different *L* Values and Different Number of Hot Spots

These values, as opposed to the plots showing the differences between number of hot spots in sub chapter 4.3, goes from 256 hot spots to 8 hot spots.

Table 3: Estimated fatigue damage for all X-joints, using L3.6, Approach Com

X-joint number	L = 3.6 m, common approach, X-joints					
	256 hot spots	128 hot spots	64 hot spots	32 hot spots	16 hot spots	8 hot spots
1	0,179249	0,179218	0,179143	0,178302	0,17829	0,162521
2	0,205439	0,205416	0,205327	0,204901	0,204896	0,183335
3	1,103573	1,103369	1,102609	1,102447	1,102447	0,987042
4	0,733179	0,73309	0,732939	0,732939	0,716205	0,70847
5	0,176632	0,176602	0,176462	0,176461	0,176461	0,153868
6	0,214249	0,214209	0,214041	0,213966	0,213963	0,184655
7	0,988894	0,988773	0,988403	0,985457	0,975671	0,975669
8	0,479983	0,479967	0,479848	0,478767	0,478195	0,478181
9	0,228277	0,22823	0,228034	0,22759	0,225062	0,213653
10	0,234146	0,234094	0,234004	0,233593	0,22992	0,221764
11	0,400069	0,400045	0,399957	0,399938	0,399864	0,39972
12	0,365551	0,365546	0,365496	0,365482	0,365472	0,365472
13	0,251445	0,251401	0,25125	0,250584	0,246049	0,236654
14	0,278142	0,278066	0,277939	0,276645	0,273683	0,259224
15	0,339624	0,339598	0,33954	0,339207	0,335849	0,332352
16	0,267958	0,267946	0,267888	0,267337	0,267261	0,256923

Table 4: Estimated fatigue damage for all X-joints, using L3.6, Approach Alt

X-joint number	L = 3.6 m, alternative approach, X-joints					
	256 hot spots	128 hot spots	64 hot spots	32 hot spots	16 hot spots	8 hot spots
1	0,179224	0,179142	0,179142	0,17829	0,17829	0,162519
2	0,205253	0,205253	0,204896	0,204896	0,204896	0,182888
3	1,103386	1,103215	1,102447	1,102447	1,102447	0,986876
4	0,733162	0,732939	0,732939	0,732939	0,71609	0,70847
5	0,176458	0,176458	0,176458	0,176458	0,176458	0,152503
6	0,214126	0,214011	0,21396	0,21396	0,21396	0,183267
7	0,988274	0,988211	0,987457	0,985418	0,975669	0,975669
8	0,4796	0,479473	0,479473	0,478171	0,478171	0,478171
9	0,227811	0,227721	0,227721	0,226569	0,224946	0,213563
10	0,233287	0,233287	0,232803	0,232792	0,228748	0,2217
11	0,399489	0,399431	0,399431	0,399431	0,399431	0,399431
12	0,365472	0,365472	0,365472	0,365472	0,365472	0,365472
13	0,251282	0,251282	0,25077	0,250582	0,246047	0,236652
14	0,278097	0,277946	0,277907	0,276635	0,273681	0,259223
15	0,339319	0,339267	0,339189	0,339189	0,334884	0,332352
16	0,267535	0,267535	0,267394	0,267097	0,267097	0,256286

Table 5: Estimated fatigue damage for all X-joints, using L4.8, Approach Com

X-joint number	L = 4.8 m, common approach, X-joints					
	256 hot spots	128 hot spots	64 hot spots	32 hot spots	16 hot spots	8 hot spots
1	0,179584	0,179556	0,179449	0,178724	0,178714	0,162521
2	0,205949	0,205916	0,205829	0,205461	0,205456	0,183637
3	1,105341	1,105088	1,104467	1,104354	1,104354	0,987086
4	0,738042	0,737976	0,737916	0,737915	0,719557	0,714711
5	0,177541	0,177517	0,177348	0,177335	0,177335	0,154952
6	0,215086	0,215053	0,214877	0,214855	0,214852	0,185155
7	0,99676	0,996668	0,996362	0,992973	0,984843	0,98484
8	0,485216	0,485164	0,485047	0,484104	0,482912	0,482899
9	0,230486	0,230468	0,230323	0,229879	0,226598	0,217157
10	0,236596	0,236568	0,236425	0,235949	0,232346	0,225396
11	0,404102	0,404083	0,40395	0,403876	0,403761	0,403593
12	0,370071	0,370034	0,369953	0,369924	0,369913	0,369913
13	0,252714	0,252658	0,252533	0,251958	0,246961	0,238363
14	0,279367	0,279308	0,279123	0,278022	0,274606	0,260933
15	0,347297	0,347277	0,347196	0,346904	0,34322	0,340106
16	0,273972	0,273943	0,27388	0,273382	0,273011	0,263224

Table 6: Estimated fatigue damage for all X-joints, using L4.8, Approach Alt

X-joint number	L = 4.8 m, alternative approach, X-joints					
	256 hot spots	128 hot spots	64 hot spots	32 hot spots	16 hot spots	8 hot spots
1	0,179559	0,179475	0,179447	0,178714	0,178714	0,162519
2	0,20574	0,20574	0,205456	0,205456	0,205456	0,182888
3	1,105168	1,10487	1,104354	1,104354	1,104354	0,986876
4	0,737947	0,737915	0,737915	0,737915	0,719413	0,714711
5	0,177361	0,177332	0,177332	0,177332	0,177332	0,154007
6	0,214958	0,214848	0,214848	0,214848	0,214848	0,183267
7	0,996194	0,995851	0,99565	0,992468	0,98484	0,98484
8	0,484785	0,484785	0,484785	0,482887	0,482887	0,482887
9	0,229993	0,229953	0,229779	0,229141	0,226465	0,217055
10	0,235673	0,235661	0,235436	0,235436	0,230317	0,225322
11	0,403486	0,403434	0,403278	0,403278	0,403278	0,403278
12	0,369994	0,369913	0,369913	0,369913	0,369913	0,369913
13	0,252549	0,252549	0,251955	0,251955	0,24696	0,238362
14	0,279317	0,279221	0,27907	0,278015	0,274605	0,260932
15	0,346988	0,346901	0,346901	0,346901	0,342027	0,340106
16	0,273538	0,273487	0,273487	0,272834	0,272834	0,262803

Table 7: Estimated fatigue damage for all X-joints, using L7.2, Approach Com

X-joint number	L = 7.2 m, common approach, X-joints					
	256 hot spots	128 hot spots	64 hot spots	32 hot spots	16 hot spots	8 hot spots
1	0,179584	0,179556	0,179449	0,178724	0,178714	0,162521
2	0,205949	0,205916	0,205829	0,205461	0,205456	0,183637
3	1,105341	1,105088	1,104467	1,104354	1,104354	0,987086
4	0,738042	0,737976	0,737916	0,737915	0,719557	0,714711
5	0,177541	0,177517	0,177348	0,177335	0,177335	0,154952
6	0,215086	0,215053	0,214877	0,214855	0,214852	0,185155
7	0,99676	0,996668	0,996362	0,992973	0,984843	0,98484
8	0,485216	0,485164	0,485047	0,484104	0,482912	0,482899
9	0,230486	0,230468	0,230323	0,229879	0,226598	0,217157
10	0,236596	0,236568	0,236425	0,235949	0,232346	0,225396
11	0,404102	0,404083	0,40395	0,403876	0,403761	0,403593
12	0,370071	0,370034	0,369953	0,369924	0,369913	0,369913
13	0,252714	0,252658	0,252533	0,251958	0,246961	0,238363
14	0,279367	0,279308	0,279123	0,278022	0,274606	0,260933
15	0,347297	0,347277	0,347196	0,346904	0,34322	0,340106
16	0,273972	0,273943	0,27388	0,273382	0,273011	0,263224

Table 8: Estimated fatigue damage for all X-joints, using L7.2, Approach Alt

X-joint number	L = 7.2 m, alternative approach, X-joints					
	256 hot spots	128 hot spots	64 hot spots	32 hot spots	16 hot spots	8 hot spots
1	0,179559	0,179475	0,179447	0,178714	0,178714	0,162519
2	0,20574	0,20574	0,205456	0,205456	0,205456	0,182888
3	1,105168	1,10487	1,104354	1,104354	1,104354	0,986876
4	0,737947	0,737915	0,737915	0,737915	0,719413	0,714711
5	0,177361	0,177332	0,177332	0,177332	0,177332	0,154007
6	0,214958	0,214848	0,214848	0,214848	0,214848	0,183267
7	0,996194	0,995851	0,99565	0,992468	0,98484	0,98484
8	0,484785	0,484785	0,484785	0,482887	0,482887	0,482887
9	0,229993	0,229953	0,229779	0,229141	0,226465	0,217055
10	0,235673	0,235661	0,235436	0,235436	0,230317	0,225322
11	0,403486	0,403434	0,403278	0,403278	0,403278	0,403278
12	0,369994	0,369913	0,369913	0,369913	0,369913	0,369913
13	0,252549	0,252549	0,251955	0,251955	0,24696	0,238362
14	0,279317	0,279221	0,27907	0,278015	0,274605	0,260932
15	0,346988	0,346901	0,346901	0,346901	0,342027	0,340106
16	0,273538	0,273487	0,273487	0,272834	0,272834	0,262803

Table 9: Estimated fatigue damage for all X-joints, using L8.4, Approach Com

X-joint number	L = 8.4 m, common approach, X-joints					
	256 hot spots	128 hot spots	64 hot spots	32 hot spots	16 hot spots	8 hot spots
1	0,179584	0,179556	0,179449	0,178724	0,178714	0,162521
2	0,205949	0,205916	0,205829	0,205461	0,205456	0,183637
3	1,105341	1,105088	1,104467	1,104354	1,104354	0,987086
4	0,738042	0,737976	0,737916	0,737915	0,719557	0,714711
5	0,177541	0,177517	0,177348	0,177335	0,177335	0,154952
6	0,215086	0,215053	0,214877	0,214855	0,214852	0,185155
7	0,99676	0,996668	0,996362	0,992973	0,984843	0,98484
8	0,485216	0,485164	0,485047	0,484104	0,482912	0,482899
9	0,230486	0,230468	0,230323	0,229879	0,226598	0,217157
10	0,236596	0,236568	0,236425	0,235949	0,232346	0,225396
11	0,404102	0,404083	0,40395	0,403876	0,403761	0,403593
12	0,370071	0,370034	0,369953	0,369924	0,369913	0,369913
13	0,252714	0,252658	0,252533	0,251958	0,246961	0,238363
14	0,279367	0,279308	0,279123	0,278022	0,274606	0,260933
15	0,347297	0,347277	0,347196	0,346904	0,34322	0,340106
16	0,273972	0,273943	0,27388	0,273382	0,273011	0,263224

Table 10: Estimated fatigue damage for all X-joints, using L8.4, Approach Alt

X-joint number	L = 8.4 m, alternative approach, X-joints					
	256 hot spots	128 hot spots	64 hot spots	32 hot spots	16 hot spots	8 hot spots
1	0,179559	0,179475	0,179447	0,178714	0,178714	0,162519
2	0,20574	0,20574	0,205456	0,205456	0,205456	0,182888
3	1,105168	1,10487	1,104354	1,104354	1,104354	0,986876
4	0,737947	0,737915	0,737915	0,737915	0,719413	0,714711
5	0,177361	0,177332	0,177332	0,177332	0,177332	0,154007
6	0,214958	0,214848	0,214848	0,214848	0,214848	0,183267
7	0,996194	0,995851	0,99565	0,992468	0,98484	0,98484
8	0,484785	0,484785	0,484785	0,482887	0,482887	0,482887
9	0,229993	0,229953	0,229779	0,229141	0,226465	0,217055
10	0,235673	0,235661	0,235436	0,235436	0,230317	0,225322
11	0,403486	0,403434	0,403278	0,403278	0,403278	0,403278
12	0,369994	0,369913	0,369913	0,369913	0,369913	0,369913
13	0,252549	0,252549	0,251955	0,251955	0,24696	0,238362
14	0,279317	0,279221	0,27907	0,278015	0,274605	0,260932
15	0,346988	0,346901	0,346901	0,346901	0,342027	0,340106
16	0,273538	0,273487	0,273487	0,272834	0,272834	0,262803

Table 11: Estimated fatigue damage for all X-joints, using L16.0, Approach Com

X-joint number	L = 16.0 m, common approach, X-joints					
	256 hot spots	128 hot spots	64 hot spots	32 hot spots	16 hot spots	8 hot spots
1	0,179584	0,179556	0,179449	0,178724	0,178714	0,162521
2	0,205949	0,205916	0,205829	0,205461	0,205456	0,183637
3	1,105341	1,105088	1,104467	1,104354	1,104354	0,987086
4	0,738042	0,737976	0,737916	0,737915	0,719557	0,714711
5	0,177541	0,177517	0,177348	0,177335	0,177335	0,154952
6	0,215086	0,215053	0,214877	0,214855	0,214852	0,185155
7	0,99676	0,996668	0,996362	0,992973	0,984843	0,98484
8	0,485216	0,485164	0,485047	0,484104	0,482912	0,482899
9	0,230486	0,230468	0,230323	0,229879	0,226598	0,217157
10	0,236596	0,236568	0,236425	0,235949	0,232346	0,225396
11	0,404102	0,404083	0,40395	0,403876	0,403761	0,403593
12	0,370071	0,370034	0,369953	0,369924	0,369913	0,369913
13	0,252714	0,252658	0,252533	0,251958	0,246961	0,238363
14	0,279367	0,279308	0,279123	0,278022	0,274606	0,260933
15	0,347297	0,347277	0,347196	0,346904	0,34322	0,340106
16	0,273972	0,273943	0,27388	0,273382	0,273011	0,263224

Table 12: Estimated fatigue damage for all X-joints, using L16.0, Approach Alt

X-joint number	L = 16.0 m, alternative approach, X-joints					
	256 hot spots	128 hot spots	64 hot spots	32 hot spots	16 hot spots	8 hot spots
1	0,179559	0,179475	0,179447	0,178714	0,178714	0,162519
2	0,20574	0,20574	0,205456	0,205456	0,205456	0,182888
3	1,105168	1,10487	1,104354	1,104354	1,104354	0,986876
4	0,737947	0,737915	0,737915	0,737915	0,719413	0,714711
5	0,177361	0,177332	0,177332	0,177332	0,177332	0,154007
6	0,214958	0,214848	0,214848	0,214848	0,214848	0,183267
7	0,996194	0,995851	0,99565	0,992468	0,98484	0,98484
8	0,484785	0,484785	0,484785	0,482887	0,482887	0,482887
9	0,229993	0,229953	0,229779	0,229141	0,226465	0,217055
10	0,235673	0,235661	0,235436	0,235436	0,230317	0,225322
11	0,403486	0,403434	0,403278	0,403278	0,403278	0,403278
12	0,369994	0,369913	0,369913	0,369913	0,369913	0,369913
13	0,252549	0,252549	0,251955	0,251955	0,24696	0,238362
14	0,279317	0,279221	0,27907	0,278015	0,274605	0,260932
15	0,346988	0,346901	0,346901	0,346901	0,342027	0,340106
16	0,273538	0,273487	0,273487	0,272834	0,272834	0,262803